

**Rutting and Fatigue Performance Evaluation of Asphalt Emulsion Modified using
Asphaltenes**

by

Manjunath Sultanipura Basavarajappa

A thesis submitted in partial fulfillment of the requirements for the degree of

Master of Science

in

Civil (Cross-Disciplinary)

Department of Civil and Environmental Engineering
University of Alberta

© Manjunath Sultanipura Basavarajappa, 2020

Abstract

Road network plays a vital role in a country's infrastructure by providing easy access from one coast to the other coast of the country through transportation which helps in supply of goods and movement of people. Basically, roads are designed and constructed to withstand specific traffic loading and climate conditions. However, the increase in traffic volume and allowable axle load weights leads to the increases in stresses exerted on pavement which subsequently results in rapid deterioration of pavement structures before reaching their intended design life. To overcome this issue, the preservation and treatment of pavement structure have become an important technique for the pavement industry. Modification of asphalt mixture is another method used to improve the performance of pavement in order to avoid the early stage of failure. The use of asphalt emulsion in pavement construction is one such a method to provide a well maintained and efficient road network. Asphalt emulsion is recently raising its popularity in pavement construction, and preservation treatment works like slurry seals, chip seals, micro-surfacing, fog seals and tack coats because of its low-temperature applications, lower viscosity and lower energy consumption. Asphalt emulsions are normally used for cold mix applications and have several advantaged over hot mix applications such as eco-friendly, easy to handle, and does not required to be heated at high temperature for its application instead it can be used at ambient temperature which provides safer working conditions by eliminating dangerous toxic fumes.

For better understanding of asphalt emulsion properties, this research focused on investigating the application of asphalt emulsion modified using asphaltenes for base course layer application. The asphaltenes used in this research were derived from Alberta oil sands. Two types of asphaltenes from different sources were used in this study. For modification, a typical

hand mixing procedure was used to mix asphaltenes with asphalt emulsion. Mix design was prepared in accordance with the standard method to determine the asphalt emulsion and water content to use in the preparation of asphalt mixture. To compare the results, various proportions of asphaltenes content were used for asphalt emulsion modification. Different types of tests were performed on a modified mixture to analyze the rutting and fatigue properties. The Marshall stability, indirect tensile strength (ITS), and Hamburg wheel tracking tests were performed on modified and unmodified asphalt mixture in accordance with ASTM/AASHTO standards. Also, indirect tensile asphalt cracking test (IDEAL-CT) was conducted to understand the cracking resistance of modified mixtures. To characterize the rheological properties of asphaltenes modified asphalt emulsion, asphalt emulsion residues were recovered using low-temperature evaporation technique. The high-temperature properties and dynamic mechanical analysis were performed on recovered residues using a dynamic shear rheometer (DSR).

Results from the study indicate that adding asphaltenes for asphalt emulsion modification improved the performance of both the asphalt mixture and the residue significantly. The Marshall stability of the asphaltenes modified samples is found to increase by 50-100% compared to the unmodified samples. It was also observed that tensile strength and rutting resistance of the modified mixtures were improved considerably than the unmodified mixture. The outcome of the Hamburg wheel tracking test results indicates that the rutting resistance index (RRI) of the modified mixtures was found to increase twice that of the unmodified mixture. From IDEAL-CT analysis, it was noticed that the fracture energy of the modified samples were increased, but the cracking tolerance index (CT_{Index}) was reduced for the modified mixture. However, the rheology tests specified that the high limiting temperature of

the modified samples were increased by 30 °C to 40 °C compared to the unmodified sample. Whereas from the dynamic mechanical analysis, it was found that asphaltene modification improves the elastic property of the asphalt emulsion, but at low-frequency range, more stiffness behaviour was observed.

Preface

All of the work presented in this report was conducted in the Asphalt and Binder engineering laboratory at the University of Alberta under the supervision of Dr. Leila Hashemian. Chapter 1 and chapter 2 represent the introduction and literature review are conducted by me based on the previous research studies.

A version of chapter 3 has been submitted for publication as M. Basavarajappa, F. Kamran, N. Bala, L. Hashemian, “Rheological characteristics and fatigue performance of asphalt emulsion modified using asphaltenes.,” in the Transportation Research Board (TRB) Annual Meeting to be held in January 2021.

A version of chapter 4 has been submitted for publication as M. Basavarajappa, F. Kamran, N. Bala, L. Hashemian, “Permanent Deformation of Stabilized Asphalt Emulsion Modified using Asphaltenes.,” in the International Journal of Pavement Research and Technology (IJPRT).

Chapter 5 in this report contains the results of dynamic mechanical analysis of the source 2 asphaltenes modified asphalt emulsion at various proportions. The result presented in this chapter is not published in any of the journal/ conference paper yet.

Chapter 6 in this report gives the summary and conclusions of this study.

The Appendix included in this report has been submitted for publication as M.M. Nojumi, M. Basavarajappa, L. Hashemian, A. Bayat, “Investigation of the Impact of Tire Configurations on Different Pavement Structures using Finite Element Analysis.,” in the Transportation Research Board (TRB) Annual Meeting to be held in January 2021.

I was responsible for all major parts of the data acquisition, analysis and interpretation of results, and preparation of the manuscript. Farshad Kamran was involved in data collection

and analysis in some parts of the work. Dr. Leila Hashemian and Nura Bala were contributed to manuscript edits. Dr. Leila Hashemian was the supervisory author on this research and was involved throughout the study in concept formation.

Dedicated to

My Father, Mother and Brother whose affection, love, encouragement and prayers make me able to achieve such a success and honor.

And to the People who have always been there to support me, congratulate me, and show me always the best path to follow.

Acknowledgements

I would like to thank the following people, without whom I would not have been able to complete this research. Throughout this research, I have received a great deal of support and assistance.

My profound thanks to my supervisor Dr. Leila Hashemian for allowing me to be part of her team. Her expertise was invaluable in articulating the research topic and methodology in particular. The door to Dr. Leila Hashemian's office was always open whenever I had a question about research, and she always steered me in the right direction whenever she thought I needed it.

I wish to thank the professor and the committee, Dr. Alireza Bayat, for providing an opportunity to work under him in one of the research projects and for sharing his valuable knowledge.

I would also like to extend my thanks to the Alberta Innovates for providing funds to this research. Also, my sincere thanks to all who contributed the materials needed for this research: Husky Energy for providing asphalt emulsion; Lafarge Canada for providing aggregates; Nestor Zerpa, and Value Creation, Inc. for providing asphaltenes.

I would like to appreciate and thank my colleagues for their most exceptional support and assistance throughout my research. My special thanks to Farshad Kamran and Amirhossein Ghasemirad for assisting in performing tests in the laboratory, collection and analysis of data; Thomas Johnson and Luis Perca for sharing their knowledge in most of the laboratory procedure. I would also like to thank Nura Bala and Lana Gutwin for providing a timeless review of all my work.

In addition, I would like to thank my parents for their wise counsel and sympathetic ear, you are always there for me. Finally, there are my friends, who were of great support in deliberating over our problems and findings, as well as providing a happy distraction to rest my mind outside of my research.

Table of Contents

1	Introduction	1
1.1	Objective	2
1.2	Methodology	3
1.3	Thesis Structure	3
2	Literature Review	5
2.1	Cold mix asphalt	5
2.2	Asphalt Emulsion in pavement construction	6
2.2.1	Processing of asphalt emulsion	7
2.2.2	Asphalt emulsion classification	9
2.3	Modified Asphalt Emulsion Mixtures	10
2.4	Properties of asphaltenes in pavement construction	10
2.5	Asphalt Emulsion Residue	11
2.6	Rheological Characteristics of Asphalt Emulsion Residue	13
2.6.1	Rutting Resistance	13
2.6.2	Dynamic Mechanical Analysis	13
2.7	Asphalt Emulsion Mixture design	16
2.8	Mechanical properties of the asphalt emulsion mixture	17
2.9	Performance evaluation of asphalt emulsion mixture	18
2.9.1	Marshall Stability and Flow	18
2.9.2	Indirect Tensile Strength (ITS)	19
2.9.3	Hamburg wheel tracking test	21
2.9.4	IDEAL-CT test	22
3	Rheological Characteristics and Fatigue Performance of Asphalt Emulsion Modified using Asphaltenes	24

3.1	Abstract.....	24
3.2	Introduction.....	24
3.3	Objective and Scope	27
3.4	Materials	28
3.4.1	Aggregates.....	28
3.4.2	Cationic slow-setting asphalt emulsion	29
3.4.3	Asphaltenes.....	29
3.4.4	SARA test on Asphaltenes	30
3.5	Methodology.....	30
3.5.1	Optimum asphalt emulsion content	30
3.5.2	Asphalt emulsion modification using asphaltenes	32
3.5.3	Penetration grading test	32
3.5.4	Residue recovery of asphalt emulsion.....	32
3.5.5	ITS and IDEAL-CT analysis.....	33
3.5.6	Dynamic mechanical analysis	34
3.6	Results and Discussion	35
3.6.1	Optimum asphalt emulsion content	35
3.6.2	Penetration grading.....	36
3.6.3	ITS and IDEAL-CT analysis.....	37
3.6.4	Dynamic mechanical analysis	39
3.7	Conclusions.....	41
4	Permanent Deformation of Stabilized Asphalt Emulsion Modified using Asphaltenes	43
4.1	Abstract.....	43
4.2	Introduction.....	43
4.3	Objectives and Scope.....	46

4.4	Materials	47
4.4.1	Aggregates	47
4.4.2	Asphalt emulsion	47
4.4.3	Asphaltenes.....	49
4.5	Mix design	51
4.5.1	Optimum asphalt emulsion content	51
4.5.2	Asphalt emulsion modification with asphaltenes	52
4.5.3	Asphalt emulsion residue recovery procedure	52
4.5.4	Marshall stability and flow	53
4.5.5	Indirect tensile strength (ITS).....	54
4.5.6	Hamburg wheel tracking test.....	54
4.5.7	Dynamic Shear Rheometer (DSR)	55
4.6	Results and discussion	55
4.6.1	Marshall stability and flow	55
4.6.2	Indirect tensile strength (ITS).....	56
4.6.3	Performance testing	57
4.7	Conclusions.....	60
5	Additional testing.....	62
5.1	Dynamic mechanical analysis of asphaltenes modified asphalt emulsion.	62
6	Summary and Conclusions.....	65
6.1	Summary.....	65
6.2	Conclusion	65
	References.....	68
	Appendix.....	87

List of Tables

Table 3-1: Aggregate gradation.....28

Table 3-2: Physical properties of the aggregates.....29

Table 3-3 SARA components of asphaltenes30

Table 3-4 Penetration grading test results37

Table 3-5 ITS and failure energy values of control and modified samples.....37

Table 4-1: Properties of asphalt binder used to produce asphalt emulsion (103)48

Table 4-2: Properties of Asphalt Emulsion (CSS-1H) (90).....48

Table 4-3: Basic chemical properties of dried asphaltenes (Source 2 type) (122)50

Table 4-4: SARA test results of asphaltenes50

Table 4-5: Design matrix to determine the optimum asphalt emulsion51

Table 4-6: Marshall stability and flow number55

Table 4-7: Indirect tensile strength test results.....56

Table 4-8: Wheel tracking test results57

Table 4-9: DSR results for high-temperature limits ($|G^*| / \sin \delta = 2.2 \text{ kPa}$).....58

List of Figures

Figure 2-1 Schematic diagram of a typical asphalt emulsion manufacturing process	8
Figure 2-2 Dynamic shear rheometer (DSR) testing equipment	14
Figure 2-3: Dynamic test outputs from DMA. [Source (52)].....	15
Figure 2-4: Two different type of failure to determine Marshall stability and flow (61)	19
Figure 2-5: ITS test specimen testing and specimen after testing	20
Figure 2-6: Key parameters of the wheel tracking test analysis (66)	21
Figure 2-7 Behaviour of specimen at different stages of the load-displacement curve (68).....	23
Figure 3-1 Asphaltenes, solid asphaltenes (left), powdered asphaltenes (right)	30
Figure 3-2 Illustration of post-peak slope and load line displacement of the curve (70).....	34
Figure 3-3 ITS and Marshall stability test results used to determine optimum emulsion content	36
Figure 3-4 Density results used to determine optimum emulsion content	36
Figure 3-5 Load-displacement relationships	38
Figure 3-6 CT_{Index} and percentage improvement of ITS for control sample and modified mixtures	39
Figure 3-7 Master curve of phase shift angle at 25 °C for control sample and modified sample	40
Figure 3-8 Master curve of complex shear modulus at 25 °C for control sample and modified samples	41
Figure 4-1: Aggregate gradation chart	47
Figure 4-2: Source 1 type of Asphaltenes. ((a) solid & (b) Powdered).....	49
Figure 4-3: Source 2 type of Asphaltenes	50

Figure 4-4: (a) Asphalt Emulsion on silicon mat at a spread rate of 1.5 to 2.0 kg/m ² (b) Recovered residue stored in a container	53
Figure 4-5: (a) Slab prepared for wheel tracking test. (b) Slab after performing Hamburg wheel tracking test	55
Figure 4-6: Rutting factor of asphalt emulsion modified with asphaltenes.....	59
Figure 4-7: Failure temperature and Rutting Resistance index	60
Figure 5-1: Master curve of phase shift angle at 25 °C for the control sample and modified sample.....	63
Figure 5-2: Master curve of complex shear modulus at 25 °C for the control sample and modified samples.....	64

1 Introduction

The road network systems are essential component of the country's infrastructure by connecting the country from coast to coast through transportation, it was estimated that over 96% of the road network around the world are paved with asphalt (1). Annually billions of dollars are spent on these roads for reconstruction, rehabilitation and maintenance (1). Maintenance of roads helps in improving the performance of the pavement, which helps in achieving the intended service life. The increase in traffic volume, extreme weather conditions, repeated traffic loading, and high tire pressure causes acute structural deterioration of pavements by generating excessive tensile stress concentrations at the bottom and top of asphalt layer (2). Adopting new design procedures, preparing better mixtures and performing reliable tests in the laboratory could avoid such pavement distress and helps to enhance pavement design life (3). One such a method to improve asphalt mixture is modifying asphalt binder using different additives (4). Currently, there are various additives like polymers, nanomaterials, fibres, etc., that have been used for improving the properties of asphalt binders. However, apart from these materials, researchers also focused on using waste materials such as paper sludge ash, high calcium fly ash, waste engine oil, palm ash and glass in the modification of asphalt emulsion mixtures (3).

Asphalt emulsion mixtures application is becoming popular nowadays compared to the conventional hot mix asphalt due to less energy consumption, fewer emissions, and more cost-effective as they do not required heat during their application process (4), because of these benefits asphalt emulsion is used as cold mix asphalt mixture. Due to its several advantages both in terms of environmental and economical factors, many research projects have been conducted by utilizing waste materials and by-products to study and develop the properties of cold mix asphalt mixtures to achieve equivalent properties of hot mix asphalt mixture. (5).

Modification of asphalt emulsion mixture is not a new concept as mentioned many researches have been conducted, one instance for that is using a cement to modify asphalt emulsion mixture to improve its properties (4). Some of the studies reported that the use of asphalt emulsion in pavement construction resulted in reduced intended service life of the pavement (2) Also increase in rutting, cracking, and surface wear are the major distress on pavement that leads to failure of the pavement structure (2). Other than these distresses, asphalt emulsion

mixtures have some issues with ravelling, compaction, stripping, low early strength and extended curing time (6). To overcome these drawbacks of asphalt emulsion, previous studies have been concluded that using additives like fly ash, Portland cement, and lime can improve the performance of asphalt emulsion mixture (7). Earlier studies proved that adding ordinary Portland cement to the asphalt emulsion mixtures have shown equivalent stiffness modulus and permanent deformation resistance as hot mix asphalt (8). Also, using cement in modification of asphalt emulsion mixture helps to eliminate delay in curing and improves high resilient modulus more rapidly, in addition to that cement enhances the stability of mixture by 250-300% than unmodified asphalt emulsion mixtures (8). Similarly, introducing polymer in asphalt emulsion modification proved that it increases the rutting performance of the mix (9).

Despite the introduction of modification in asphalt emulsion and asphalt emulsion mixture, there are still some challenges associated with their properties such as high material cost, lack of availability, higher molecular weight and long-term performance (10). To overcome these issues, researchers focused on implementing waste materials in asphalt emulsion modification. One such an example of potential waste material is asphaltenes. The asphaltenes fraction has an ability to combine into micelles and form networks (11). The compatibility between the asphaltenes and maltene phases that has a major effect on asphalt rheological properties (11). The polarity of asphalt binder materials and their interactions play a significant role in determining the rheological properties of the asphalt binder. Also, earlier studies proved that the increased content of asphaltenes as polar fractions helps to increase the indirect tensile strength of the binders (12).

1.1 Objective

The main objective of this research is to investigate and compare the performance of modified asphalt emulsion using two types of waste asphaltenes obtained from different sources. Other specific objectives of the study are as follows:

- To determine the performance of the modified mixture and unmodified mixture using indirect tensile strength (ITS) at intermediate temperature of 25 °C and Marshall stability test.

- To determine the cracking indices and fatigue resistance of modified asphalt emulsion mixtures using indirect tensile asphalt cracking test (IDEAL-CT) analysis with the help of the load-displacement curve of IDT test results.
- To evaluate the permanent deformation (rutting) of the asphalt emulsion mixture containing different proportion of asphaltenes based on relationship of the results of rheology test and wheel tracking tests.
- To perform dynamic mechanical analysis (DMA) and superpave performance grading (PG) tests at high temperatures to characterize rheological properties of asphalt emulsion residues modified with asphaltenes.
- To evaluate the penetration grading of modified and unmodified residues by performing penetration test and verify the suitability of the binders for pavement construction.

1.2 Methodology

The performance of asphaltenes modified cationic slow setting (CSS-1H) asphalt emulsion in a granular base course was analyzed by performing various tests in the laboratory. Unless otherwise mentioned, the asphalt emulsion used in this research shall be identified by a cationic slow setting (CSS-1H). The asphalt emulsion modification was done by hand mixing, and for the modification various proportions of asphaltenes at 0.2%, 0.5%, 1% and 2% by weight of total mixture were used. At each proportion, at least three samples were prepared for each test to compare the results. The prepared specimens were tested for Marshall stability, ITS, Hamburg wheel tracking test and IDEAL-CT analysis and the results were compared with the control sample (unmodified sample).

For the rheological investigation of modified and unmodified samples, the asphalt emulsion residues were recovered using the “low-temperature evaporation technique”. The recovered residues were analyzed for dynamic mechanical stability and rutting performance using a dynamic shear rheometer. All the tests performed in this research were conducted in accordance with ASTM/AASHTO standards specifications.

1.3 Thesis Structure

The thesis structure is presented as follows:

Chapter 1 – Introduction: This chapter contains a background, motivation of the research, objective, methodology, and thesis structure.

Chapter 2 – Literature Review: Advantages/disadvantages and performance of asphalt emulsion in pavement construction are discussed. Modification of asphalt emulsion and asphalt mixture using various types of materials and its performance has been discussed. Also, the residue recovery procedure and its effect on asphalt emulsion are included in this chapter. Relevant case studies are also presented.

Chapter 3 – Rheological Characteristics and Fatigue Performance of Asphalt Emulsion Modified using Asphaltenes: The cracking indices of asphalt emulsion-stabilized mixtures modified with asphaltenes using load-displacement curves of the ITS tests at intermediate temperatures are presented, and dynamic mechanical analysis of the modified and unmodified asphalt emulsion residues are also compared in this chapter.

Chapter 4 – Permanent Deformation of Stabilized Asphalt Emulsion Modified using Asphaltenes: This chapter contains the results of performance testing of asphaltenes modified asphalt emulsion mixtures are presented. The rutting performance of both modified and unmodified stabilized mixes are evaluated and compared. The high limiting performance grading of the asphalt emulsion residues are also included.

Chapter 5 – The dynamic mechanical analysis for the asphalt emulsion modified samples using source 2 types of asphaltenes is demonstrated in this chapter. Based on the frequency sweep conducted for the modified asphalt emulsion residues, the master curves have been plotted over a range of frequencies.

Chapter 6 – Summary and conclusions: In this chapter, based on the various tests results, the effects of asphalt emulsion modification using asphaltenes at different proportions on rheological properties and performance of mixture are summarized and explained.

2 Literature Review

2.1 Cold mix asphalt

Cold mix asphalt is the type of asphalt mixture used in pavement construction, as the name indicates, cold mix asphalt does not require heating for its application (13, 14). The cold mix asphalt is a mixture of unheated aggregates and asphalt emulsion mixed and compacted at ambient temperature (14, 15). Several environmental and cost-effective benefits can be achieved through the use of cold mixes over hot mix asphalt mixtures (14). Cold mix asphalt can be produced either in plant or at the worksite with the help of pug mill mixers; this reduces the hauling charges and energy consumption, which makes this mixture a very cost-effective (15). Similarly, by using more proportion of recycled asphalt pavement (RAP) in mixture, the cold mix asphalt reduces significantly the material cost of the pavement (15).

Mostly, cold mix asphalts are suitable to use as a base course for low to medium traffic conditions, cold climate regions, wearing course/surface coat, and for reinstatement works (16, 17). Cold mix asphalt is considered as inferior to hot mix asphalt (17) because it has to meet with the requirements of carrying heavy traffic loads, and also it requires to resist the environmental impact in terms of durability (5). However, despite the benefits of cold mix application, there are three main major concerns on cold mix asphalt application compared to hot mix asphalt (17).

- a. The high porosity of the compacted mixture
- b. Weak early life strength
- c. Long curing time required to achieve maximum performance

Mechanical properties of asphalt mixture such as stiffness modulus, permanent deformation and fatigue resistance are affected by many parameters such as base binder grade, mixture void content, curing time, aggregate characteristics and additives (14, 18, 19). Several studies have been conducted to improve the mechanical properties of cold mix asphalt by using polymers, latex, cement, waste glass, etc., as additives to modify the mixture. A study conducted by M. A. Kadhim et al. (2019) used waste glass as a replacement of virgin fine aggregates in cold bituminous emulsion mixture at proportions of 25%, 50%, 75% and 100%. Results indicated that the modified mixture had shown greater efficiency to work as a

structural surface layer; however, ITS values of all the modified samples including control samples were found to be greater than 1000 kPa. The cold bituminous emulsion mixture modified with 75% of waste glass as fine aggregates had shown ITS value equivalent to hot mix asphalt (3).

The use of reclaimed asphalt pavement is becoming popular due to reduction in production process cost, substituting natural aggregates and virgin binder of asphalt (20). S. Arimilli et al., (2016) conducted a study using cement as a filler and reclaimed asphalt pavement by replacing virgin aggregates at 30%, 50%, 60%, 70% and 80%. The study concluded that the use of 60% reclaimed asphalt pavement in cold asphalt mixture exhibited better results in ITS, dynamic creep and wheel tracking tests (21).

Additionally, for the mechanical performance analysis of emulsion treated base layer, several of heavy vehicle simulator (HVS) analysis were performed to obtain real field behaviour data from typical roads, a recent study developed a model on fatigue cracking based on heavy vehicle simulator in a research conducted by Jordan (2000), the outcome of the study showed that emulsion treated base layer can carry a high traffic loading up to 30 million ESAL's under relatively high surface deflection, however, fatigue failure was observed in the emulsion treated base layer (22).

2.2 Asphalt Emulsion in pavement construction

The demand for a low periodic maintenance roadway urges industries and government agencies to find a cost-effective, easy to apply and environmentally friendly preservation treatment technique (23, 24). Due to less availability of quality raw materials, it is necessary to utilize road materials in an efficient and conservative manner. This leads to the increased use of recycling and high-performance material like modified emulsion (23). The use of asphalt emulsion for preservation treatment techniques is growing popular due to its various advantages, such as lower viscosity and lower application temperatures (24). The emulsions were first advanced in the early 1900's, and it was introduced in pavement applications in the 1920's (23). In the beginning stage, asphalt emulsions were limited to use only in spray applications and dust palliatives due to the availability of limited type of emulsion and lack of knowledge on how to implicate in pavement construction (23). However, the increased in

traffic loads and volumes during World War II, the roadway designers urge to use of asphalt emulsions (23).

Apart from mentioned reason above, several factors mentioned below have contributed to an increase in the use of asphalt emulsions, most prominent ones are as follows (23).

- Very less or absence of hydrocarbon emissions from asphalt emulsion reduces atmospheric pollution.
- Asphalt emulsions have ability to coat damp aggregates, which reduces the fuel requirements for heating and drying aggregates.
- The availability of various types of asphalt emulsions helped to develop laboratory procedures to satisfy design and construction requirements.
- Asphalt emulsions can also be used in pavement preservation and treatment to enhance the service life of slightly distressed pavements.

The United States is the largest producer of emulsion in the world (25, 26). The lower viscosity of asphalt emulsion allows to its application at a lower temperature (23-25). This low-temperature technique in road construction and maintenance reduce emissions, energy consumption, provides safer working condition and avoids releasing toxic gases, because of all these applications asphalt emulsion is considered as environmentally friendly construction material and also well-known as green technology in road construction (23-26).

2.2.1 Processing of asphalt emulsion

The asphalt emulsion is a combination of asphalt, water and emulsifying agents. Setting time of asphalt emulsion depends on the chemical composition, asphalt emulsion can be prepared to have a different setting time based on the type of surfactants; their concentration and additives used (24), the setting time is defined as the time required for asphalt emulsion to break and set. Asphalt emulsions are designed to be in a stable suspension when stored; however, when they come into contact with aggregate surfaces, the emulsions are formulated to break and form a layer of asphalt around aggregate particles (24). The cations in aggregates help to raise the OH⁻ ions in emulsion and lead to setting. The rate at which the asphalt

emulsion breaks depends on the chemical design and emulsifier used and on the nature of the aggregates the emulsion comes in contact with (24).

For processing asphalt emulsion, a colloidal mill is the basic equipment consists of high-speed, high-shear mechanical devices used to divide the asphalt to tiny drops. Also, the manufacturing process requires emulsifier solution tank, heated asphalt tank, pumps and flow-metering gauges (23). Figure 2.1 shows a schematic diagram of a typical asphalt emulsion manufacturing process.

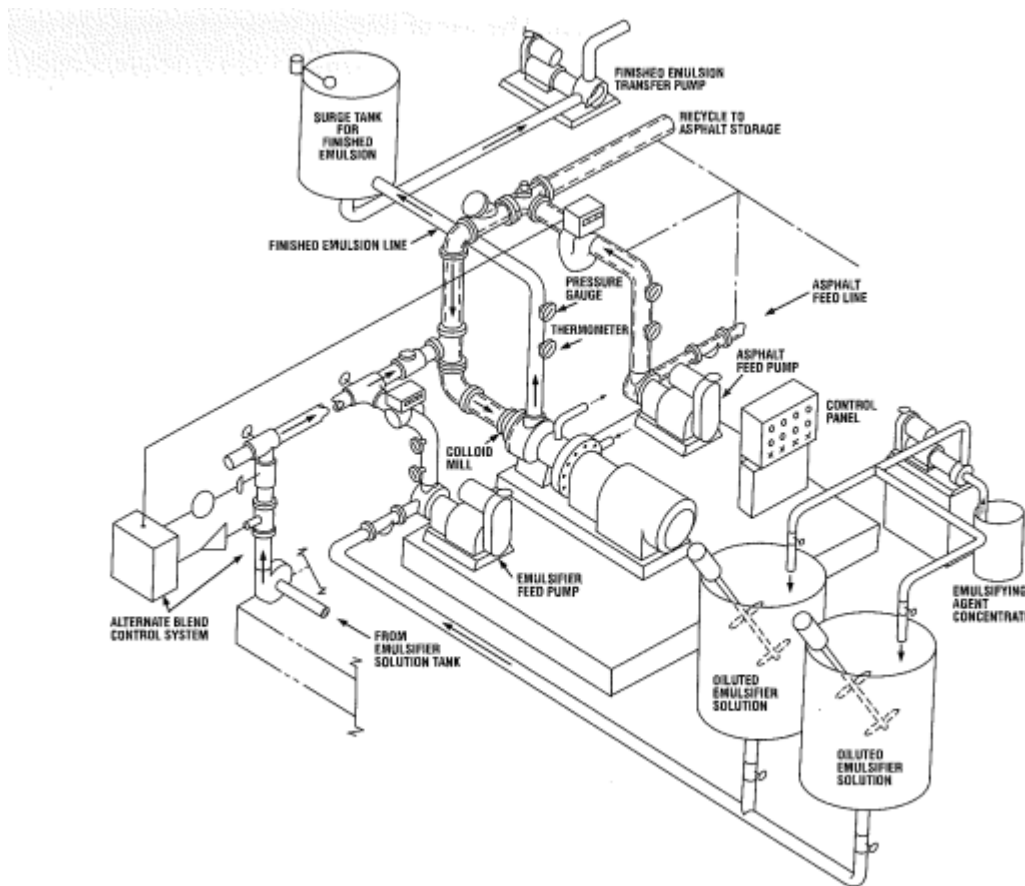


Figure 2-1 Schematic diagram of a typical asphalt emulsion manufacturing process [Source 23]

The high-speed rotor in colloidal mill revolves at 1000 to 6000 rpm with mill clearance settings of about 0.25 to 0.50mm. The asphalt emulsion droplets are in the size between 0.001 to 0.010 m. However, asphalt emulsion sizes relied on the mechanical energy density transmitted by the mill (23). This particle analyzers are commonly used to describe the asphalt emulsion quality. In the asphalt emulsification process the heated asphalt is transferred to the

colloidal mill to divide into tiny droplets and simultaneously the water containing emulsifying agent will also be transferred to the colloid mill. The asphalt and emulsifiers are supplied to the colloid mill using separate pumps. Due to highly corrosive nature of emulsifier solution it is necessary to use the corrosive resistant equipment's (23).

Later, the asphalt in colloid mill is heated to a low viscosity and water in colloid mill also adjusted to a temperature to optimize emulsification. This temperature depends on the emulsification property and the compatibility between the asphalt and the emulsifying agent. However, very high temperature asphalt emulsions are not used due to the reason that the emulsion transferring from the colloid mill to the storage tank should be within the boiling point of water. The mechanical agitation will be equipped in the storage tank to keep the emulsion uniformly blended (23).

2.2.2 Asphalt emulsion classification

There are different types of asphalt emulsions available for various purposes, and asphalt emulsion type for a particular application is decided based on the performance properties required for such work (23, 27). Asphalt emulsions are generally classified based on particle charge and setting properties of the emulsion (27). The anionic, cationic and non-ionic are three main types of asphalt emulsions based on the particle charge. Anionic and cationic are widely used in pavement construction works and are readily available, but non-ionic emulsions have limited applications in the pavement. As all aggregates are negatively charged at the surface, the cationic emulsion uses this property as an advantage for fast and effective binding (27). Usually, asphalt emulsions are manufactured to have four different setting properties, which are rapid setting (RS), medium setting (MS), slow setting (SS) and quick setting (QS). Some of the modified asphalt emulsions are identified by using additional letters, for example polymer-modified asphalt emulsions are indicated by the letter "P" and latex modified emulsions are indicated by letter "L" at the end of their identification. Apart from these, asphalt emulsions are also identified by using numbers 1 or 2, and letter (H) for hard emulsion or (S) for soft emulsion. The number "1" indicates low viscosity, and number "2" indicates high viscosity, and "hard" (H) represents the high penetration base asphalt whereas "soft" (S) represents the lower penetration base asphalt. (23, 27).

2.3 Modified Asphalt Emulsion Mixtures

In earlier days unmodified asphalt emulsion were able to withstand the traffic volume and loads applied on them, but at present due to higher vehicle load and heavy traffic volume, the stress exerted on pavement surfaces increased, which results in early pavement deterioration and distress before reaching their intended service life (26). To address this premature failure of pavement structure, many studies focused on modifying asphalt emulsion with different types of polymers, cement and other additives. The early stage of studies on using polymers for modification exhibited improvement in pavement performance, which helps to increase the pavement service life even though the pavement surfaces experience an unexpected increase in traffic volume (26). It was also proved that polymer modified asphalt emulsion pavement showed better resistance to rutting and thermal cracking, and it helps to decrease fatigue damage and stripping (26).

S. Du (2014) conducted a study by using cement as a filler to modify asphalt emulsion. In this study, limestone was used as filler for an unmodified mixture where for modified samples, cement was used as filler. The results from the study showed that increasing cement content to the mixture decreases the optimum emulsion content; meanwhile, ITS of the samples were increased. In addition to that, adding cement to the mixture improved moisture and rutting performance of the asphalt emulsion mixture considerably. These improvement results were found due to the ability of hydration products to enhance the rigidity of cement asphalt emulsion mixture and due to improvement in interface adhesion between mastic and aggregates (4).

2.4 Properties of asphaltenes in pavement construction

The asphaltenes are considered as the least valuable component of crude oil (28). The Canadian oil sand bitumen is ranked as one of the highest producer of large amounts of asphaltenes (16-20 weight %) (29). The viscosity of crude oil increases significantly due to the presence of asphaltenes content and making it difficult to transport and process (30). Asphaltenes are very difficult to biodegrade because of the presence of heavy metal components, and this makes asphaltenes the most undesired component in the petroleum waste management perspective (31). However, despite these properties which make the

asphaltenes undesirable, asphaltene is also very useful in pavement industry. One such an example is that asphalt a derivative of asphaltene is the most suitable material for pavement surfaces construction (28, 32, 33). The asphalt properties such as bio-inertness, rheological toughness and adhesion make it an ideal material in the application on pavement surface coating (28). The molecular structure of the asphaltene phase in the bitumen is considered to have a significant effect on its rheological properties (28, 34). Because of its polar characteristics, asphaltene is prone to react with oxygen and create carbonyl and sulfoxide compounds. This reaction results in the increase in stiffness and viscosity of the binder (35). From earlier studies, it had been concluded that the increase in the content of asphaltene in asphalt blend apparently increases the viscosity of the blends (34).

2.5 Asphalt Emulsion Residue

The recovery method of asphalt emulsion residue plays a vital role in analyzing the rheological characteristics of a particular asphalt emulsion. However, the primary purpose of residue recovery is to obtain the part of the non-water phase in the emulsion to perform necessary testing (36). At present, there are over ten different recovery methods and some of these methods have been accepted as consensus standards and outlined in ASTM and AASHTO standards (37). Some of these techniques required a higher temperature, and some requires mainly a lower temperature. Below listed are some standards that have been accepted as consensus standards and are outlined in ASTM and AASHTO standards.

- Low-temperature evaporation technique – AASHTO PP 72-11/ ASTM D7497-09
- Distillation Technique – ASTM D 6997
- Evaporation Technique – ASTM D 6934
- Moisture Analyzer Balance – ASTM D 7404
- Low-temperature Vacuum Distillation – ASTM D 7497

Apart from above standard procedures, below mentioned are some of the methods which are proposed by different researchers during their study.

- Recovering using Simple Aging Test Plate (38)
- Simple Air-Drying Technique (27)
- Rapid Residue Recovery Procedure using RTFOT (27)

Many of these procedures involved a distillation or evaporation technique to recover residue. In the distillation process, usually high-temperature heat is used to recover residue compare to the evaporation technique (26). The main issue in the high-temperature recovery process is obtaining a laboratory specimen representative to field condition, where at field construction is held at an ambient temperatures (27). A study conducted by D. Salomon et al., (2008) compare the rheological properties of asphalt emulsion residue recovered using distillation (ASTM D 6997), evaporation (ASTM D 6934) and moisture analyzer balance (ASTM D 7404) methods for five different type of asphalt emulsions. Based on the complex shear modulus obtained at 60 °C and 0.4 Hz which was used to evaluate how each asphalt emulsion type and residue recovery procedure affected rheological properties. From the analysis it was concluded that distillation and evaporation are considered as more dynamic recovery procedures compared to static moisture analyzer balance process because the samples recovered under distillation and evaporation methods were subjected to more turbulent conditions, boiling and stirring respectively which affect their rheological properties. Also, higher oxidation was noticed during the moisture analyzer balance recovery method due to the static nature of the process and to the higher surface to volume ratio of the sample compared to other methods (39).

However, K. Takamura (2000) showed that the use of high temperature in some of the recovery procedures affected the microscopic structure of the emulsion considerably; hence the residues recovered using some of the high-temperature methods does not represent the field conditions. Therefore, to simulate the recovered residue to the field conditions Takamura proposed a new procedure called simple air-drying process to recover residue by drying emulsion at ambient temperature for 5-6 hours, this process could be accelerated by drying samples in rolling thin film oven test (RTFOT) apparatus for 75 min at 85 °C (40). A study was conducted to compare the results of the recovered residues samples by using the simple air-drying procedure and RTFOT procedure; from the results and observation, it was concluded that RTFOT procedure produces stiffer residues compare to the simple air-drying method (27).

2.6 Rheological Characteristics of Asphalt Emulsion Residue

2.6.1 Rutting Resistance

The rheological properties of asphalt binder, temperature and traffic conditions are the main parameters determining pavement distress such as rutting, fatigue and thermal cracking (41, 42). Due to this, a well-established performance grading system is needed to choose the appropriate asphalt binder based on the required applications (43). The physical properties of asphalt materials tend to make asphalt concrete to be more susceptible to rutting at a high temperature when the asphalt binder has a lower viscosity and more chances to creep under heavy traffic (44).

As per Superpave fundamentals, the permanent deformation of an asphalt binder at a high-performance temperature will be measured using a $G^*/\sin \delta$ as a prime factor. Similar to asphalt binder, the rheological properties of asphalt emulsion residue can also be analyzed using a dynamic shear rheometer (DSR). To understand the high-temperature properties of asphalt emulsion residue at the construction stage, the high-temperature performance grade of asphalt emulsion residue was determined by using failure temperature at the original unaged condition. The viscous and elastic behaviour of the residues were characterized by measuring the complex modulus (G^*) and phase angle (δ). The G^* is the sum of the elastic component, and the viscous component which can be obtained from the ratio of the stress amplitude to the strain amplitude is a measure of binder resistance to shear deformation. The δ is the time lag between the applied stress and the resulting strain and is an indication of the binder's response to shear deformation (44, 45). The parameters G^* and δ were measured by performing DSR tests in accordance with the Superpave test method (46) and AASHTO T315 (47) at a strain rate of 0.5% with an angular frequency of 10 rad/s and an 8mm diameter spindle with a 2-mm gap.

2.6.2 Dynamic Mechanical Analysis

Initially, dynamic mechanical analysis (DMA) has been used by polymer and food processing industries for several years (48). Eventually, researchers started using DMA to analyze the fatigue and healing characteristics of asphalt mastics and mixtures (48, 49). Like asphalt mixtures, DMA can also be used to obtain G^* and δ of binders by performing frequency

sweep tests to determine the effects of time, temperature, strain and loading frequency on asphalt emulsion (48, 50, 51). The viscoelastic behaviour of the asphalt emulsion residues/binders can be obtained through DMA over a wide range of temperatures and frequencies. To determine this, the samples are sandwiched between two parallel plates and subjected to alternate shear stress and shear strain. Depending on the variables controlled by the test apparatus, the test can be either stress controlled, or strain-controlled (52). Usually, the strain-controlled condition will be used to determine the dynamic rheological properties of the samples (45, 53, 54). Figure 2-1 shows the model of the dynamic shear rheometer (DSR) equipment used in this study.

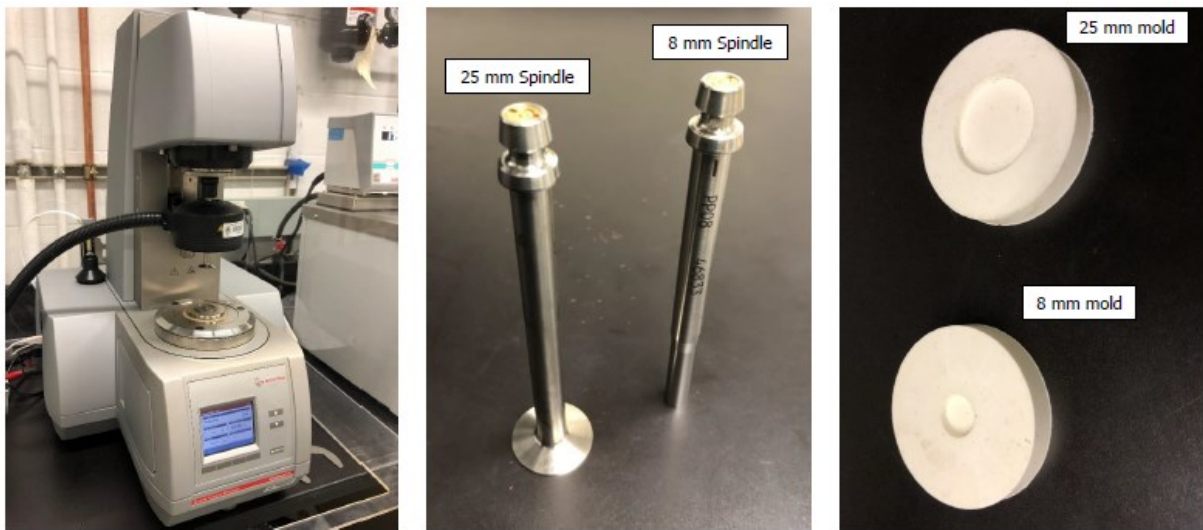


Figure 2-2 Dynamic shear rheometer (DSR) testing equipment

The dynamic mechanical analysis (DMA) of the samples are conducted by using a dynamic shear rheometer (DSR). As mentioned, strain-controlled testing is more common in DMA, where a sinusoidal strain is exerted on the specimens, and the subsequent stress is noted as a function of frequency. However, the stress-controlled DMA method in which sinusoidal stress is applied and the strain response is measured is not quite familiar as strain-controlled DMA (45). Figure 2-2 shows the sinusoidal, oscillatory, stresses, strains wave forms and dynamic test outputs.

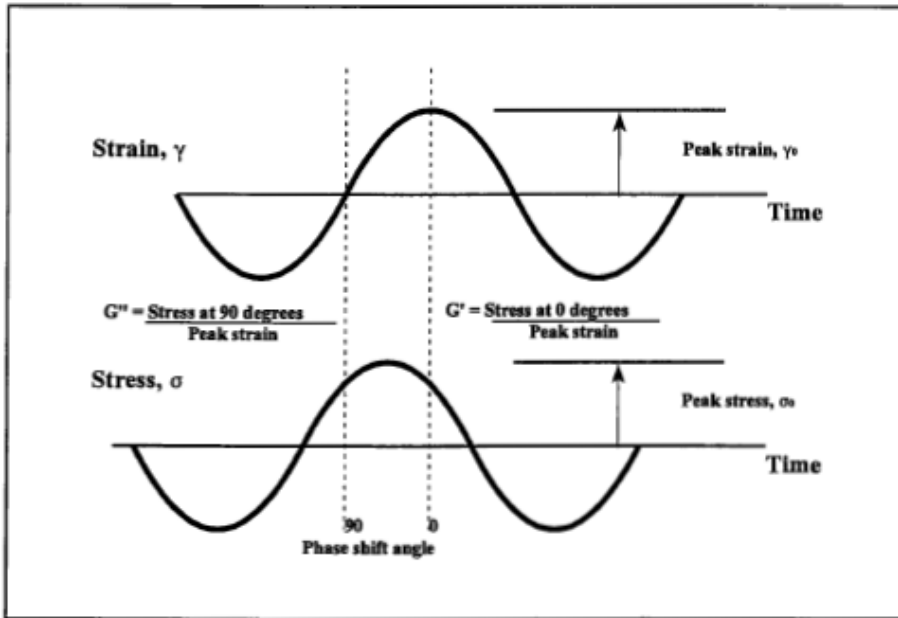


Figure 2-3: Dynamic test outputs from DMA. [Source (52)]

The primary viscoelastic components obtained from DSR are the complex shear modulus (G^*) and the phase angle (δ). The complex shear modulus is the ratio of the subsequent stress to the applied strain, and the phase difference between stress and strain is defined as phase angle. The phase angle will be zero for purely elastic material and will be 90° for purely viscous material. The complex shear modulus contains in-phase and out-phases components called storage modulus (G') and loss modulus (G''), respectively. The storage modulus is an elastic component in which the amount of energy that is stored and released elastically in each oscillation, whereas, the loss modulus is a viscous component and defines the average energy dissipation rate in the continuous steady oscillation in the dynamic test (52).

The DMA comprises the creation of master curves using interrelationship between temperature and frequency to create a continuous rheological parameter curve at a reduced frequency or time scale (55). From the study conducted by previous researchers, it has been found that there is interrelationship between temperature and frequency through which the data obtained at different temperatures can be fit into one overall continuous curve at reduced frequency or time scale. The obtained continuous curve provides the behaviour of the binder at a temperature over a large range of frequencies. The time-temperature superposition principle is used to generate a master curve by relating the equivalency between time and temperature. In overall time-temperature superposition principle is used to calculate the

rheological properties at different temperatures. It should also note that while analyzing the rheological properties of viscoelastic material through the master curve, both time dependency (as indicated by master curve) and temperature dependency (as indicated by shift factors) must be taken into consideration.

2.7 Asphalt Emulsion Mixture design

The mix design procedure includes various steps and many tests depending on the type of road and magnitude of traffic (56). In early-stage application of cold mix asphalt in pavement construction, the widely used mix design procedures were the Haveem mix design, which was used in California and Marshall mix design developed by Illinois department of transportation (15). In recent days, a basic asphalt manual from Asphalt emulsion manufacturers association is the widely used design procedure for cold mix asphalt (15).

First, the optimum moisture content for the selected aggregates are determined by preparing a specimen at different water contents using Marshall hammer or standard/modified proctor compactor. The maximum density obtained at specific water content is considered as optimum moisture content. A few researchers used Marshall stabilities of the specimen prepared using different water content to determine the optimum water content.

The amount of asphalt emulsion required for the mixture is calculated based on aggregates gradations using equations provided in ASTM D7229 (15). Using the initial asphalt emulsion content determined from the equations and with the different combinations of asphalt emulsion and water content, samples are prepared to determine the optimum emulsion content. As per the basic asphalt emulsion manual, the samples with a minimum of three different emulsion contents are prepared for at least one content above and below initial asphalt emulsion content. It should also be considered that in the coating test if the mixture appears dry, the trials mixes should be started from initial asphalt emulsion content. If the asphalt emulsion mixture seems to be rich in the coating test, reduce the content for other levels with 1% of the normal difference between the emulsion contents (15).

A study conducted by Y. Pi et al., (2019) (57) determined the optimum emulsion content by performing the Marshall stability test and by void content for the mixtures prepared at different emulsion contents. The test specimens were prepared using four different emulsion

contents and three different cement content by mass of total aggregates. The test results showed that the maximum Marshall stability was achieved at 2.9% asphalt emulsion content, also the void ratio was less than 12% at 2.9% emulsion content. By considering these two factors, for further study, 2.9% of asphalt emulsion content was considered as optimum emulsion content.

2.8 Mechanical properties of the asphalt emulsion mixture

There are various tests developed currently to evaluate the performance of asphalt mixtures to determine the capabilities of such mixtures to perform well for particularly designed traffic and climate condition. It is not possible to use a mix design of a particular project for the other project, because the best mix for one project may be the worst mix for another project (46). A detailed mix design analysis would provide the capability to understand the properties of the mixture. The two main components that influence the performance of pavement are mechanical properties and durability characteristics of the asphalt mixture.

Pavements are designed to have suitable layer thickness and materials to address particular pavement distresses such as rutting, fatigue and thermal cracking. Rutting is defined as the permanent settlement of each layer of the pavement structure under repetitive loading condition (58). Rutting is caused due to shear displacement or the densification of a loosely compacted layer (58). Rutting resistance can be assessed for asphalt mixture at the laboratory to provide an appropriate mixture design based on the climatic condition and traffic capacity. Marshall stability test, static creep test, dynamic creep test, and wheel tracking tests are the main tests perform in the laboratory to assess the quality of the asphalt mixture (59). Also, from these tests, the amount and type of additives required to modify asphalt mixture can be quantified before implementing the modified mixture at the site. Rutting can be reduced in pavement structure by introduction of suitable additives to the asphalt mixture and by preparing a stiffer mixture. However, these improvements may results in the development of fatigue cracking in pavement structure (52).

Fatigue cracking is the most common distress that occurs in pavement structure due to the deterioration of adhesive and cohesive properties as a result of repeated traffic loading and together with ultraviolet-irradiation aging (60). This type of cracking develops slowly inside

the asphalt pavement layer throughout the life span, which leads to the formation of roughness and potholes on the surface. To achieve the design life of pavement structure and to provide low maintenance, a comprehensive study is required to understand fatigue cracking. Previous studies have developed various methods to analyze the fatigue life of asphalt mixtures, shear fatigue test for asphalt mortar, indirect tensile fatigue test (ITFT), four points bending beam test (60), semi-circular testing, and indirect tensile asphalt cracking test (IDEAL-CT) (2) are the most prominent methods (2, 60). The proper analysis of cracking properties of asphalt mixture at the mix design stage can reduce the fatigue cracking.

2.9 Performance evaluation of asphalt emulsion mixture

2.9.1 Marshall Stability and Flow

Most of the agencies around the world uses Marshall stability test for mix design and as well as to evaluate the performance of the asphalt mixture (46). Marshall stability is one of the most common laboratory experiments applied to develop a suitable asphalt mixture using stability/flow and density/voids analysis. One of the major advantages of the Marshall stability test is it provides attention to the density and void properties of asphalt mixture, which ensures the proper volumetric ratios of the mixture (46). Apart from that, the Marshall stability test equipment is not expensive and it is portable; this makes it easy for remote quality control operations (46).

The Marshall stability and flow of asphalt mixtures are determined by conducting tests on compacted specimens of 100mm in diameter and 60mm in height. The test can be performed using a load-deformation recorder in conjunction with a load cell and an automatic recording device (61). Marshall stability is defined as the peak resistance load obtained during a constant rate of the deformation loading sequence, or it can also be defined as the load obtained at the time of loading increase begins to decrease. Figure 2-3 illustrates the two different types of failure to determine Marshall stability and flow. Measuring the deformation of asphalt mix determined through stability test is defined as the Marshall flow (61). It is measured as the complete deformation of the sample from the point at the extended tangent of the straight part of the curve meets the x-axis to the point that curves start to become horizontal.

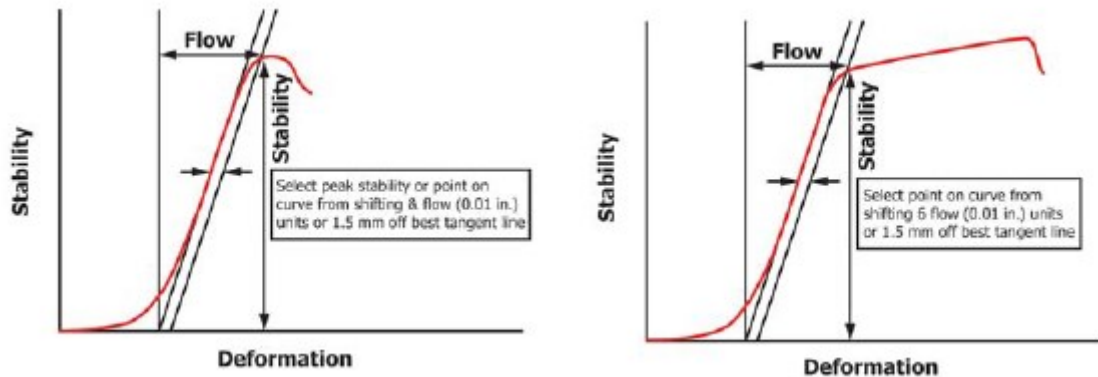


Figure 2-4: Two different type of failure to determine Marshall stability and flow (61)

2.9.2 Indirect Tensile Strength (ITS)

ITS test is used to determine the tensile strength properties of the asphalt mixture. ITS is also considered as a cost-effective test as sample preparation and sample collection from the field, testing and analyzing the data is uncomplicated (35). However, the tensile properties of the asphalt mixture are associated with the cracking properties; the higher ITS values correspond to stronger cracking resistance (35). Through the ITS test, the properties of asphalt mixtures such as tensile strength, fatigue characteristics and permanent deformation can be determined (62). The performance of the asphalt mixture to fatigue cracking is dependent on the tensile properties, as mentioned earlier due to repeated traffic load on the pavement layers which generates tensile stress and strains at the bottom of the pavement structure that lead to the fatigue failure (62). The magnitude of the strain is reliant on the stiffness of the asphalt mixture. So, the results from ITS test is considered as an indicator of strength and adherence against fatigue failure, cracking and rutting of the asphalt mixture (62).



Figure 2-5: ITS test specimen testing and specimen after testing

The tensile strength of the asphalt mixtures can be assessed using a Marshall specimen of approximately 100mm in diameter and 60mm thick by performing tests in a universal testing machine (UTM). The specimens will be subjected to loading along a diametric plane with a constant compressive load at a rate of 50mm/min acting parallel and along the vertical diametrical plane through two 13mm wide loading strips on both the directions. Figure 2-4 shows the sample testing and the sample after breaking. Through this loading arrangement, a uniform tensile stress perpendicular to the direction of the applied load will generate along with the vertical diametrical plane, which makes the specimen fail by splitting along the vertical axis. The compressive load applied to the sample will indirectly generate a tensile load along the horizontal axis of the sample (62). The peak load recorded before the failure of the sample will be used to calculate the indirect tensile strength of the specimen using Equation 2.1 given in AASHTO T 283 (63).

$$S_t = \frac{2000 P}{\pi t D} \dots\dots\dots 2.1$$

Where,

S_t = indirect tensile strength (ITS), kPa

P = maximum load, N

t = average specimen thickness, mm

D = specimen diameter, mm

2.9.3 Hamburg wheel tracking test

The Hamburg wheel tracking is the indicator of rutting resistance of asphalt mixtures, and the rutting resistance can be analyzed by running a simulative test in the laboratory equipment, the test contains small steel rolling wheel device used repeatedly rolling across an asphalt mixture specimen. The prepared specimens are of 260 x 320 x 40mm in dimensions. The steel rolling wheel of 47mm wide is used to roll across a submerged sample till the sample reaches either 20,000 cycles of rolling or until 20mm of deformation achieved (64, 65).

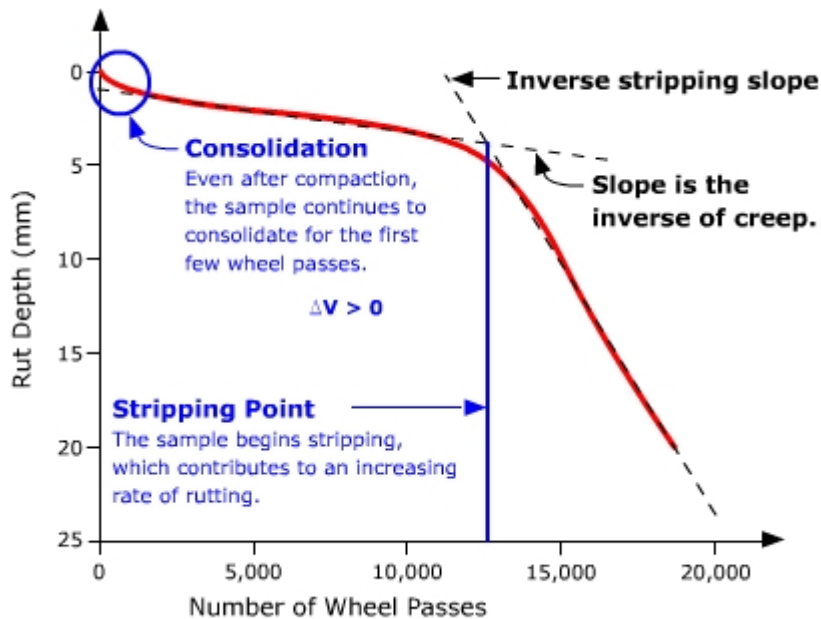


Figure 2-6: Key parameters of the wheel tracking test analysis (66)

Figure 2-5 shows the illustration of the parameters of the typical plot from the wheel tracking test. These parameters indicate the performance of the asphalt mixture. The consolidation point is considered as the rut depth achieved within the first 1,000 loading cycles due to post compaction consolidation. The creep slope is the inverse of the rutting slope after consolidation but before the stripping inflection point, where it is used to analyze rutting potential instead of rut depth. The stripping point is the point where creep slope and stripping slope-intercept, and it can be used to measure moisture damage potential of the asphalt mixture. The mixture is considered as susceptible to moisture damage if the stripping point occurs at a low number of load cycles. And at last, the stripping slope is a determination of the accumulation of moisture damage (64-66).

The data obtained from the wheel tracking test can be used to determine the rutting resistance index (RRI) of the sample using Equation 2.2.

$$RRI = \text{no. of Cycles @ end of test} \times (1 - \text{Rut Depth}) \dots\dots\dots 2.2$$

2.9.4 IDEAL-CT test

The cracking initiation and propagation are the main phases of the cracking mechanism, which directly affect the service life of the asphalt pavements (2, 67-69). Therefore, by proper assessment of cracking properties of asphalt mixture at mix design stage can minimize cracking in pavement structure (2, 69). Even though many cracking tests have been developed earlier but no single test is accepted for routine tests such as quality check and analysis, and development of mix design in the laboratory due to the complexity of testing procedures. Recently for analyzing cracking indices of the asphalt mixture indirect tensile asphalt cracking test (IDEAL-CT) is introduced. The IDEAL-CT is considered as one of the most cost and time-efficient tests due to simple, practical, and repeatable and also has been developed as a routine cracking test to be used by contractors and researchers (2, 67-69). The IDEAL-CT test uses the same principle used for indirect tensile strength test, the test runs at room temperature with a cylindrical specimen of size 100mm or 150mm in diameter and for various thickness (38, 50, 62, 75mm, etc.) with a loading rate of 50 mm/min (2, 68). Figure 2-6 shows the behaviour of specimen at different stage of load displacement curve under ITS.

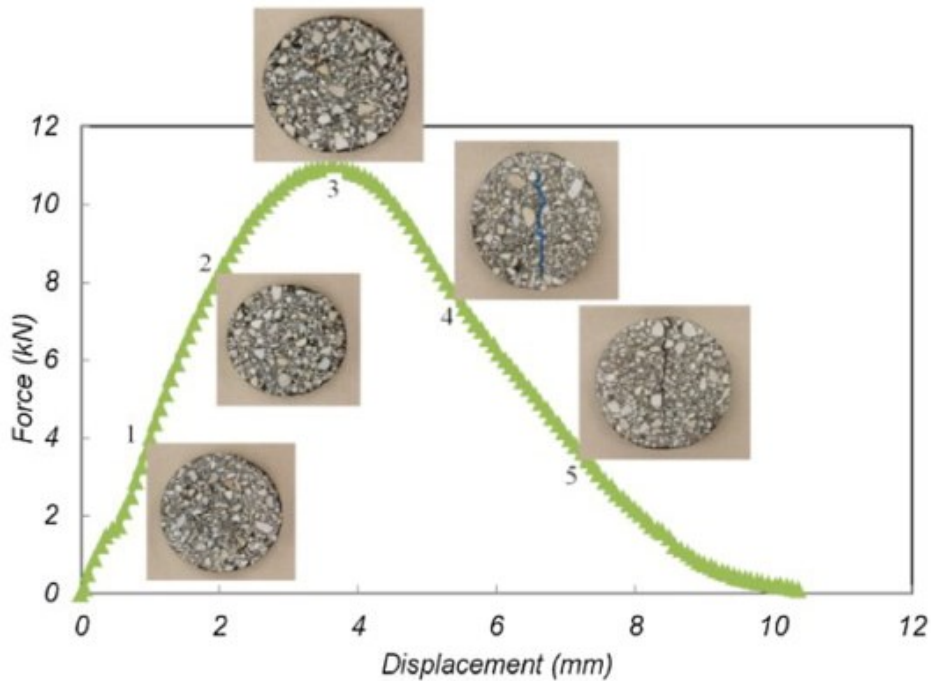


Figure 2-7 Behaviour of specimen at different stages of the load-displacement curve (68)

The cracking tolerance (CT_{Index}) of an asphalt mixture specimen is calculated with the post-peak slope of the load-displacement curve. The CT_{Index} value of the asphalt mixture depends on the aggregate gradation, air-voids and the type of additive used for the mix, the higher the CT_{Index} value, the better the cracking resistance of the asphalt mixture. With the help of fracture energy and deformation tolerance at 75% of the peak load, the CT_{Index} of the asphalt mixture can be calculated using Equation 2.3 (70).

$$CT_{Index} = \frac{t}{62} \times \frac{l_{75}}{D} \times \frac{G_f}{|m_{75}|} \times 10^6 \dots\dots\dots 2.3$$

where,

CT_{Index} = cracking tolerance index

G_f = fracture energy, joules/m²

$|m_{75}|$ = absolute value of the post-peak slope, N/m

l_{75} = displacement at 75% of post-peak slope, mm

D = specimen diameter, mm

t = thickness of specimen, mm

3 Rheological Characteristics and Fatigue Performance of Asphalt Emulsion Modified using Asphaltenes

3.1 Abstract

This study investigates the application of asphaltenes derived from Alberta oil-sands bitumen to modify asphalt emulsion for base course layer application. The asphaltenes used for modification is a waste material obtained from oil refineries that has no other valuable function in pavement industry. Cracking resistance of the asphaltenes-modified asphalt emulsion mixtures is analyzed through indirect tensile asphalt cracking tests (IDEAL-CT) performed at intermediate temperatures. Also, for the purpose of investigating the viscoelastic rheological properties of the modified samples, a dynamic shear rheometer is used to perform a frequency sweep test on residues recovered from asphalt emulsion, the asphalt emulsion residues have been recovered using a low-temperature evaporation technique. The results indicate that mixtures stabilized with asphaltenes-modified asphalt emulsion show better performance in terms of fracture energy, but the cracking tolerance index (CT_{Index}) is reduced for the modified samples. Similarly, in terms of the indirect tensile strength (ITS), the asphaltenes modified mixtures show higher values than all the other samples. Finally, dynamic mechanical analysis is conducted on asphaltenes modified samples, with the results showing that asphaltenes modification increases considerably the elastic property of the asphalt emulsion, whereas the master curve of the complex modulus shows that asphaltenes modification is associated with more stiffness behavior at low-frequency ranges.

3.2 Introduction

In recent years, increases in traffic volume and axle loads, and higher tire pressure on pavement surfaces have increased the exposure of pavement to more stresses, which in turn result in distresses such as permanent deformation (rutting), cracking, and surface wear on the pavement structure (59). Among these distresses, rutting is one of the key failure criteria for pavement deterioration (71). In recent decades, researchers have focused on finding methods to minimize rutting defects in pavement, with common methods applied, having included modifying binders with different new additives and recycled materials in combination with various trials of aggregate gradation (67, 68). These methods have resulted in a significant reduction of rutting in flexible pavements (67, 72). However, although these modifications of

pavement materials have improved rutting resistance but consequently lead to early fatigue cracking problems in the asphalt layers (67, 73). The fatigue cracking due to repeated traffic loading is one of the most significant distresses in asphalt pavements (2, 74), causing a significant decrease in serviceability (23, 74, 75). It is known that tensile strains at the bottom of the asphalt layer are the main cause of fatigue cracking (76). Fatigue cracking can be minimized through careful analysis of the cracking properties of the mixtures during the mix design stage (2, 69, 77). Many test procedures have been developed to analyze the cracking susceptibility of asphalt mixtures; however, no single test has been widely accepted as suitable for routine applications such as quality analysis and quality control, lab testing, etc. (2).

The use of asphalt emulsion has been gaining popularity in recent years in pavement construction and preservation treatment works such as slurry seals, chip seals, micro-surfacing, fog seals, and tack coats (23, 24, 75). Asphalt emulsion comprises three basic materials asphalt, water and an emulsifying agent (23); asphalt emulsions are manufactured to have a stable dispersion under storage, mixing, and pumping, where, upon contact with aggregates, it breaks down quickly and creates a layer of asphalt around the aggregate particles (24, 27). Asphalt emulsions are easy to handle at ambient temperature and are an energy-saving material, as they do not need to be heated to high temperatures for application (26). This provides safer working conditions by eliminating the toxic fumes generated from heating of asphalt binder to high temperatures (37).

The use of unmodified asphalt emulsions has been found to offer limited resistance to the stresses associated with the increasing number of heavy vehicles and increasing allowable axle loads on today's roads; this results in rapid deterioration of pavement structures prior to their designed service life (26). To enhance the performance of pavement, asphalt emulsions can be modified with polymers or other materials (9, 10, 26). A study conducted by Shafii et al. (26), for instance, showed that polymer modification of asphalt emulsion improves the physical properties, performance, and durability of base courses. Their study further indicated that the use of polymers in emulsion modification could reduce temperature susceptibility and increase rutting performance of cold mixes (26). A study performed by Babagoli et al. (9) described how an asphalt emulsion modified with cement, lime, and styrene-butadiene-styrene (SBS) polymer showed a significant improvement in Marshall quotient, dynamic creep, and rutting

performance. However, despite these achievements, the high cost, reduced penetration resistance, and higher molecular weight of polymers (10) have led researchers to continue searching for materials that can replace polymers for emulsion modification.

Asphalt cracking analysis requires a proper cracking test that not only performs well but is reliable, repeatable, sensitive to asphalt mix, and conducive to routine use in the mix design process, quality control, and quality analysis (2, 67, 68, 78). Indirect tensile strength (ITS) and semi-circular bending (SCB) tests are popular tests for evaluating the susceptibility of asphalt mixtures to cracking at intermediate temperatures (2). Despite the fact that the SCB test is simple, rapid, and reliable, though, the process of preparing SCB specimens is complicated, as it requires cutting and notching (79). Moreover, non-homogeneous characteristics of asphalt concrete can result in the top of the sample ending with a different material (aggregate or asphalt mastic) due to notching, in turn leading to changes in crack propagation (79). Furthermore, several researchers have concluded that the nominal maximum size of the aggregate increases the variance in SCB results. This is due to the fact that a specimen with a large nominal maximum aggregate size has a greater chance of having a notch in an aggregate particle (79-82). To overcome this issue, the indirect tensile asphalt cracking test (IDEAL-CT) has been introduced; this test does not require notching or cutting of the specimen, and it can be widely applied in industry due to its simplicity, practicality, efficiency, repeatability, sensitivity, and high correlation to field performance (67, 68, 73).

Similar to ITS, IDEAL-CT runs at room temperature with cylindrical specimens of 100 mm or 150 mm in diameter and various thicknesses (38, 50, 62, 75 mm, etc.) at a loading rate of 50 mm/min. The IDEAL-CT test, it should be noted, is not only simple, but it can also be performed within a duration of just one minute, and it is more repeatable due to its relatively low coefficient of variation (less than 20%) compared to other laboratory tests (68). Because of these features, IDEAL-CT is the ideal cracking test for contractors and researchers alike for routine tests (68). The value of the cracking tolerance index (CT_{Index}) in the IDEAL-CT test is the performance indicator parameter of asphalt binders and modifiers and aggregate blends in asphalt mixtures, where a higher CT_{Index} value of an asphalt material is indicative of better cracking resistance performance (70). Dong and Charmot (83) conducted a study to analyze the CT_{Index} of cold recycling mixtures prepared using asphalt emulsion and portland cement at

various proportions. In their study, it was observed that cold recycling mixtures with low emulsion and high cement content express quasi-brittle behavior, whereas mixtures with high emulsion content and a low amount of cement are indicative of compliant behavior (83). This suggests that adding more emulsion and reducing cement content increases the cracking resistance of cold recycling mixture (83).

The rheological properties of asphaltic material are also important, as they are a key determinant of the extent of a particular distress in an asphalt mixture. The rheological characteristics of an asphalt binder at high, intermediate, and low temperatures can be investigated through performance grading testing of the asphalt binder (84). For characterization of the flow characteristics of asphalt binders, researchers have developed a master curve that shifts the stiffness of the asphalt binder measured at various temperature to the individual stiffness curve along the time axis in order to obtain a stiffness curve at reference temperature (84). Similarly, the relationship between binder stiffness and reduced frequency over a series of temperatures and frequencies can also be obtained by plotting the master curve of the asphalt binder (84).

Asphaltenes are large hydrocarbon molecules found in a lower amount in light crude oil and in a higher amount in heavier crude oil. Asphaltenes are rich in heteroatom content such as sulphur, oxygen, and nitrogen, and they also have a high metal content (e.g., nickel and vanadium) (29). Asphaltenes are most commonly available in petroleum products and in heavy oil from oil sand deposits (85). Asphaltenes can be obtained in the form of waste material as a by-product of the deasphaltation process with negligible value in pavement construction in current practice. The polar fractions in asphalt binder, such as asphaltenes and resins, are responsible for the elastic behavior of the asphalt binder, where saturates and aromatics are partially responsible for the viscous behavior of the asphalt binder (12, 86). Previous studies have shown that application of asphaltenes material for modification of asphalt emulsion to improve the low- and high-temperature performance has been limited.

3.3 Objective and Scope

The objective of this study is to perform IDEAL-CT analysis to determine the cracking indices of asphalt emulsion-stabilized mixtures modified with asphaltenes using load-displacement

curves of the ITS tests at intermediate temperatures. A cationic slow setting (CSS-1H) asphalt emulsion was used in this study for modification with waste asphaltenes derived from Athabasca oil sands. The asphalt emulsion was modified using different amounts of asphaltenes. The asphalt emulsion residue was recovered using a low-temperature evaporation technique. The viscoelastic properties of the modified asphalt emulsions were analyzed by performing frequency sweep tests at temperatures ranging from 4 °C to 40 °C and within a frequency range of 0.1 rad/s to 100 rad/s.

3.4 Materials

3.4.1 Aggregates

A well-graded aggregate gradation with 57.27% coarse aggregates, 36.73% fine aggregates, and 6% filler was used for this study. This aggregate gradation was selected based on the limitations provided in the Wirtgen cold recycling manual (56), City of Edmonton standards (87), and Alberta Transportation specifications (88). The bulk specific gravity of the aggregate, as per AASHTO T 85 (89), was determined to be 2.601. The optimum moisture content (OMC) of the aggregate, meanwhile, was determined, by means of the proctor test and in accordance with ASTM D698 (90) to be 6.3%. The aggregate gradation employed in preparing the mixtures is presented in Table 3.1, while the physical properties of the aggregates are given in Table 3.2.

Table 3-1: Aggregate gradation

Sieve size (mm)	Percentage Passing	Percentage Retained
20.000	100.00	0.00
12.500	75.17	24.83
10.000	61.23	13.94
8.000	55.00	6.23
6.300	48.00	7.00
5.000	42.73	5.27
2.500	32.08	10.65
1.250	25.61	6.47
0.630	18.93	6.68
0.315	13.00	5.93
0.160	9.00	4.00
0.080	6.00	3.00
Filler (Pan)	0.00	6.00

Table 3-2: Physical properties of the aggregates

Properties	Standard	Result
Specific gravity of coarse aggregates (Gca)	ASTM C127	2.598
Water absorption of coarse aggregates in %		0.870
Specific gravity of fine aggregates (Gfa)	ASTM C128	2.604
Water absorption of fine aggregates in %		0.624
Abrasion value of coarse aggregates in %	ASTM C131	23.000
Optimum moisture content (OMC) in %	ASTM D698 (90)	6.300
Maximum dry density in kN/m ³		15.400

3.4.2 Cationic slow-setting asphalt emulsion

The asphalt emulsion used in this research was a cationic slow-setting asphalt emulsion (CSS-1H) consisting of 61% asphalt and 39% water. According to the data sheet provided by the material supplier, the asphalt emulsion had a density of 1.020 kg/L, a viscosity at 25 °C of 22 S.F.S, and a penetration of residue at 25 °C of 95 dmm (91).

3.4.3 Asphaltenes

The asphaltenes used for the asphalt emulsion modification in this study were obtained from Athabasca oil-sands bitumen from Alberta, Canada. The waste asphaltenes were obtained in solid form. Asphaltenes, are macro-polar structures obtained in solution within the oil matrix. The asphaltenes used in this study had been extracted in industry through deasphaltation process by adding the required amount of non-polar solvent to the oil matrix, a method which disrupts the solubility of the asphaltenes and forces them out of the solution. To ensure adequate dispersion of asphaltenes during asphalt emulsion modification, the asphaltenes obtained in solid form were crushed into powder and sieved through a no. 100 sieve. Figure 3.1 shows chunk asphaltenes and powdered asphaltenes after crushing and sieving through a no. 100 sieve.



Figure 3-1 Asphaltenes, solid asphaltenes (left), powdered asphaltenes (right)

3.4.4 SARA test on Asphaltenes

To determine the purity of the asphaltenes used in this study, the percentage of SARA components (saturates, aromatic, resin, and asphaltenes) were determined through a SARA test in accordance with ASTM D6560 (92) and ASTM D2007 (93). The SARA test results are presented in Table 3.3. From the results it can be seen that almost 80% of the material was asphaltenes.

Table 3-3 SARA components of asphaltenes

Material	Saturate (%)	Aromatic (%)	Resin (%)	Asphaltenes (%)
Asphaltenes	6.85	9.68	3.84	79.62

3.5 Methodology

3.5.1 Optimum asphalt emulsion content

Based on the data sheet provided by material supplier (91), the amount of asphalt emulsion residue after distillation was determined to be 61%. Using a well-graded aggregate gradation as per the specifications given by the Asphalt Institute, the asphalt emulsion content to be used for this study was calculated using **Equation 3.1**.

$$\text{Base mixture: Asphalt emulsion \%} = \frac{(0.06B+0.01C)100}{A} \dots\dots\dots 3.1$$

where

A = Amount of the residue of asphalt emulsion remaining after distillation (%)

B = Amount of dry aggregates passing through No. 4 sieve (%)

C = Amount of dry aggregates retained on No. 4 sieve (%)

Using Equation 3.1, the asphalt emulsion content was determined to be 4.89% of the total mixture. Using this as the base asphalt emulsion content and considering the OMC of aggregates as listed in Table 3.2, Marshall and ITS samples were prepared along with different contents of asphalt emulsion at different intervals to determine the optimum emulsion content.

Marshall and ITS samples were prepared by mixing oven-dried aggregates and water until mixed uniformly. After asphalt emulsion had been added to the mix, the mixture was compacted using a Marshall hammer with 50 blows on each side of the sample. The compacted samples were cured in molds in an oven for 48 hours at 60 °C. Three specimens were prepared for each of the asphalt emulsion content.

After curing, the samples were ejected from the molds and tested for Marshall stability and ITS. Marshall stability and ITS tests were performed in accordance to ASTM D6927-15 (61) and AASHTO T283 (63), respectively. The prepared samples were conditioned before conducting the tests. For the Marshall stability test, samples were conditioned for at least 2 hours in a 25 °C air bath, whereas, for the ITS test, the samples were conditioned for 3 hours at 25 °C air bath. To calculate the tensile strength of the samples, the test was conducted by applying load at a rate of 50 mm/min; using the recorded maximum load applied on samples before reaching failure point, the tensile strength of the samples was calculated using **Equation 3.2**.

$$S_t = \frac{2000P}{\pi tD} \dots\dots\dots 3.2$$

where

St = Indirect tensile strength, kPa

P = Maximum applied load, N

t = Average height of specimen, mm

D = Diameter of specimen, mm

3.5.2 Asphalt emulsion modification using asphaltenes

Asphaltenes were mixed manually with the asphalt emulsion for modification. Various proportions of asphaltenes were mixed at 54.37%, 26.95%, 13.475%, and 5.39% by weight of emulsion, equivalent to 2%, 1%, 0.5% and 0.2% by weight of the total mixture, respectively. Asphaltenes content was calculated by performing Marshall stability and ITS tests on the modified mixture at different proportions. The modification was carried out by adding asphalt emulsion and asphaltenes into a measuring glass and mixed manually using a spatula. The mixing process was continued for about 60 seconds (until the asphaltenes were dispersed thoroughly in the emulsion). It was observed that the breaking point of the 1% modified sample was at 7 hours to 8 hours. During the modification process, mixing the 2% modified sample was found to be difficult, as adding more asphaltenes causes the breaking of the asphalt emulsion to occur very rapidly. To overcome this difficulty and ease the modification process, an additional 25% of water was added to the sample (based on the assumption that the additional water would evaporate during the residue recovery procedure).

3.5.3 Penetration grading test

In order to check the penetration grading of the modified samples, a penetration test was conducted on the recovered residue of the asphaltenes-modified samples and unmodified samples as per ASTM D5 (94). The test was performed at a temperature of 25 °C, applying a weight of 100 g to the needle and allowing the needle to penetrate for a duration of 5 seconds.

3.5.4 Residue recovery of asphalt emulsion

At present, a number of different residue recovery methods are in use by researchers, some of them outlined in the ASTM and AASHTO standards (37). Among these methods, the majority require exposure of the asphalt emulsion to a high temperature, a practice which affects the rheological properties of the recovered binder. Moreover, high-temperature techniques do not simulate actual field curing conditions, where the asphalt emulsion would be exposed to ambient temperatures (38). In this regard, previous studies have concluded that using exposure to high temperatures as the recovery technique alters the microscopic structure of the emulsion significantly (40). To avoid such issues with the residue recovery, this study used a simple low-temperature evaporation technique to recover the residue in order to maintain the asphalt

emulsion's rheological properties. The residue recovery method "low-temperature evaporation technique", described in AASHTO PP 72-11 Procedure A (95), was used in this research. This technique involves pouring the modified and unmodified asphalt emulsions into a silicon mat at a spread rate of 1.5 to 2.0 kg/m². To recover the residue, the prepared samples were dried in a forced draft oven at 25 °C for 24 hours, then cured at 60 °C for another 24 hours. After 48 hours of oven drying, the samples were allowed to cool at room temperature for 1 hours. After cooling, the recovered residue would be carefully peeled out from the silicon mat using a round-edged steel rod and stored in a container for further testing.

3.5.5 ITS and IDEAL-CT analysis

The IDEAL-CT results for the asphaltenes-modified and unmodified mixtures were analyzed as per ASTM D8225-19 (70). The CT_{Index} was determined by computing the area under load displacement curve, and calculating the work of failure, fracture energy, and other required parameters using the load displacement curve from the ITS results. Figure 4 illustrates the post-peak slope and load line displacement of the curve.

The ITS test was performed in accordance with AASHTO T283 (63). The test specimens were prepared for asphalt emulsion modified with 0.2%, 1% and 2% asphaltenes content. Before mixing, the aggregates required for each specimen were oven dried in order to remove any moisture in the aggregates. ITS specimens with 100 mm diameter were prepared by mixing oven dried aggregates, water and asphaltenes-modified asphalt emulsion in an asphalt mixer. Prepared mixtures were poured into molds and compacted with 50 blows on each side using Marshall compactor. For testing, three specimens were prepared for each of the samples of different asphaltenes content thresholds and the control sample without asphaltenes. The compacted specimens were cured in an oven for 48 hours at 60 °C. The samples were extracted from the molds after being allowed to cool down at room temperature. Before performing the test, it should be noted, the samples were conditioned in an air chamber at 25 °C for 3 hours. Testing was conducted using a universal testing machine (UTM) applying a load at a rate of 50 mm/min.

The analysis was conducted by calculating the required parameters work of failure, fracture energy, post-peak load and displacement at 85% (P_{85} , l_{85}), 75% (P_{75} , l_{75}), 65% (P_{65} , l_{65}), post-

peak slope by following the procedure mentioned in ASTM D8225-19 (70). (An illustration of post-peak slope and load line displacement of the curve is shown in Figure 3.2.) Using these parameters, the CT_{Index} of the modified and unmodified mixtures were calculated using Equation 3.3.

$$CT_{Index} = \frac{t}{62} \times \frac{L_{75}}{D} \times \frac{G_f}{|m_{75}|} \times 10^6 \dots\dots\dots 3.3$$

where

CT_{Index} = Cracking tolerance index

G_f = Failure energy (Joules/m²)

$|m_{75}|$ = Absolute value of the post-peak slope m_{75} (N/m)

L_{75} = Displacement at 75% post-peak load (mm)

D = Specimen diameter (mm)

t = Specimen thickness (mm)

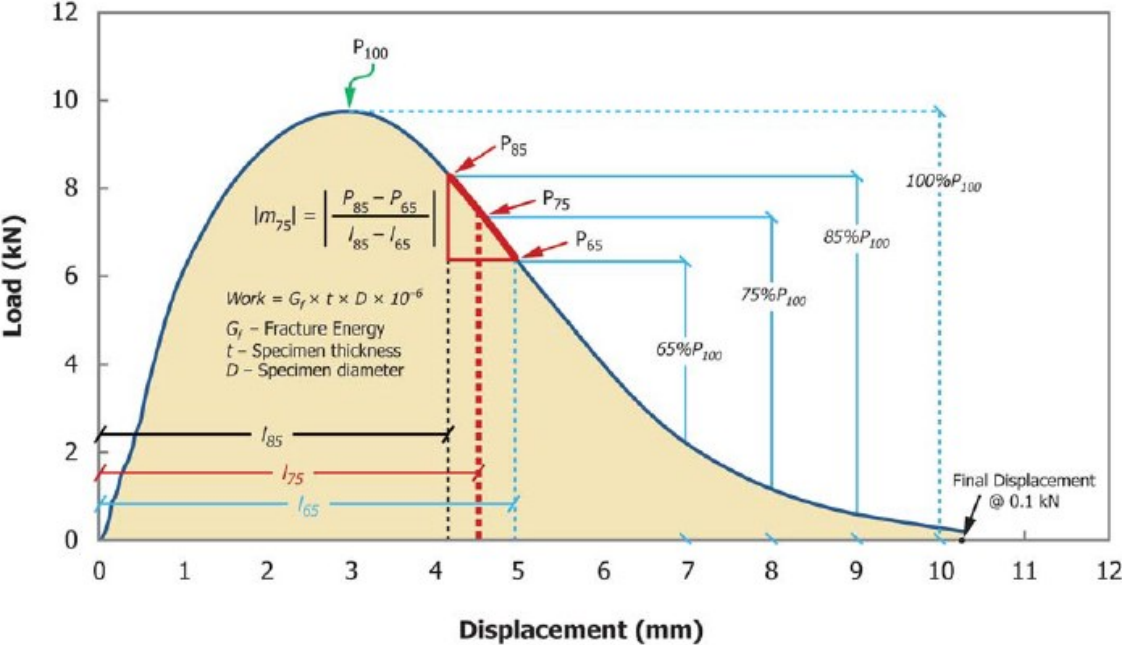


Figure 3-2 Illustration of post-peak slope and load line displacement of the curve (70).

3.5.6 Dynamic mechanical analysis

The rheological performance of the residues from the control samples and asphaltene-modified samples at percentages of 0.2%, 0.5%, 1% and 2% was ascertained by conducting a

frequency sweep test at various temperatures and loading frequencies. The frequency sweep test was performed using a dynamic shear rheometer (DSR) with 8 mm diameter plates and a gap of 2 mm. The test samples were prepared by oven-heating the asphalt emulsion residue at 135 °C until sufficiently fluid to pour inside molds; the residue was then poured into a silicon mold of 8 mm diameter. Tests were performed at temperatures loop of 4 °C, 10 °C, 20 °C, 25 °C, 30 °C, and 40 °C with an angular frequency range of 0.1 to 100 rad/s. Three tests were performed for each of the samples. The time-temperature superposition (TTS) principle and Williams-Landel-Ferry (WLF) regression analysis were applied using RheoCompass software in order to plot the master curves for the complex modulus and phase angle at 25 °C over a wider range of frequencies.

3.6 Results and Discussion

3.6.1 Optimum asphalt emulsion content

Figure 3.3 presents the results of the ITS and Marshall stability tests and Figure 3.4 presents density of the mixtures that were applied in order to determine the optimum emulsion content. From these results it can be seen that the ITS samples showed better performance overall for the samples prepared with 3.7% emulsion. However, considering the trend of the Marshall stability and density results, it was observed that the maximum stability was achieved at 3.7% asphalt emulsion content. Based on the results of the Marshall stability and ITS tests, it was decided that a 3.7% asphalt emulsion by weight of total mix should be used for further tests.

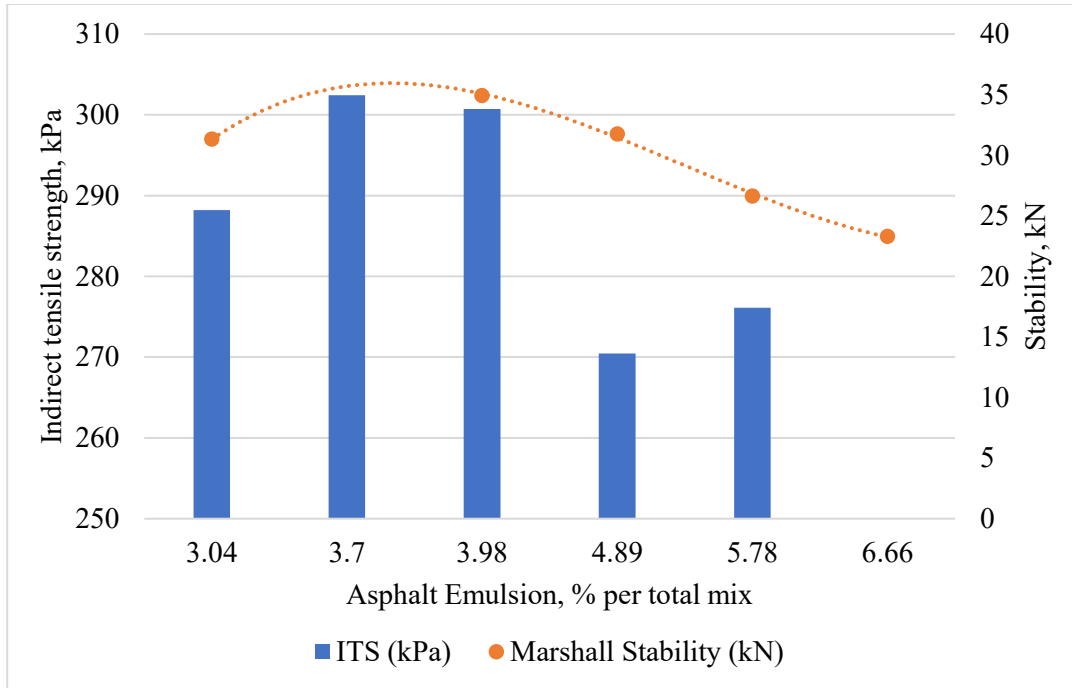


Figure 3-3 ITS and Marshall stability test results used to determine optimum emulsion content

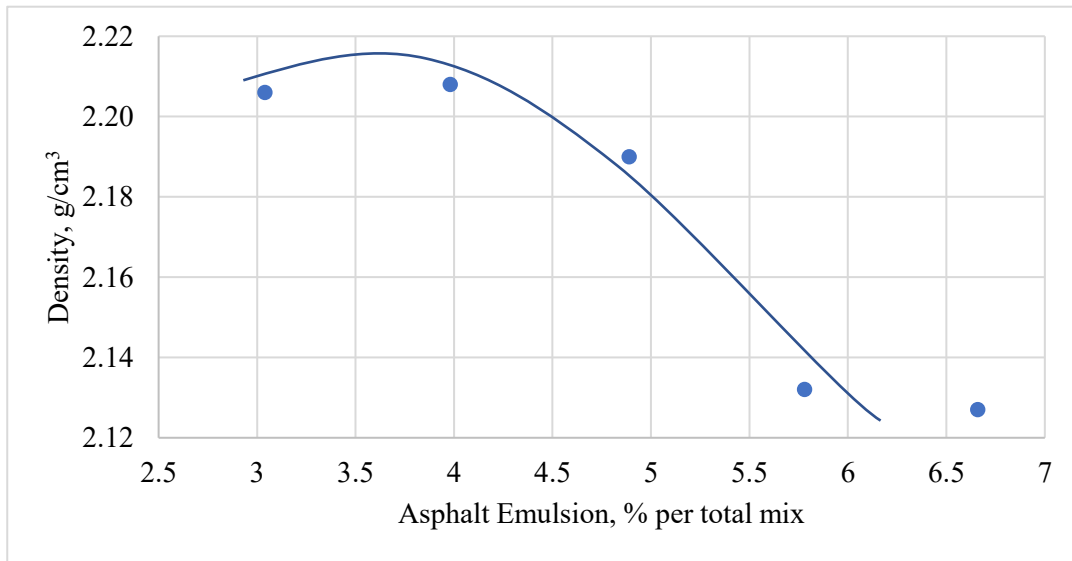


Figure 3-4 Density results used to determine optimum emulsion content

3.6.2 Penetration grading

Table 3.4 shows the penetration grading result for the control sample without asphaltenes and modified samples with asphaltenes. From the results it was observed that the 0.2% asphaltenes-modified asphalt emulsion had a higher penetration grade 60/70 compared to the other modified samples. This indicates that adding more asphaltenes for modification makes

the residue stiffer. However, the 0.2% modified sample was found to be within the range of specified minimum penetration grading of 40/50. (Asphalt emulsion with a penetration grade of 60/70 is the most common type of emulsion used in the market.)

Table 3-4 Penetration grading test results

Sample Type	Penetration at 25 °C, (100 g weight, 5 s duration) in 1/10 mm	Specification (37)	
		Min.	Max.
Control sample (unmodified sample without asphaltenes)	95	40	125
0.2% Asphaltenes-modified asphalt emulsion	62	40	125
0.5% Asphaltenes-modified asphalt emulsion	21	40	125
1% Asphaltenes-modified asphalt emulsion	10	40	125
2% Asphaltenes-modified asphalt emulsion	2	40	125

3.6.3 ITS and IDEAL-CT analysis

Table 3.5 present the values for the ITS and fracture energy of control and asphaltenes-modified samples; from these results, the 2% asphaltenes modified sample with 25% additional water was found to have higher fracture energy and tensile strength as compared to control sample and other modified samples. This indicates that the sample is more resistant to cracking than the control sample and the 0.2% asphaltenes-modified sample. It was also observed that the 2% asphaltenes-modified sample exhibited better performance in terms of tensile strength compared to the other samples. Figure 3.5 represents the load-displacement curves of the control and asphaltenes-modified samples used to calculate the CT_{Index} . It can be seen that the sample with 2% asphaltenes content and 25% additional water failed at a load almost three times greater than the failure load of the control sample. Moreover, both of the 2% modified samples failed at a higher load compared to the control sample and 0.2% and 1% asphaltenes-modified samples. This shows that asphaltenes modification significantly improves the load capacity of the mixture.

Table 3-5 ITS and failure energy values of control and modified samples

	Control Sample	0.2% Asphaltenes	1% Asphaltenes	2% Asphaltenes with 25% extra water
Fracture Energy (J/m ²)	984.56	1,416.26	1,819.38	2,314.26
ITS, kPa	302.45	438.3	636.59	824.75

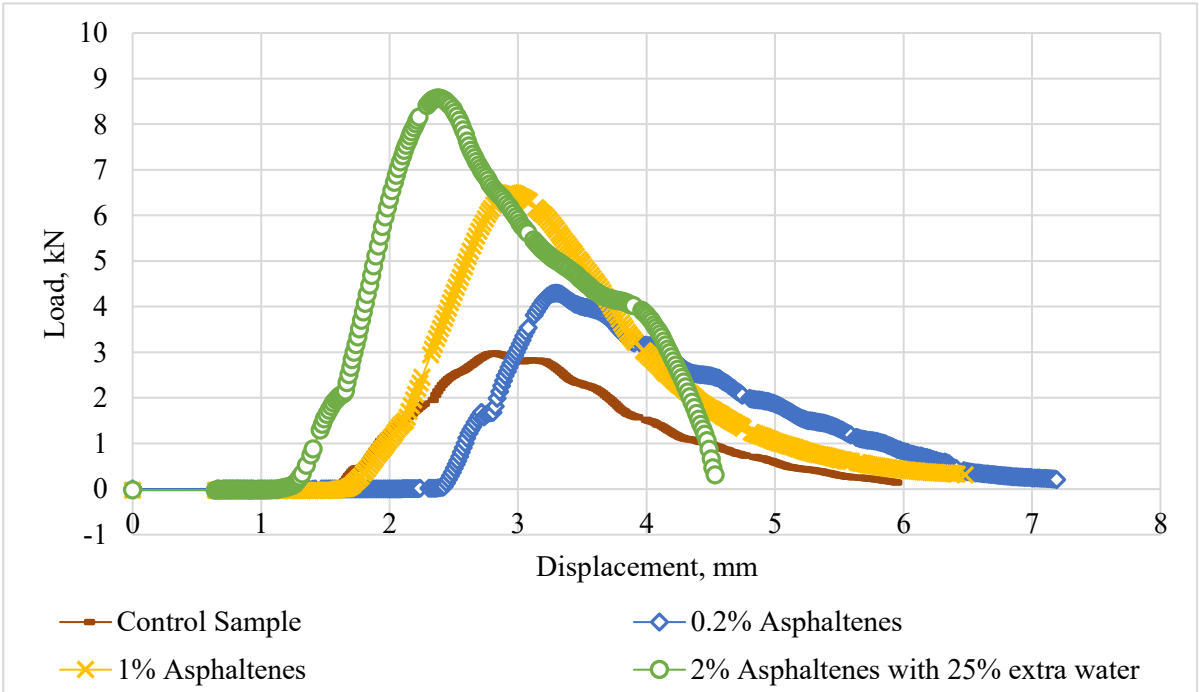


Figure 3-5 Load-displacement relationships

Figure 3.6 shows the CT_{Index} and percentage improvement in ITS of the control and asphaltenes modified samples. From the results it can be seen that the samples modified with 1% and 2% asphaltenes content with an additional 25% of water exhibited minimal reduction in CT_{Index} compared to the control sample; however, the 0.2% asphaltenes-modified sample exhibited better cracking resistance than the control and the other modified samples. This could be attributed to the fact that the asphaltenes-modified samples were brittle compared to the control samples. As seen in Figure 3.5, the control sample has a uniform load-displacement chart, whereby the modified samples have sharp initial and post-peak slopes, resulting in a lower CT_{Index} value for the modified sample compared to the control sample.

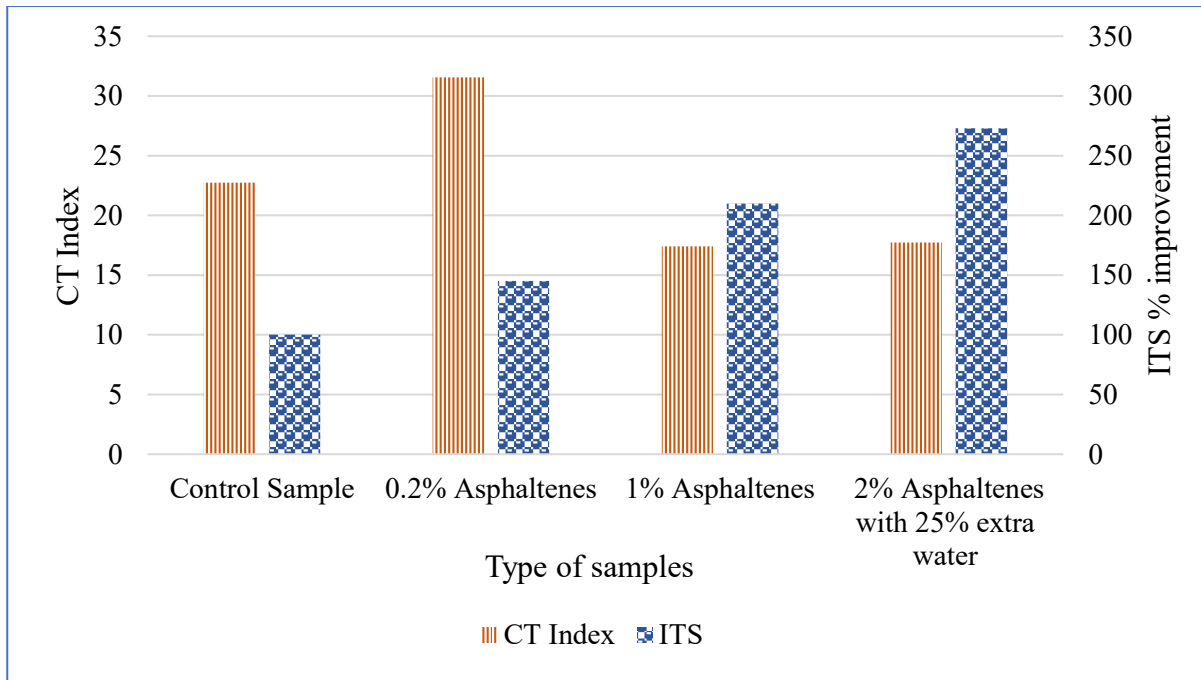


Figure 3-6 CT_{Index} and percentage improvement of ITS for control sample and modified mixtures

3.6.4 Dynamic mechanical analysis

The complex modulus and phase angle for the control and asphaltenes-modified samples were evaluated by means of rheological master curves using frequency sweep test data. Figure 3.7 presents the master curve for the phase angle at 25 °C; as can be observed in the figure, the phase angle master curves for the asphaltenes modified samples shows a reduction in phase angle at both low and high ranges of frequency compared to that of the control sample. The trend from the graph suggests that an increase in asphaltenes content decreases the phase angle values of the samples. Also, the modified samples show similar trends to the control sample over a wide range of frequencies. However, from the chart it can also be seen that the control sample has a phase angle of approximately 70° at the angular frequency of 1 Hz, whereas the 0.2%, 0.5%, 1%, and 2% modified samples have phase angles of approximately 65°, 55°, 45°, and 30°, respectively. Overall, it can be concluded that adding asphaltenes for modification at greater proportions reduces the viscous behavior of the asphaltenes-modified samples.

Figure 3.8 illustrates the master curve of the complex modulus at 25 °C over a range of frequencies. As can be seen, the trends with respect to complex modulus for the asphaltenes-modified samples show a significant improvement at lower frequencies and a very minimal

change at higher frequencies. Similar to with the phase angle master curve, the asphaltenes-modified samples show similar trends to the control sample. From the graph it can be observed that the complex shear modulus of the control sample and the 0.2% modified sample at an angular frequency of 1 Hz are within the range of 1×10^5 Pa to 1×10^6 Pa; meanwhile, the complex shear modulus values of the 0.5%, 1% and 2% modified samples fall within the range of 1×10^6 Pa to 1×10^7 Pa at 1 Hz angular frequency. This indicates a stiffening effect and an increase in temperature susceptibility of the asphaltenes-modified samples corresponding to an increase in asphaltenes content.

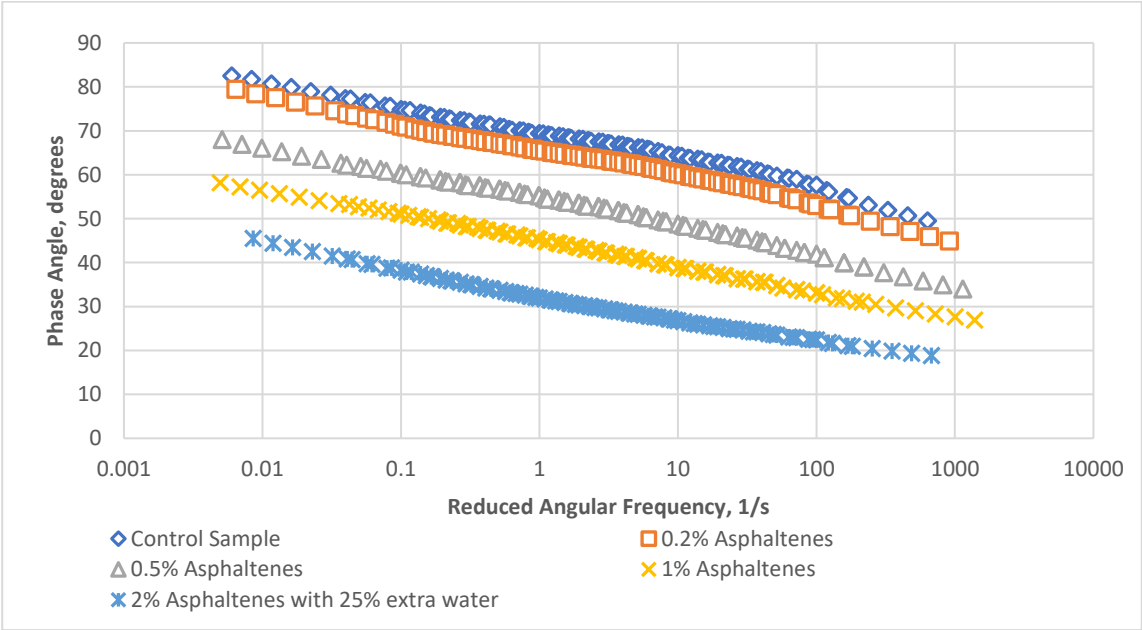


Figure 3-7 Master curve of phase shift angle at 25 °C for control sample and modified sample

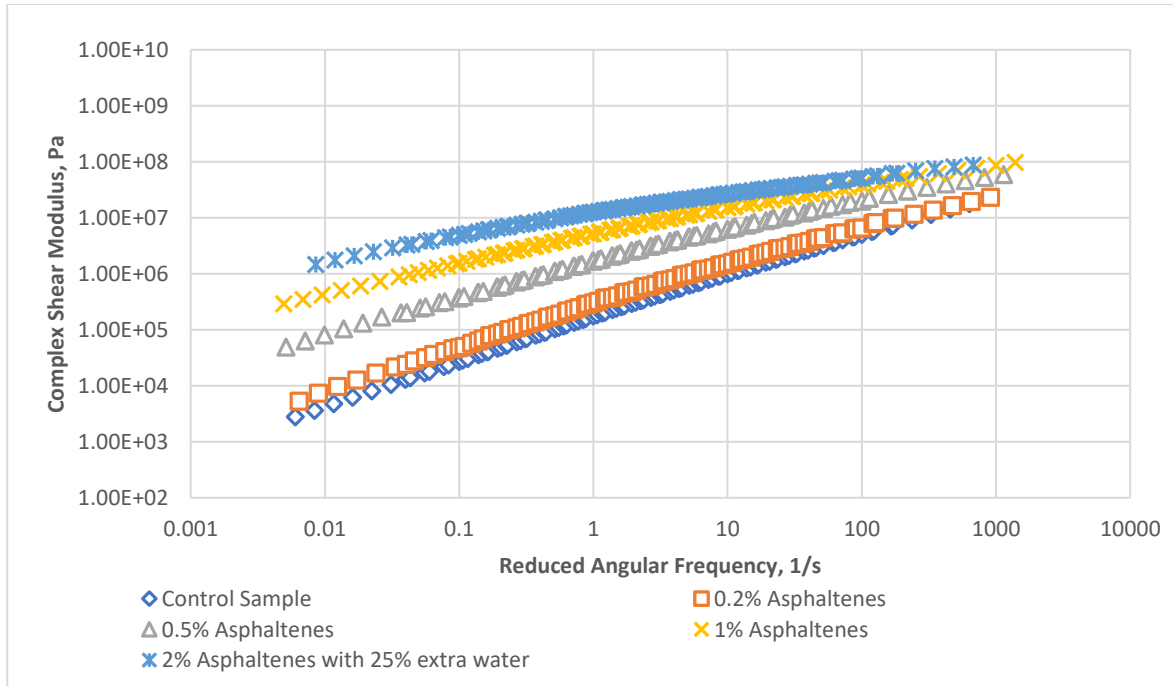


Figure 3-8 Master curve of complex shear modulus at 25 °C for control sample and modified samples

3.7 Conclusions

Based on the experimental results and analysis performed on the asphaltenes-modified asphalt emulsion, the following conclusions have been drawn.

- Higher performance values of ITS test observed for asphaltenes-modified samples confirmed a significant increase for tensile strength and fracture energy of mixtures compared to the control samples. It was observed that the sample modified with 2% asphaltenes have the highest tensile strength which is almost three times greater than the control sample, also the same asphaltenes content was found to have the highest fracture energy almost twice of the control sample.
- Penetration grading results showed that the addition of asphaltenes will significantly change the penetration grade of the asphalt residue. To keep the asphalt residue in the specification recommended range, the added asphaltenes amount should be limited to 0.2%.
- From IDEAL-CT result analysis, it can be concluded that 0.2% asphaltenes-modified sample has higher performance in terms of cracking resistance compared to the control and other asphaltenes-modified samples. Also, it was observed that there is a slight decrease in

terms of CT_{Index} for the 1% and 2% asphaltenes-modified samples compared to control sample despite improvements in tensile strength and fracture energy. Hence, it can be concluded that the addition of higher amounts of asphaltenes to the mixture improves the tensile strength but, consequently, decreases the cracking resistance.

- The dynamic mechanical analysis indicated that increasing asphaltenes content for modification decreases the phase angle at both low and high-frequency ranges, which indicates less viscous behavior of the modified samples compared to control sample. From the complex shear modulus master curve analysis, it was observed that asphaltenes-modified samples exhibit higher complex modulus at the lower frequency ranges compared to the control sample, but this change for higher frequency ranges was less. This behavior indicates that asphaltenes-modified samples could be less prone to rutting compared to unmodified samples.

4 Permanent Deformation of Stabilized Asphalt Emulsion Modified using Asphaltenes

4.1 Abstract

Asphalt emulsion is one of the most common materials used in the pavement industry for surface treatment and other applications such as stabilization of pavement base course. Because asphalt emulsions do not require heating at high temperatures for these applications, this feature makes it environmentally friendly due to energy savings and provide safer working conditions by eliminating dangerous toxic fumes. This study investigates the application of using asphaltenes derived from Alberta oil sands to modify asphalt emulsion for base course layer application. Asphaltenes is a waste material of insignificant value with no notable applications in the pavement industry. The amount of asphaltenes to be added for asphalt emulsion modification is determined in the present study through the Marshall stability test, indirect tensile strength test, and wheel tracking test. Asphaltenes from two different sources are used for the asphalt emulsion modification. The modified asphalt emulsion is cured using a low-temperature evaporation technique to recover the asphalt residue. The rheological properties of recovered residue from modified asphalt emulsions are evaluated at high temperatures using a dynamic shear rheometer (DSR). The results indicate that the asphaltenes from both sources significantly increase the Marshall stability and indirect tensile strength of the mixes. The rutting resistance of the modified mixes from the wheel tracking test is found to improve significantly by increasing the number of passes by more than 200% compared to the control sample. Furthermore, the modified asphalt emulsion residues show an improvement in rheological properties at high temperatures.

4.2 Introduction

Due to their lower application temperature, lower energy consumption, and lower viscosity, asphalt emulsions have gained popularity around the world, primarily for application in pavement surface treatments (24). Asphalt emulsion is a combination of asphalt droplets dispersed in water using a chemical emulsifier (27). The preparation of these emulsions is a complex task since the type and amount of emulsifier and shearing force used in the dispersion of the mixture greatly affect the stability of the emulsion and influence its properties (24). Asphalt emulsion is one of the most commonly used materials for pavement surface treatment such as chip seal, slurry seal, and micro-surfacing. Asphalt emulsion is also

used in asphalt recycling, and in other applications such as stabilizing base courses using cold mixing procedure (26). Moreover, the asphalt emulsion does not need to be heated at a high temperature for these applications; this feature contributes to energy savings and provides safer working conditions by eliminating toxic fumes, and has contributed to its reputation as a green technology for road construction (37).

Currently due to increase in volume of using heavy vehicles with increasing their allowable axle weights have resulted in a significant increase in the stresses exerted on pavement surfaces. This, in turn, results in premature deterioration and distresses of the pavement surface before reaching their intended design service life (26). Consequently, modification of asphalt emulsion using different materials such as polymers has emerged as a promising alternative for improving the service life of asphalt emulsion pavement layers (26). Recently, polymer modification of asphalt emulsion has increasingly been employed to achieve higher performance in asphalt emulsion layers. Polymer-modified asphalt emulsion exhibits improvements in performance, durability, and reduced life cycle cost compared to unmodified asphalt emulsion (26). Due to these benefits, the use of polymer-modified asphalt emulsion in pavement construction has been found to increase the service life of the pavement despite increase in traffic volume and axle loads.

A research study conducted using asphalt emulsion (CSS-1) modified with SBS polymer, lime and cement showed an increase in Marshall Quotient and dynamic creep for the modified samples. Also, rutting test results showed a decrease in permanent deformation for the modified mixtures (9), while a study conducted by Shafii et al. (26) showed that polymer modification of asphalt emulsion improves the physical properties, performance, and durability of base courses. Their study further indicated that the use of polymers in emulsion modification could increase the temperature susceptibility and rutting performance of cold mix asphalt (26). Along with these advantages of polymer modification of asphalt emulsions, some specific drawbacks with its applications have been noted, such as its high cost, reduced penetration resistance, and higher molecular weight (10). As a result of these drawbacks, researchers continue to work on finding a replacement for polymers in emulsion modification. In this context, the use of asphalt by-products is a promising alternative to polymers, since higher flexibility is required (96).

Asphaltenes are large hydrocarbon molecules found in a lower concentration in light crude oil, but found in higher quantities in heavier crude oil (97). Asphaltenes are present in most petroleum products, and in all heavy oils from oil sands deposits (29). Asphaltenes are defined by their solubility, specifically that of the components that are soluble in aromatic solvents but insoluble in straight-chain solvents such as pentane or heptane (97). They are the lowest-value fraction of asphalt, with a very complex mixture. Asphaltenes are rich in heteroatom elements such as sulphur, oxygen, and nitrogen, and they also have high content of metals such as nickel and vanadium (29).

According to their polarity, asphalt binders are classified in terms of chemical composition as saturates, aromatics, resins, and asphaltenes, a categorization often abbreviated as “SARA” (98, 99). The polarity of asphalt binder materials and their interactions play a significant role in determining the rheological properties of the asphalt binder (100). The polar fractions of the asphalt binder, including asphaltenes and resins, are the components that give it its elastic behavior, while the non-polar components, including saturates and aromatics, are responsible for its viscous behavior (12, 86)

A recent study conducted by Sultana et al. (12) investigated the indirect tensile strength (ITS) of asphalt binders by increasing the polar fractions (asphaltenes or resins). The results indicated that augmented asphaltene content improves the binder’s tensile strength. From this finding they concluded that the presence of more polar fractions in the binder will not only increase the stiffness, but also improves its tensile strength (12).

The performance of a pavement structure depends on the stability of the underlying layers, and these layers are constructed on the assumption that each layer has the minimum defined structural quality to withstand and distribute the superimposed loads (101). Base stabilization is termed as a permanent improvement of the base layer that results in significant development of elastic and strength characteristics (102). A laboratory mix design is necessary to analyze the type and quantity of additives that will allow the mixture to meet the performance requirements in terms of strength, elasticity and durability, where the performance testing is governed by the stabilization technique employed and the additives used (102).

For the purpose of studying the rheological characteristics of asphalt emulsion, the asphalt emulsion residue must first be recovered in a timely and accurate manner. In recent decades, various asphalt emulsion recovery methods have been implemented; among them, most prominent methods are oven evaporation, distillation, moisture analyzer balance, weathering rack, thermostatically controlled hot plate, and dehydrator methods (37). However, these existing standard methods for residue recovery of emulsified asphalts are time-consuming (37). Nevertheless, many of these methods have been accepted as consensus standards and are outlined in ASTM and AASHTO standards (37). However, many of these recovery methods require subjection of asphalt emulsion to high temperatures that exceed the temperatures asphalt emulsions are exposed to in the field; these high temperatures significantly affect the rheological properties of the recovered binder material (38). Due to this drawback of high-temperature recovery methods, a residue recovery technique that stimulates actual field curing and application conditions is needed.

A study conducted by Takamura (40) showed that using high temperatures in residue recovery significantly alters or damages the microscopic structure of the emulsion. As a result, the asphalt emulsion residue recovery does not represent the practical field conditions where construction is taking place in ambient temperatures (27). To address this issue and more accurately simulate actual field conditions, Takamura proposed a recovery method that employs airflow under ambient temperature (27). Under this method, the recovery process does not require any subjection to high temperature; residue is recovered at room temperature (23 °C) for 24 hours, with the sample subsequently placed in an oven at 60 °C for 2 hours to remove excess moisture (27).

4.3 Objectives and Scope

The objective of this study was to investigate the rutting performance of granular base course stabilized using asphalt emulsion and asphaltenes derived from Alberta oil sands, and to characterize the rheological properties of asphaltenes-modified asphalt emulsion residue. A cationic slow setting (CSS-1H) asphalt emulsion was modified using asphaltenes and was used to stabilize a well-graded granular base course. The rutting performance of both modified and unmodified stabilized mixes were evaluated and compared. For the purpose of analyzing

the rheological properties, asphalt emulsion residue was recovered using a low-temperature evaporation method and was tested using a dynamic shear rheometer (DSR).

4.4 Materials

4.4.1 Aggregates

Aggregate gradation was selected based on the parameters provided by the Wirtgen cold recycling manual (56), the City of Edmonton (87) and Alberta Transportation (88). To satisfy these limitations, a well-graded aggregate gradation was selected as shown in Figure 4.1. The selected gradation comprised 57.27% coarse aggregates and 6% filler, with fine aggregates constituting the remaining portion. According to ASTM D698 (90), the proctor test was conducted to determine the optimum moisture content (OMC) of the aggregates; based on the results, the OMC was determined to be 6.3%. The bulk specific gravity of the aggregates was determined to be 2.601.

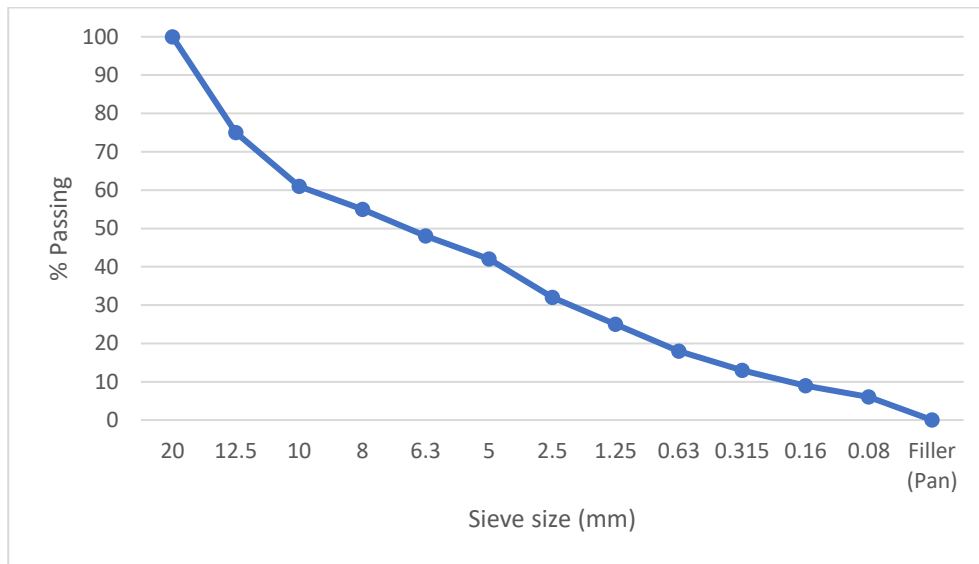


Figure 4-1: Aggregate gradation chart

4.4.2 Asphalt emulsion

A cationic slow setting asphalt emulsion (CSS-1H) consisting of 61% asphalt and 39% water was used in this research. This asphalt emulsion is used in a wide range of pavement applications such as tack coat, base stabilization, dust control, fog seal, slurry seal, and crack sealing. Table 4.1 shows the properties of asphalt binder used to produce the asphalt emulsion, while Table 4.2 presents the properties of the asphalt emulsion used for this study.

Table 4-1: Properties of asphalt binder used to produce asphalt emulsion (103)

Properties	Standard	Specification		Typical Analysis
		Min.	Max.	
Specific gravity (Density) at 15 °C, kg/L	ASTM D70 (104)	-	-	1.0341
Penetration at 25 °C (100 g, 5 s), dmm	ASTM D5 (94)	80	100	90
Flash Point (COC) °C	ASTM D92 (105)	230	-	276
Ductility at 25 °C (5cm/min), cm	ASTM D113 (106)	100	-	150+
Solubility in trichloroethylene, %	ASTM D2042 (107)	99.5	-	99.9
Absolute viscosity at 60 °C, Pa.s	ASTM D2171 (108)	150	-	183
Viscosity at 135 °C, Pa.s	ASTM D4402 (109)	-	3	0.42
RTFO mass loss, %	ASTM D1754 (110)	-	1	0.37

Table 4-2: Properties of Asphalt Emulsion (CSS-1H) (91)

Properties	Standard (ASTM/AASHTO)	Specification		Typical Analysis
		Min.	Max.	
Tests on Emulsion				
Specific Gravity (Density) at 15.6 C, kg/L	D6937/T59 (111, 112)	-	-	1.020
Residue by distillation, % by mass	D6997/T59 (112, 113)	57	-	61
Viscosity at 25°C, S.F.S	D7496-D88/T59 (112, 114, 115)	20	100	22
Oversized particles (sieve), % by mass	D6933/T59 (112, 116)	-	0.3	0.008
Settlement (24 hours), % by mass	D6930/T59 (112, 117)	-	1	0.5
Particle charge test	D7402 (118)	Positive		Positive
Tests on Residue				
Penetration at 25°C (100 g, 5 s), dmm	D5/T49 (94, 119)	40	125	95
Ductility at 25°C (5 cm/min), cm	D113/T51 (106, 120)	40	-	>40

Solubility in Trichloroethylene, % by mass	D2042/T44 (107, 121)	97.5	-	>97.5
--	----------------------	------	---	-------

4.4.3 Asphaltenes

Asphaltenes from two different Alberta oil sands sources were used in this study. The Source 1 asphaltenes, shown in Figure 4.2, were obtained in solid form after extraction through deasphaltation process. The solid asphaltenes was crushed into powder form and passed through a No. 100 sieve. The crushed asphaltenes passing through this sieve was used for asphalt emulsion modification. The Source 2 asphaltenes, as shown in Figure 4.3, was obtained in powder form. This asphaltenes was also sieved through a sieve No. 100 to ensure sufficient fineness for dispersion in asphalt emulsion during modification. Table 4.3 outlines the basic chemical properties of dried asphaltenes from Source 2.



Figure 4-2: Source 1 type of Asphaltenes. ((a) solid & (b) Powdered)



Figure 4-3: Source 2 type of Asphaltenes

Table 4-3: Basic chemical properties of dried asphaltenes (Source 2 type) (122)

Test items	Typical Analysis
Sample Name	Vacuum Dried Asphaltene Solids
Origin of Sample	Cold Lake bitumen
Bulk Density, Kg/m ³	403.6
True Density, Kg/m ³	1135
C5 Insoluble, Wt% ASTM D-4055 (123)	74.5
Gross Calorific Value, MJ/Kg (ASTM D-5865-04 (124))	38.6
Net Calorific Value, MJ/Kg	36.4
Micro Carbon residue (MCR), Wt% ASTM D-4530 (125)	37.2

For the purpose of checking the purity of the two asphaltenes types, the SARA test conducted on the asphaltenes to determine the relative percentage of each SARA component (saturates, aromatic, resin, and asphaltenes). The SARA test results for the two asphaltenes are shown in Table 4.4. As can be seen in the table, both asphaltenes sources were found to have some impurities, but the asphaltenes content was around 80% for each source.

Table 4-4: SARA test results of asphaltenes

Type of Asphaltenes	Saturate (%)	Aromatic (%)	Resin (%)	Asphaltenes (%)

Source 1	6.85	9.68	3.84	79.62
Source 2	2.35	7.3	6.62	83.63

4.5 Mix design

4.5.1 Optimum asphalt emulsion content

Optimum emulsion content was determined by preparing trial mixtures with different asphalt emulsion contents. Based on Asphalt Institute specifications (23), the amount of asphalt emulsion to be used for this research was calculated using Eq. (4.1) for well-graded aggregate gradation considering the result from ASTM D6997 (113).

$$\text{Base mixture: Asphalt Emulsion \%} = \frac{(0.06B + 0.01C)100}{A} \dots\dots\dots 4.1$$

where

A = Percentage of residue of asphalt emulsion remaining after distillation

B = Percentage of dry aggregate passing through a No. 4 sieve

C = Percentage of dry aggregate retained on a No. 4 sieve.

The approximate asphalt emulsion content was determined to be 4.89%. Later samples were prepared for 4.89% asphalt emulsion, with an additional different contents of asphalt emulsion at various intervals. Table 4.5 shows the design matrix used to determine the optimum emulsion content. The prepared samples were tested for Marshall stability and ITS in order to select the optimum emulsion content. Based on the results obtained and the trend observed for density, stability, and tensile strength results, 3.7% asphalt emulsion content shows a maximum value. By considering all these factors 3.7% asphalt emulsion per total mix was used as the optimum asphalt emulsion content, with 4.8% water added to the aggregates in order to prepare the samples for further testing.

Table 4-5: Design matrix to determine the optimum asphalt emulsion

Emulsion content (% per total mix)	Additional water (% per total mix)
---	---

3.04	5.10
3.70	4.80
3.98	4.70
4.89	4.30
5.79	3.90
6.66	3.50

4.5.2 Asphalt emulsion modification with asphaltenes

The modification was done by manually mixing asphaltenes into the asphalt emulsion at two ratios 1% and 2% by weight of total mixtures, which is equivalent to 26.95% and 54.37% by weight of asphalt emulsion. Two asphaltenes from different sources were used in this research. The modification process includes mixing asphalt emulsion and asphaltenes by manual mixing for 60 seconds (until the asphaltenes were dispersed thoroughly in the emulsion) using a measuring glass and spatula.

During the modification process, it was observed that mixing asphaltenes at 2% makes modification difficult by fast-breaking the emulsion. In order to ease the modification process, an additional 25% of water was added to the sample, based on the assumption that additional water would evaporate during the residue recovery procedure. The same modification procedure was used for both asphaltenes types.

4.5.3 Asphalt emulsion residue recovery procedure

The residue recovery method used in this study was “Low-temperature evaporation technique as per AASHTO PP 72-11 – Procedure A” (95). Following this simple low-temperature evaporation technique, the modified and unmodified asphalt emulsion was poured on a silicon mat at a spread rate of 1.5 to 2.0 kg/m². Subsequently, the evenly spread asphalt emulsion was dried in a forced draft oven at 25 °C for 24 hours, then stored at 60 °C for another 24 hours. After oven drying, the samples were allowed to cool at room temperature for 1 hour. The residue was then peeled from the silicon mat, and the recovered residue was stored in a

container for further testing. Figure 4.4a shows the asphalt emulsion on the silicon mat at a spread rate of 1.5 to 2.0 kg/m², while Figure 4.4b shows the recovered residue.

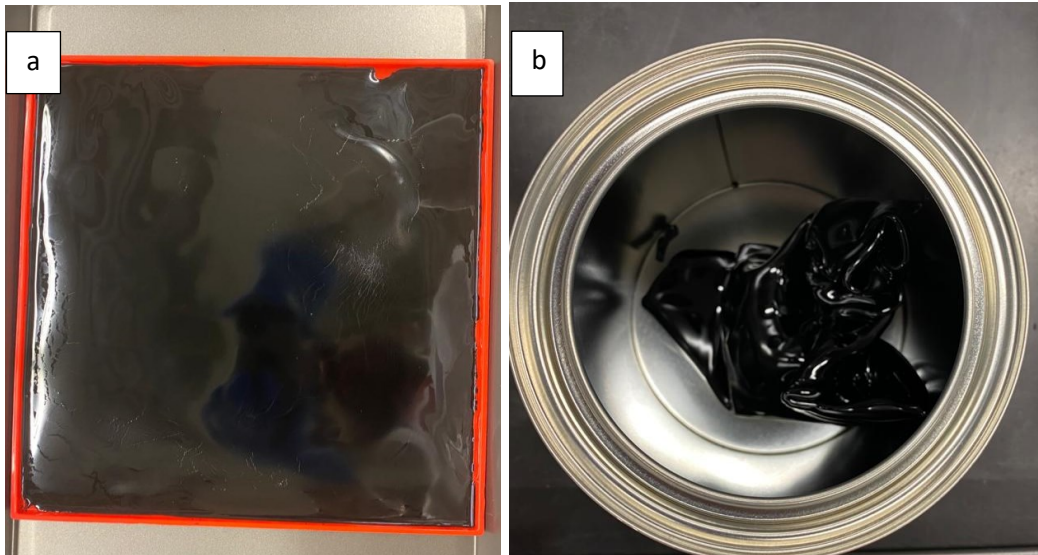


Figure 4-4: (a) Asphalt Emulsion on silicon mat at a spread rate of 1.5 to 2.0 kg/m² (b) Recovered residue stored in a container

4.5.4 Marshall stability and flow

The Marshall stability test was performed in accordance with ASTM D6927-15 (61). The test specimens were prepared for asphalt emulsion modified with two different proportions of asphaltenes from Source 1 and one proportion from Source 2 due to less availability of material. The Marshall samples were prepared with a 100 mm diameter, and, in order to remove the moisture in the aggregates, the aggregates required for each sample were weighed and oven-dried before mixing. The mixing process involved adding oven-dried aggregates, water, and asphaltenes modified asphalt emulsion. Specimens were compacted with 50 blows on each side using a Marshall compactor. Before ejecting the samples from the molds, the compacted samples were cured in the oven for 48 hours at 60 °C. After allowing them to cool down for at least two hours, samples were extracted from the molds. Three specimens were prepared at each asphaltene content for the purpose of testing. Finally, the Marshall stability test was conducted after conditioning the specimens in a water bath at 60 °C for 2 hours (23).

4.5.5 Indirect tensile strength (ITS)

The ITS test was performed as per AASHTO T283 [51] standard. The ITS test specimens were prepared using the determined optimum asphalt emulsion content of 4.2% and asphaltenes contents of 1%, and 2% by total weight of the mixture. The samples were compacted and cured using the same procedure as that used for the Marshall stability test, where three samples were prepared for each asphaltenes content and control samples without asphaltenes. Conditioning was achieved by keeping the samples in an air chamber at 25 °C for 3 hours. The samples were tested using a universal testing machine (UTM) and applying a load at a rate of 50 mm/min. Tensile strength was calculated by using the maximum load applied to the samples before failure.

4.5.6 Hamburg wheel tracking test

The Hamburg wheel tracking test was conducted as per AASHTO T 324-17 (126) standard to determine the rutting resistance of the samples prepared with asphalt emulsion modified with asphaltenes. The slab specimens were prepared with dimensions of 60 mm (height), 320 mm (length) and 260 mm (width). The mixtures were prepared with the optimum emulsion content modified with 1% and 2% asphaltenes (as a proportion of the total weight of the mixture). The specimens were compacted to the required height using a roller compactor. They were then oven-cured in a mold for 48 hours at 60 °C. After cooling them for at least 2 hours, the specimens were removed from the mold. Figure 4.5a and 4.5b shows the slab specimens prepared for testing.



Figure 4-5: (a) Slab prepared for wheel tracking test. (b) Slab after performing Hamburg wheel tracking test.

4.5.7 Dynamic Shear Rheometer (DSR)

A DSR was used to characterize the viscoelastic behavior of the asphalt binder material. This test is conducted by measuring the properties of thin asphalt binder specimen sandwiched between oscillating spindle and a fixed plate (46). In this study, the DSR test for high temperatures properties was performed in accordance with the parameters specified in AASHTO T 315-12 (47). Tests were conducted at a single frequency of 10 rad/s using a 25 mm spindle for high temperatures with 1 mm thick specimens. For the sample preparation, residues were first heated in an oven at 135 °C for 60 min, and poured into DSR molds, and allowed to cool at room temperature prior to testing. A minimum of three tests were performed for each of the modified asphalt emulsion residues and control asphalt emulsion residue samples.

4.6 Results and discussion

4.6.1 Marshall stability and flow

The Marshall stability, flow number, and Marshall quotient for the control and modified samples are presented in Table 4.6. It can be seen that adding asphaltenes increases the Marshall stability of the mixtures considerably. Moreover, it was observed that the mixtures modified with 2% asphaltenes improved the stability value almost two-fold compared to the control samples. Also, it was observed that the modified mixtures using different sources of asphaltenes at 1% content exhibit nearly the same effect on stability values as one another. Additionally, the Marshall quotient for the modified mixtures was found to increase significantly compared to control samples.

Table 4-6: Marshall stability and flow number

Asphaltenes type	Sample Description	Density (gr/cm³)	Air voids (% per total mix)	G_{mb}	Stability (kN)	Flow number (mm)	Marshall Quotient (kN/mm)
N/A	Control Sample	2.197	11.113	2.272	11.536	5.545	2.080

Source 1	1% Asphaltenes	2.150	11.395	2.244	17.059	5.263	3.241
	2% Asphaltenes, with 25% extra water	2.143	12.574	2.195	22.718	7.482	3.036
Source 2	1% Asphaltenes	2.094	13.798	2.184	16.730	4.575	3.657

4.6.2 Indirect tensile strength (ITS)

Table 4.7 presents the ITS test results for the control sample and modified mixtures with asphaltenes from Source 1 and Source 2. It can be seen that the modified mixtures with 2% asphaltenes and 25% extra water were found to have higher tensile strength values compared to the other modified mixtures, whereas the samples modified with 1% asphaltene content were found to exhibit similar results for both Source 1 and Source 2 asphaltenes. Moreover, the modified mixtures were observed to have higher tensile strength compared to control samples. Therefore, it can be concluded that modifying mixtures by adding asphaltenes increases the tensile strength capacity of the mixtures.

Table 4-7: Indirect tensile strength test results

Asphaltenes type	Sample Description	Indirect Tensile Strength (kPa)
N/A	Control Sample	297.784
Source 1	1% Asphaltenes	613.200
	2% Asphaltenes, with 25% extra water	872.803
Source 2	1% Asphaltenes	644.128

4.6.3 Performance testing

Hamburg wheel tracking test

The results of the wheel tracking test are presented in Table 4.8. Similar to the Marshall stability and ITS results for optimum emulsion content and modified mixtures, the asphaltenes modified mixtures showed a significant increase in rutting resistance based on the results of the wheel tracking test. It was found that the control samples failed at 3,940 passes, whereas the modified mixtures at 1% and 2% asphaltenes content reached failure at much higher numbers of passes 8,712 and 8,604 respectively. Using the maximum number of passes for each sample, permanent deformation under repeated wheel tracking load cycles was calculated in terms of Rutting Resistance Index (RRI) using Eq. (2). From the results it can be seen that RRI of the modified samples were found to be twice that of the control samples. The modified samples with 1% and 2% asphaltenes were found to exhibit approximately the same effect as one another on number of passes, rut depth, and RRI values.

$$RRI = \text{No. of Passes @ end of test} \times (1'' - \text{Rut Depth}) \dots\dots\dots 4.2$$

Table 4-8: Wheel tracking test results

Asphaltenes type	Sample Description	No. of Passes	Rut depth (mm)	Rutting Resistance Index
N/A	Control Sample	3940	11.09	2219.74
Source 1	1% Asphaltenes	8712	9.77	5360.97
	2% Asphaltenes with 25% extra water	8604	9.78	5291.12

Dynamic shear rheometer

Recovered asphalt emulsion residue was used for the rheological testing at high temperatures. Asphalt emulsions eliminate the requirement of hot mix plant operations, so the recovered residues were considered as approximately proportionate to the rolling thin-film oven (RTFO) aged binder [2]. A Superpave rutting criterion $G^*/\sin \delta$ greater or equal to the 2.2 kPa limit for high temperature was used. Table 4.9 presents the results corresponding to the high-temperature rheological test parameters. The results indicate that modifying the asphalt

emulsion with asphaltenes significantly increases the high-temperature limit. It can be seen that the high-temperature limit of the control (unmodified) asphalt emulsion residue was 69.33 °C, while the high-temperature limit of the asphalt emulsion modified with 1% of Source 1 asphaltenes was found to be 101.56 °C, and that of the Source 2 asphaltenes modified asphalt emulsion was found to be 110.12 °C. Both the Source 1 and Source 2 asphaltenes at 1% were observed to increase the high-temperature limit of asphalt emulsion, by 32.22 °C and 40.78 °C, respectively. Furthermore, the results of the asphalt emulsion modified with 2% asphaltenes from Source 2 show an increase in high-temperature limit to almost twice that of the control samples.

Table 4-9: DSR results for high-temperature limits ($|G^*| / \sin \delta = 2.2 \text{ kPa}$)

Type of Asphalt Emulsion Residue	Standard Temperature at Failure (°C)	Temperature at failure (°C)
Control Sample	64	69.33
Source 1 Asphaltenes - 1%	100	101.56
Source 1 Asphaltenes - 2%	118	121.97
Source 2 Asphaltenes - 1%	106	110.12
Source 2 Asphaltenes - 2%	130	134.98

The rutting factor results of the samples are shown in Figure 4.6. As can be observed, the rutting factor of the modified samples was found to increase significantly compared to that of the control samples. Furthermore, the samples modified with 2% of asphaltenes were found to have a higher rutting factor than those modified with 1%; this effect was the same for both sources of asphaltenes.

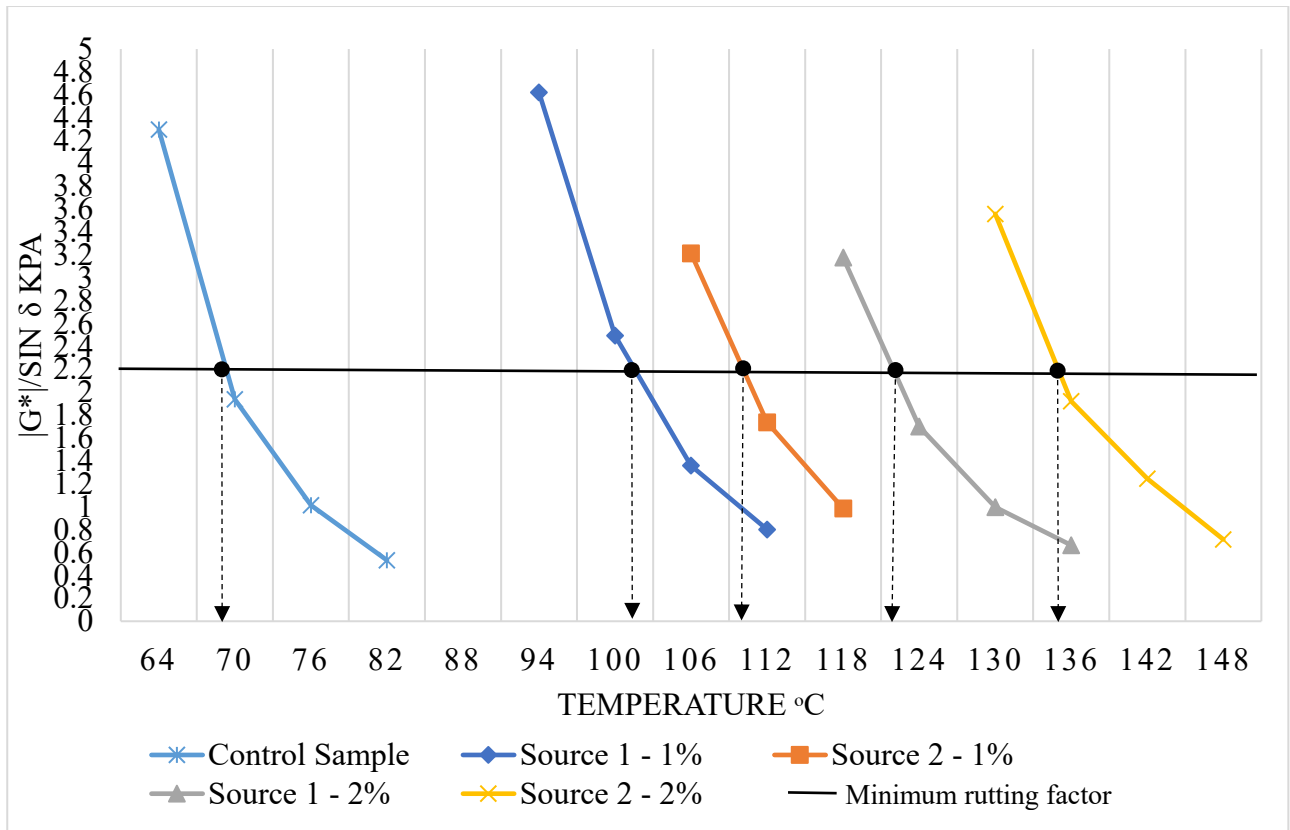


Figure 4-6: Rutting factor of asphalt emulsion modified with asphaltenes

Figure 4.7 presents the DSR results for high-temperature limit when $G^*/\sin \delta = 2.2$ kPa, Marshall quotient, and rutting resistance index (RRI) from Hamburg wheel tracking test. From the graph, a significant difference can be seen between the results of the control samples and those of the modified asphalt emulsion, it is noticed that the asphalt emulsion modified with asphaltenes brought significant improvement in terms of high-temperature limit for both sources and both asphaltenes contents (1% and 2%) in the DSR test. Despite the improvement in high-temperature limit for the samples modified with 2% asphaltenes, the wheel tracking test results show that the 2% asphaltenes modified samples did not significantly improve the rutting resistance of the mixtures. This is due to the fact that compaction is achieved with greater difficulty after adding more asphaltenes to the mixture. It should be noted that the Hamburg wheel tracking tests were not performed on Source 2 asphaltenes due to a shortage of material, but, similar to with the rheology test results, it can reasonably be assumed that the same performance would be observed with the Source 2 asphaltenes as with Source 1.

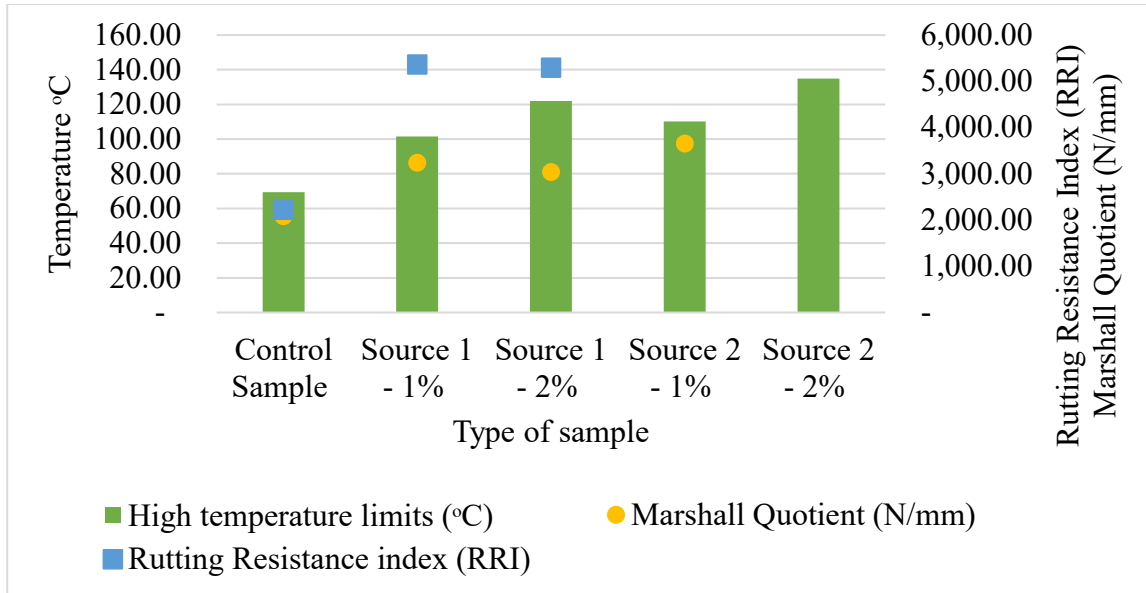


Figure 4-7: Failure temperature and Rutting Resistance index

4.7 Conclusions

Based on the experimental results and analysis performed on the modified asphalt emulsion with two sources of asphaltenes under different proportions, the following conclusions can be drawn.

- Asphaltenes modification was found to enhance the Marshall stability and tensile strength by almost double compared to the control samples, with the 2% asphaltenes modified mixture being found to have the highest tensile strength and stability. However, it was observed that the addition of 2% asphaltenes does not increase the Marshall Quotient compared to the 1% asphaltenes samples.
- The results of the Hamburg wheel tracking test show that the modified samples were associated with a considerably higher rutting resistance compared to the control samples after adding 1% asphaltenes by the weight of total mix. However, it was observed that increasing asphaltenes to 2% was not effective in terms of improving rutting performance, since the increased asphaltene content made compaction more difficult.
- Based on the DSR results, both sources of asphaltenes were found to exhibit significant improvement with respect to all the performance test results conducted. Modification of the asphalt emulsion with 1% asphaltenes increases the high-temperature limit

for both Source 1 and Source 2 asphaltenes by 33.3 °C and 41.7 °C, respectively in comparison to the control samples. The asphalt emulsion modified with 2% asphaltenes, meanwhile, was found to increase the high-temperature limit to almost twice that of the control samples.

- Comparing the results of the DSR, Marshall Quotient, and wheel tracking tests, it can be concluded that the addition of 1% asphaltenes was more effective in terms of improving the rutting resistance of the asphalt emulsion stabilized mixes compared to modifying the mix with 2% asphaltenes.

5 Additional testing

5.1 Dynamic mechanical analysis of asphaltenes modified asphalt emulsion.

In chapter 3 of this report, the dynamic analysis was done for source 1 type of asphaltenes; in this chapter, a similar analysis was performed for source 2 types of asphaltenes using the data from frequency sweep test.

The rheological performance of the residues from the control samples and asphaltenes-modified samples at percentages of 0.2%, 0.5%, 1% and 2% was ascertained by conducting a frequency sweep test at various temperatures and loading frequencies. The frequency sweep test was performed using a dynamic shear rheometer (DSR) with 8 mm diameter plates and a gap of 2 mm. The test samples were prepared by oven-heating the asphalt emulsion residue at 135 °C until sufficiently fluid to pour inside molds; the residue was then poured into a silicon mold of 8 mm diameter. Tests were performed at temperatures loop of 4 °C, 10 °C, 20 °C, 25 °C, 30 °C, and 40 °C with an angular frequency range of 0.1 to 100 rad/s. Three tests were performed for each of the samples. The time-temperature superposition (TTS) principle and Williams- Landel-Ferry (WLF) regression analysis were applied using RheoCompass software to plot the master curves for the complex modulus and phase angle at 25 °C over a broader range of frequencies.

Figure 5-1 represents the master curve for the phase angle at 25 °C for source 2 asphaltenes modified residue. From the master curve analysis, it can be seen that the phase angle master curves for the asphaltenes modified samples shows a reduction in phase angle at both low and high ranges of frequency compared to that of the control sample. Similar to source 1 asphaltenes, the master curve trend depicts that an increase in asphaltenes content decreases the phase angle of the samples. However, from the chart, it can also be seen that the control sample has a phase angle of approximately 70° at the angular frequency of 1 Hz. In contrast, 0.2%, 0.5%, 1%, and 2% modified samples have phase angles of approximately 60°, 50°, 40°, and 25°, respectively. By looking at the curves of the samples, it can be concluded that adding asphaltenes for modification at greater proportions reduces the viscous behaviour of the asphaltenes-modified samples.

Figure 5-2 demonstrates the master curve of the complex modulus at 25 °C over a range of frequencies. From the analysis it can be seen that the complex modulus for the asphaltene-modified samples shows a significant improvement at lower frequencies and a very minimal change at higher frequencies. Also, It can be observed from the figure that the complex shear modulus of the control sample and the 0.2% modified sample at an angular frequency of 1 Hz are within the range of 1×10^5 Pa to 1×10^6 Pa. The complex shear modulus values of the 0.5% and 1% modified samples fall within the range of 1×10^6 Pa to 1×10^7 Pa and 1×10^7 Pa to 1×10^8 respectively at 1 Hz angular frequency. But, some inconsistency in source 2, 2% modified sample was observed compared to source 1 asphaltene, it can be seen from the analysis that source 2 2% modified sample has complex shear modulus values in the range of 1×10^6 Pa to 1×10^7 Pa. In contrast, the value of source 1 modified sample falls within the range of 1×10^6 Pa to 1×10^7 Pa at 1 Hz angular frequency. This result indicates a stiffening effect and an increase in temperature susceptibility of the asphaltene-modified samples corresponding to an increase in asphaltene content.

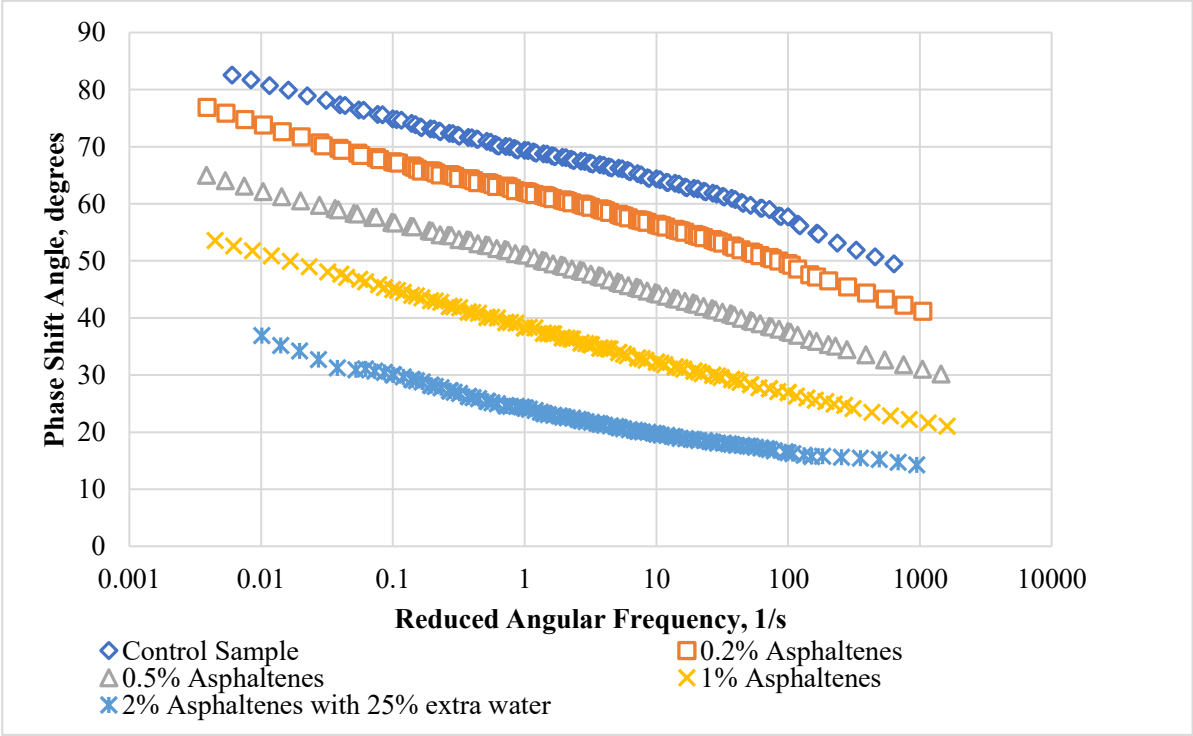


Figure 5-1: Master curve of phase shift angle at 25 °C for the control sample and modified sample

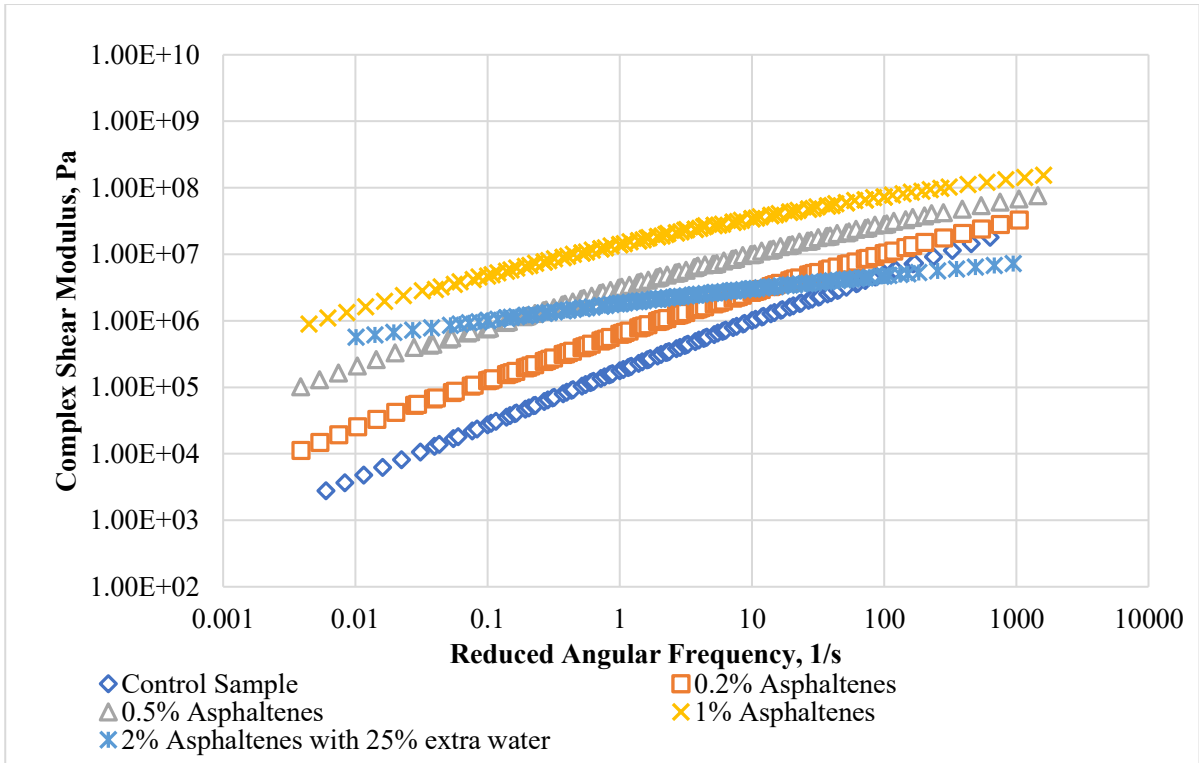


Figure 5-2: Master curve of complex shear modulus at 25 °C for the control sample and modified samples

6 Summary and Conclusions

6.1 Summary

The use of asphalt emulsion as a stabilized cold mix in pavement construction has seen a dramatic growth throughout the world. As mentioned earlier in this report, asphalt emulsion benefits are not only limited to improving performance, but also it has more advantages environmentally as compared to hot mix asphalt mixtures. Several studies conducted on asphalt emulsion to understand the performance using various additives. However, still the correlation and assessment of test results vary among researchers and institutions due to lack of uniform procedure for laboratory evaluation of cold mix asphalt mixtures.

This research study focused on investigating the mechanical performances and rheological properties of asphalt emulsion modified using asphaltenes. Both modified asphalt emulsion mixtures and residues were subjected to various tests based on Superpave binder testing protocols and AASHTO/ASTM standards. Due to less availability of source 2 asphaltenes for modification, to perform Marshall stability and indirect tensile strength (ITS) test, mixtures were prepared and tested only for 1% asphaltenes by total weight of mix, and wheel tracking tests were not performed with source 2 type of asphaltenes. However, due to less requirement of material to perform rheological tests, the high temperature limiting test and dynamic mechanical analysis were performed for both the source of asphaltenes at 0.2%, 0.5%, 1% and 2%.

6.2 Conclusion

Based on the various test results and analysis conducted in this study, the mechanical performance and rheological properties of asphaltenes modified asphalt emulsion were compared, and the following conclusions are drawn from this study.

- The content of asphaltenes for modification was determined by performing tests on trial mixes prepared at different proportions. Based on the trial test results, 1% and 2% asphaltenes by weight of total mix was used for further performance testings. From the observation, it was seen that adding 2% asphaltenes to the emulsion was found difficult due to the fast-breaking of emulsion which makes the modified

sample stiff. To overcome this, an additional 25% of water by weight of total mix was added to allow the modification consistent. From this, it can be concluded that adding more asphaltenes makes the sample stiffer.

- The percentage of air voids of the modified mixtures were calculated from specimen's bulk specific gravity (G_{mb}) and theoretical maximum specific gravity (G_{mm}). Values from the results showed that the modification had not shown any significant impact on air voids. Only minimal changes in the results were observed for modified samples compared to the control sample.
- From Marshall stability test results, the stability of the modified samples was found to improve by 50% for 1% and 100% improvement for 2% asphaltenes modified sample compared to the control sample. But, from Marshall quotient analysis, it was observed that 1% asphaltenes modified sample from both asphaltenes sources had shown better performance than 2% asphaltenes modified sample and control sample.
- Indirect tensile strength (ITS) results have shown a significant improvement in the results of samples modified with asphaltenes compared to the control sample. From the test results the following developments were observed for the modified samples: 1% modified sample from both source of asphaltenes have improved the tensile strength by approximately two times the value of control sample, whereas 2% asphaltenes modified sample has improved three times than that of control sample.
- Modification of asphalt emulsion with asphaltenes enhanced the indirect tensile asphalt cracking performance of the 0.2% modified mixture. It was also observed that the cracking tolerance of 1% and 2% asphaltenes modified mixtures were found to decrease than that of the control sample. However, from the results, it was observed that adding a higher proportion of asphaltenes improves the tensile strength of the mixture, but it decreases the cracking resistance.
- The rutting performance result from Hamburg wheel tracking test shows that adding asphaltenes for modification improves the rutting resistance of the mixture. From the

results, the control sample reached the rut depth of 11.09mm at 3940 passes, whereas 1% and 2% modified sample have reached the rut depth of 9.77mm and 9.78mm at 8712 and 8604 passes respectively. The rutting resistance index (RRI) of the asphaltenes modified samples were also improved significantly compared to the control sample, however, 1% modified sample has better performance than 2% modified and control sample in terms of RRI.

- High-temperature performance grade of the asphalt emulsion residues was found to be improved for asphaltenes modified samples. The 1% modified samples increased the high-temperature limits by 50%, while 2% modified samples have improved by 100% compared to the control sample.
- Dynamic mechanical analysis from the frequency sweep test shows that adding asphaltenes for modification improves the rheological properties of the asphalt emulsion. However, master curves indicated that adding asphaltenes for modification reduces phase angle at both low and high-frequency range, which signifies less viscous behaviour of modified samples compared to the control sample. Modified samples significantly increase complex shear modulus at low-frequency ranges; thus, the modified samples exhibit more stiffness at lower frequency range compared to the control sample but show almost similar stiffness behaviour at higher frequency range.

References

1. Borhan MN, Suja E, Ismail A, Rahmat RAO. Used Cylinder Oil Modified Cold—Mix Asphalt Concrete. *Journal of Applied Sciences*. 2007;7(22):3485-91.
2. Seitllari A, Boz I, Habbouche J, Diefenderfer SD. Assessment of cracking performance indices of asphalt mixtures at intermediate temperatures. *International Journal of Pavement Engineering*. 2020:1-10.
3. Kadhim MA, Al-Busaltan S, Almuhan RR. An evaluation of the effect of crushed waste glass on the performance of cold bituminous emulsion mixtures. *International Journal of Pavement Research and Technology*. 2019;12(4):396-406.
4. Du S. Interaction mechanism of cement and asphalt emulsion in asphalt emulsion mixtures. *Materials and structures*. 2014;47(7):1149-59.
5. Nassar AI, Mohammed MK, Thom N, Parry T. Mechanical, durability and microstructure properties of Cold Asphalt Emulsion Mixtures with different types of filler. *Construction and Building Materials*. 2016;114:352-63.
6. Thomas T, Karmas A. Performance-related tests and specifications for cold in-place recycling: lab and field experience. *Transport Research Board*. 2002.
7. Cross SA. Experimental cold in-place recycling with hydrated lime. *Transportation Research Record*. 1999;1684(1):186-93.
8. Terrell R, Wang C. Early curing behavior of cement modified asphalt emulsion mixtures. *Association of Asphalt Paving Technologists Proc*. 1971.

9. Babagoli R, Ameli A, Shahriari H. Laboratory evaluation of rutting performance of cold recycling asphalt mixtures containing SBS modified asphalt emulsion. *Petroleum Science and Technology*. 2016;34(4):309-13.
10. Becker Y, Mendez MP, Rodriguez Y, editors. *Polymer modified asphalt*. Vision tecnologica. 2001.
11. Bearsley S, Forbes A, G. HAVERKAMP R. Direct observation of the asphaltene structure in paving-grade bitumen using confocal laser-scanning microscopy. *Journal of microscopy*. 2004;215(2):149-55.
12. Sultana S, Bhasin A. Effect of chemical composition on rheology and mechanical properties of asphalt binder. *Construction and Building Materials*. 2014;72:293-300.
13. Jiang J, Ni F, Zheng J, Han Y, Zhao X. Improving the high-temperature performance of cold recycled mixtures by polymer-modified asphalt emulsion. *International Journal of Pavement Engineering*. 2020;21(1):41-8.
14. Al-Busaltan S, Al Nageim H, Atherton W, Sharples G. Mechanical properties of an upgrading cold-mix asphalt using waste materials. *Journal of materials in civil engineering*. 2012;24(12):1484-91.
15. Piratheepan M. *Designing Cold Mix Asphalt (CMA) and Cold-In-Place Recycling (CIR) Using SUPERPAVE Gyratory Compactor*. MSc thesis, Civil and Environmental Engineering, University of Nevada, Reno. 2011.
16. Ojum CK. *The design and optimisation of cold asphalt emulsion mixtures*: PhD thesis University of Nottingham. 2015.

17. Thanaya INA. Review and recommendation of cold asphalt emulsion mixtures CAEMS design. *Civil Engineering Dimension*. 2007;9(1):pp. 49-56.
18. Needham D. Developments in bitumen emulsion mixtures for roads: PhD thesis, University of Nottingham Nottingham. 1996.
19. Thanaya I, Forth P, Zoorob S, editors. Utilisation of coal ashes in hot and on cold bituminous mixtures. *International Coal Ash Technology Conference*. 2006.
20. Sangiorgi C, Tataranni P, Simone A, Vignali V, Lantieri C, Dondi G. A laboratory and field evaluation of Cold Recycled Mixture for base layer entirely made with Reclaimed Asphalt Pavement. *Construction and Building Materials*. 2017;138:232-9.
21. Arimilli S, Jain PK, Nagabhushana M. Optimization of recycled asphalt pavement in cold emulsified mixtures by mechanistic characterization. *Journal of Materials in Civil Engineering*. 2016;28(2):04015132.
22. Jordaan G, editor Behaviour of an emulsion treated base (Etb) layer as determined from heavy vehicle simulator (Hvs) testing. *Proceedings of the 10th Conference on Asphalt Pavements for Southern Africa (CAPSA), Drakensberg, South Africa*. 2011.
23. Asphalt Institute. *A Basic Asphalt Emulsion Manual*. 4th ed: Asphalt Emulsion Manufacturer Association. 2008.
24. Buss A, Pinto I, Guirguis M, Cochran E, Panthani M. Enhancing the Fundamental Knowledge and Use of Asphalt Emulsions Using Systematic Scientific and Engineering Approaches: Final Report August 2018. *Midwest Transportation Center*. 2018.
25. James A. *Asphalt Emulsion Technology, Overview of asphalt emulsion*. *Transportation research circular E-C102*. 2006:1-15.

26. Shafii M, Rahman MA, Ahmad J. Polymer modified asphalt emulsion. International journal of civil and environmental engineering. 2011. Vol:11, No. 06.
27. Marasteanu MO, Clyne TR. Rheological characterization of asphalt emulsions residues. Journal of materials in civil engineering. 2006;18(3):398-407.
28. Yen TF, Chilingarian GV. Asphaltenes and asphalts, 2, Developments in Petroleum Science: Elsevier Science. 1994.
29. Carvalho do Prado GH. Asphaltenes conversion by chemical modification. PhD thesis Department of Chemical and Material Engineering, University of Alberta. 2015.
30. Werner A, Behar F, De Hemptinne J, Behar E. Viscosity and phase behaviour of petroleum fluids with high asphaltene contents. Fluid phase equilibria. 1998;147(1-2):343-56.
31. Al-Maghrabi IM, Aqil AB, Islam M, Chaalal O. Use of thermophilic bacteria for bioremediation of petroleum contaminants. Energy Sources. 1999;21(1-2):17-29.
32. Islam M. New Methods of Petroleum Sludge Disposal and Utilization. Asphaltenes: Springer. 1995. p. 219-35.
33. Mullins OC. Sulfur and nitrogen molecular structures in asphaltenes and related materials quantified by XANES spectroscopy. Asphaltenes: Springer. 1995. p. 53-96.
34. Rajan N, Selvavathi V, Sairam B, Krishnan J. Influence of asphaltenes on the rheological properties of blended paving asphalts. Petroleum science and technology. 2010;28(4):331-50.
35. Islam MR, Hossain MI, Tarefder RA. A study of asphalt aging using Indirect Tensile Strength test. Construction and Building Materials. 2015;95:218-23.

36. Transportation Research Board. Asphalt Emulsion Technology: Review of Asphalt Emulsion Residue Procedures. 2007.
37. Motamed A, Salomon D, Sakib N, Bhasin A. Emulsified asphalt residue recovery and characterization: combined use of moisture analyzer balance and dynamic shear rheometer. Transportation Research Record. 2014;2444(1):88-96.
38. Farrar MJ, Salmans SL, Planche J-P. Recovery and laboratory testing of asphalt emulsion residue: application of simple aging test and 4-mm dynamic shear rheometer test. Transportation research record. 2013;2370(1):69-75.
39. Salomon D, Thompson M, Dur G, Gueit C, Deneuvillers C, Robert M, et al. Comparison of Rheological Properties for Recovered Residue from Emulsified Asphalt obtained by Three Recovery Procedures. 2008.
40. Takamura K, Lubbers C. Comparison of emulsion residues recovered by forced airflow and RTFO drying. ISSA/AEMA Proceedings. 2000.
41. Alataş T, Yılmaz M, Kök BV, Fatih Koral A. Comparison of permanent deformation and fatigue resistance of hot mix asphalts prepared with the same performance grade binders. Construction and Building Materials. 2012;30:66-72.
42. Isacsson U, Zeng H. Relationships between bitumen chemistry and low temperature behaviour of asphalt. Construction and Building Materials. 1997;11(2):83-91.
43. Behnood A, Shah A, McDaniel RS, Beeson M, Olek J. High-temperature properties of asphalt binders: Comparison of multiple stress creep recovery and performance grading systems. Transportation Research Record. 2016;2574(1):131-43.

44. Amirkhanian AN, Xiao F, Amirkhanian SN. Evaluation of high temperature rheological characteristics of asphalt binder with carbon nano particles. *Journal of Testing and Evaluation*. 2011;39(4):583-91.
45. Airey GD. Rheological properties of styrene butadiene styrene polymer modified road bitumens. *Fuel*. 2003;82(14):1709-19.
46. Superpave Fundamental Reference Manual. U.S. Department of Transportation, Federal Highway administration. 2000.
47. AASHTO. T 315-12, Standard Method of Test for Determining the Rheological Properties of Asphalt Binder Using a Dynamic Shear Rheometer (DSR) Washington D.C.: American Association of State Highway and Transportation Officials. 2012.
48. Hossain Z, Zaman M. Rheological properties of performance grade binders using a dynamic mechanical analyzer. *Pavements and Materials: Modeling, Testing, and Performance*. 2009. p. 140-9.
49. Lytton RL, Masad EA, Zollinger C, Bulut R, Little DN. Measurements of surface energy and its relationship to moisture damage. Texas Department of Transportation and Federal Highway Administration, Texas. 2005.
50. Hossain Z, Zaman M, editors. Dynamic Mechanical Analysis of Performance Grade Asphalt Binder. Proc 12th International Conference of International Association for Computer Methods and Advances in Geomechanics (IACMAG). 2008.
51. Hossain Z. Evaluation of rheological properties of asphalt binders for pavement design applications. PhD thesis, School of Civil Engineering and Environmental Science, University of Oklahoma. 2011.

52. Airey GD. Rheological characteristics of polymer modified and aged bitumens. PhD thesis, Department of Civil Engineering, University of Nottingham. 1997.
53. Goodrich JL, editor Asphalt and polymer modified asphalt properties related to the performance of asphalt concrete mixes (with discussion). Association of Asphalt Paving Technologists Procedure. 1988.
54. Pink HS, Merz RE, Bosniack D, editors. Asphalt rheology: Experimental determination of dynamic moduli at low temperature. Association of Asphalt Paving Technologists Proceedings. 1980.
55. Airey GD. Use of black diagrams to identify inconsistencies in rheological data. Road Materials and Pavement Design. 2002;3(4):403-24.
56. Wirtgen Cold Recycling Manual, 1st edition. Wirtgen GmbH. Windhagen, Germany. 2004.
57. Pi Y, Huang Z, Pi Y, Li G, Li Y. Composition Design and Performance Evaluation of Emulsified Asphalt Cold Recycled Mixtures. Materials. 2019;12(17):2682.
58. Nagabhushana M, Tiwari D, Jain P. Rutting in flexible pavement: an approach of evaluation with accelerated pavement testing facility. Procedia-Social and Behavioral Sciences. 2013;104:149-57.
59. Tayfur S, Ozen H, Aksoy A. Investigation of rutting performance of asphalt mixtures containing polymer modifiers. Construction and Building Materials. 2007;21(2):328-37.
60. Yu J, Yu X, Gao Z, Guo F, Wang D, Yu H. Fatigue resistance characterization of warm asphalt rubber by multiple approaches. Applied Sciences. 2018;8(9):1495.

61. ASTM International. ASTM D6927-15, Standard test method for Marshall Stability and flow of bituminous mixtures. West Conshohocken, PA: American Society for Testing and Materials. 2015.
62. Technology CUoSa. Chapter 5 - Indirect tensile strength characteristics, School of Engineering, Cochin University of Science and Technology
63. AASHTO. T 283-14, Standard Method of Test for Resistance of Compacted Asphalt Mixtures to Moisture-Induced Damage. Washington, D.C.: American Association of State Highway and Transportation Officials. 2017.
64. Aschenbrener T. Evaluation of Hamburg wheel-tracking device to predict moisture damage in hot-mix asphalt. Transportation Research Record. 1995;1492:193.
65. Izzo RP, Tahmoressi M. Use of the Hamburg wheel-tracking device for evaluating moisture susceptibility of hot-mix asphalt. Transportation Research Record. 1999;1681(1):76-85.
66. Pavement Interactive. Laboratory Wheel Tracking Devices [Available from: <https://pavementinteractive.org/reference-desk/testing/asphalt-tests/laboratory-wheel-tracking-devices/>].
67. Zhou F, Im S, Sun L, Scullion T. Development of an IDEAL cracking test for asphalt mix design and QC/QA. Road Materials and Pavement Design. 2017;18(sup4):405-27.
68. Zhou F. Development of an IDEAL Cracking Test for Asphalt Mix Design, Quality Control and Quality Assurance. NCHRP-IDEA Program Project Final Report. 2019(195).
69. Harvey JT, Tsai B-W. Effects of asphalt content and air void content on mix fatigue and stiffness. Transportation research record. 1996;1543(1):38-45.

70. ASTM International. ASTM D8225-19, Standard Test Method for Determination of Cracking Tolerance Index of Asphalt Mixture Using the Indirect Tensile Cracking Test at Intermediate Temperature. West Conshohocken, PA: American Society for Testing and Materials. 2019.
71. Perraton D, Di Benedetto H, Sauzéat C, De La Roche C, Bankowski W, Partl M, et al. Rutting of bituminous mixtures: wheel tracking tests campaign analysis. *Materials and structures*. 2011;44(5):969-86.
72. Brown E. Performance survey of superpave mixes. National Center for Asphalt Technology. 1998.
73. Im S, Zhou F. New and simpler cracking test method for asphalt mix designs. *Transportation Research Record*. 2017;2631(1):1-10.
74. Shu X, Huang B, Vukosavljevic D. Laboratory evaluation of fatigue characteristics of recycled asphalt mixture. *Construction and Building Materials*. 2008;22(7):1323-30.
75. Abedini H, Naimi S, Abedini M. Rheological properties of bitumen emulsion modified with NBR latex. *Petroleum Science and Technology*. 2017;35(15):1576-82.
76. Molenaar AA. Prediction of fatigue cracking in asphalt pavements: do we follow the right approach? *Transportation research record*. 2007;2001(1):155-62.
77. Seitllari A, Lanotte MA, Kutay ME. Calibration of the MEPDG rutting model: issues and consequences on rutting prediction. 2019.
78. Zhou F, Newcomb D, Gurganus C, Banihashemrad S, Park ES, Sakhaeifar M, et al. Experimental design for field validation of laboratory tests to assess cracking resistance of asphalt mixtures. NCHRP Project. 2016(9-57).

79. Yan C, Zhang Y, Bahia HU. Comparison between SCB-IFIT, un-notched SCB-IFIT and IDEAL-CT for measuring cracking resistance of asphalt mixtures. *Construction and Building Materials*. 2020;252:119060.
80. Cannone Falchetto A, Moon KH, Lee CB, Wistuba MP. Correlation of low temperature fracture and strength properties between SCB and IDT tests using a simple 2D FEM approach. *Road Materials and Pavement Design*. 2017;18(sup2):329-38.
81. El Khatib AK. Development of a performance-based test method for quantification of cracking potential in asphalt pavement materials. MSc thesis, Department of Civil and Environmental Engineering, University of Illinois at Urbana-Champaign. 2016.
82. Molenaar JMM. Performance related characterisation of the mechanical behaviour of asphalt mixtures. PhD thesis, Road and hydraulic Engineering Institute, Delft University of Technology. 2004.
83. Dong W, Charmot S. Proposed tests for cold recycling balanced mixture design with measured impact of varying emulsion and cement contents. *Journal of Materials in Civil Engineering*. 2019;31(2):04018387.
84. Booshehrian A, Mogawer WS, Bonaquist R. How to construct an asphalt binder master curve and assess the degree of blending between RAP and virgin binders. *Journal of Materials in Civil Engineering*. 2013;25(12):1813-21.
85. Petersen J, Robertson R, Branthaver J, Harnsberger P, Duvall J, Kim S, et al. Binder characterization and evaluation: Volume 1. Rep No SHRP-A-367, Strategic Highway Research Program, National Research Council, Washington, DC. 1994.
86. Xu Y, Zhang E, Shan L. Effect of SARA on Rheological Properties of Asphalt Binders. *Journal of Materials in Civil Engineering*. 2019;31(6):04019086.

87. City of Edmonton. Design and Construction standards, Volume 2: Roadways. Edmonton, Alberta. 2015.
88. SOLIMAN H, Shalaby, A., KASS, S., editor Overview of Specifications for Unbound Granular Base Materials in Selected Canadian Provinces and Neighbouring States. Transportation 2014: Past, Present, Future-2014 Conference and Exhibition of the Transportation Association of Canada. 2014.
89. AASHTO. T 85-91. Standard Method of Test for Specific Gravity and Absorption of Coarse Aggregate. Washington, D.C: American Association of State Highway and Transportation Officials. 2004.
90. ASTM International. ASTM D698-12, Standard test methods for laboratory compaction characteristics of soil using standard effort. West Conshohocken, PA.: American Society of Testing and Materials. 2012.
91. Husky Asphalt. Specification and typical analyses of CSS-1H emulsified asphalt, product 573. Saskatoon, Canada. 2019.
92. ASTM International. ASTM D6560, Standard Test Method for Determination of Asphaltenes (Heptane Insolubles) in Crude Petroleum and Petroleum Products. West Conshohocken, PA: American Society for Testing and Materials. 2012.
93. ASTM International. ASTM D2007, Fractionation of Crudes by SARA Analysis. West Conshohocken, PA: American Society for Testing Materials. 2000.
94. ASTM International. ASTM D5 / D5M-20 Standard Test Method for Penetration of Bituminous Materials. West Conshohocken, PA: American Society for Testing and Materials. 2020.

95. AASHTO. PP 72-11, Standard Practice for Recovering Residue from Emulsified Asphalt Using Low Temperature Evaporative Technique. Washington, D.C.: American Association of State Highway and Transportation Officials. 2013.
96. Aziz MMA, Rahman MT, Hainin MR, Bakar WAWA. An overview on alternative binders for flexible pavement. *Construction and Building Materials*. 2015;84:315-9.
97. Oil sands glossary, Alberta Oil Sands [Available from: <https://www.alberta.ca/oil-sands-glossary.aspx>].
98. Lesueur D. The colloidal structure of bitumen: Consequences on the rheology and on the mechanisms of bitumen modification. *Advances in colloid and interface science*. 2009;145(1-2):42-82.
99. Yang C, Xie J, Wu S, Amirkhanian S, Zhou X, Ye Q, et al. Investigation of physicochemical and rheological properties of SARA components separated from bitumen. *Construction and Building Materials*. 2020;235:117437.
100. Michalica P, Kazatchkov IB, Stastna J, Zanzotto L. Relationship between chemical and rheological properties of two asphalts of different origins. *Fuel*. 2008;87(15-16):3247-53.
101. Little DN, Nair S. Recommended practice for stabilization of subgrade soils and base materials. 2009.
102. Wegman DE, Sabouri M, Korzilius J, Kuehl R, Intertec B. Base Stabilization Guidance and Additive Selection for Pavement Design and Rehabilitation. Minnesota. Dept. of Transportation. Research Services Section. 2017.
103. Husky Energy. Specification and typical analyses for 80/100A PEM asphalt binder, product 0330. Canada. 2018.

104. ASTM International. ASTM D70-09, Standard Test Method for Density of Semi-Solid Bituminous Materials (Pycnometer Method). West Conshohocken, PA: American Society for Testing and Materials. 2009.
105. ASTM International. ASTM D92, Standard test method for flash and fire points by Cleveland open cup tester. West Conshohocken, PA: American Society of Testing and Materials. 2016.
106. ASTM International. ASTM D113-17 Standard Test Method for Ductility of Asphalt Materials. West Conshohocken, PA: American Society for Testing and Materials. 2017.
107. ASTM International. ASTM D2042-15 Standard Test Method for Solubility of Asphalt Materials in Trichloroethylene. West Conshohocken, PA: American Society for Testing and Materials. 2015.
108. ASTM International. ASTM D 2171/ D 2171M-18, Standard test method for viscosity of asphalts by vacuum capillary viscometer. West Conshohocken, PA: American Society for Testing and Materials. 2018.
109. ASTM International. ASTM D4402 / D4402M-15, Standard test method for viscosity determination of asphalt at elevated temperatures using a rotational viscometer. West Conshohocken, PA: American Society for Testing and Materials. 2015.
110. ASTM International. ASTM D 1754 / D1754M-09, Standard Test Method for Effects of Heat and Air on Asphaltic Materials (Thin-Film Oven Test). West Conshohocken, PA: American Society for Testing and Materials. 2014.
111. ASTM International. ASTM D 6937-16, Standard Test Method for Determining Density of Emulsified Asphalt. West Conshohocken, PA: American Society for Testing and Materials. 2016.

112. AASHTO. T 59-16, Standard method of test for Emulsified Asphalts. Washington, D.C: American Association of State Highway and Transportation Officials. 2016.
113. ASTM International. ASTM D6997-12, Standard Test Method for Distillation of Emulsified Asphalt. West Conshohocken, PA: American Society of Testing and Materials. 2012.
114. ASTM International. ASTM D 7496-18, Standard Test Method for Viscosity of Emulsified Asphalt by Saybolt Furol Viscometer. West Conshohocken, PA: American Society for Testing and Materials. 2018.
115. ASTM International. ASTM D88-07, Standard Test Method for Saybolt Viscosity. West Conshohocken, PA: American Society for Testing and Materials. 2007.
116. ASTM International. ASTM D6933-18, Standard Test Method for Oversized Particles in Emulsified Asphalts (Sieve Test). West Conshohocken, PA: American Society for Testing and Materials. 2018.
117. ASTM International. ASTM D6930-19, Standard Test Method for Settlement and Storage Stability of Emulsified Asphalts. West Conshohocken, PA: American Society for Testing and Materials. 2019.
118. ASTM International. ASTM D7402-09 Standard Practice for Identifying Cationic Emulsified Asphalts. West Conshohocken, PA: American Society for Testing and Materials. 2017.
119. AASHTO. T 49-15, Standard method of test for Penetration of Bituminous Materials. Washington, D.C: American Association of State Highway and Transportation Officials. 2017.

120. AASHTO. T 51-09, Standard method of test for Materials for Ductility of Asphalt Materials. Washington, D.C: American Association of State Highway and Transportation Officials. 2013.
121. AASHTO. T 44-14, Standard method of test for Materials for Solubility of Bituminous Materials. Washington, D.C: American Association of State Highway and Transportation Officials. 2017.
122. VC Tek Inc. Summary of key tests on Asphaltenes. Calgary, AB, Canada. 2006.
123. ASTM International. ASTM D4055-04 Standard Test Method for Pentane Insolubles by Membrane Filtration. West Conshohocken, PA: American Society for Testing and Materials. 2019.
124. ASTM International. ASTM D5865 / D5865M-19 Standard Test Method for Gross Calorific Value of Coal and Coke. West Conshohocken, PA: American Society for Testing and Materials. 2019.
125. ASTM International. ASTM D4530-15 Standard Test Method for Determination of Carbon Residue (Micro Method). West Conshohocken, PA: American Society for Testing and Materials. 2015.
126. AASHTO. T 324-17, Hamburg Wheel-Track Testing of Compacted Asphalt Mixtures. Washington, D.C.: American Association of State Highway and Transportation officials. 2017.
127. Ang-Olson J, Schroeer W. Energy efficiency strategies for freight trucking: potential impact on fuel use and greenhouse gas emissions. Transportation Research Record. 2002;1815(1):11-8.

128. Al-Qadi I, Elseifi M, Yoo P. Pavement damage due to different tires and vehicle configurations. Final Report submitted to Michelin Americas Research and Development Corporation. 2004;515.
129. Al-Qadi IL, Hernandez JA, Gamez A, Ziyadi M, Gungor OE, Kang S. Impact of wide-base tires on pavements: a national study. *Transportation research record*. 2018;2672(40):186-96.
130. Al-Qadi IL, Loulizi A, Janajreh I, Freeman TE. Pavement response to dual tires and new wide-base tires at same tire pressure. *Transportation Research Record*. 2002;1806(1):38-47.
131. Al-Qadi IL, Yoo PJ, Elseifi MA, Janajreh I. Effects of tire configurations on pavement damage. *Journal of the Association of Asphalt Paving Technologists*. 2005;74(1):921-61.
132. Elseifi MA, Al-Qadi IL, Yoo PJ, Janajreh I. Quantification of pavement damage caused by dual and wide-base tires. *Transportation research record*. 2005;1940(1):125-35.
133. Papagiannakis A, Haas R, editors. Wide base truck tires: industry trends and state of knowledge of their impact on pavements. Roads and Transportation Association of Canada Conference, Ottawa. 1987.
134. Ponniah J. Use of New Technology Single Wide-Base Tires: Impact on Pavements. Final Report Ontario Ministry of Transportation Engineering Standards Branch Report. 2003.
135. Greene J, Toros U, Kim S, Byron T, Choubane B. Impact of wide-base single tires on pavement damage. *Transportation research record*. 2010;2155(1):82-90.
136. Group GC. Economic Study Use of Supersingle Tires by Heavy Vehicles Operating in Quebec. Report published by GENIVAR Consulting Group Montreal, QC, Canada. 2005.

137. Sebaaly PE. Pavement damage as related to tires, pressures, axle loads, and configurations. *Vehicle, Tire, Pavement Interface*: ASTM International. 1992.
138. Al-Qadi IL, Wang H. Pavement damage due to different tire and loading configurations on secondary roads. NEXTRANS Center (US). 2009.
139. Hernandez JA, Gamez A, Al-Qadi IL. Effect of wide-base tires on nationwide flexible pavement systems: Numerical modeling. *Transportation Research Record*. 2016;2590(1):104-12.
140. Hernandez JA. Development of deformable tire-pavement interaction: contact stresses and rolling resistance prediction under various driving conditions: University of Illinois at Urbana-Champaign. 2015.
141. Himeno K, Kamijima T, Ikeda T, Abe T, editors. Distribution of tire contact pressure of vehicles and its influence on pavement distress. *Eighth International Conference on Asphalt Pavements* Federal Highway Administration. 1997.
142. Anghelache G, Moisescu R, Sorohan Ş, Bureţea D. Measuring system for investigation of tri-axial stress distribution across the tyre-road contact patch. *Measurement*. 2011;44(3):559-68.
143. De Beer M, Fisher C. Stress-In-Motion (SIM) system for capturing tri-axial tyre-road interaction in the contact patch. *Measurement*. 2013;46(7):2155-73.
144. Akram T, Scullion T, Smith R, Fernando E. Estimating damage effects of dual vs. wide base tires with multidepth deflectometers. *Transportation Research Record*. 1992;1355.

145. Sharp K, Sweatman P, Potter D, editors. The comparative effects of dual and wide single tyres on pavement response. Australian Road Research Board (ARRB) Conference, 13th, 1986, Adelaide, Australia. 1986.
146. Grellet D, Doré G, Bilodeau J-P. Comparative study on the impact of wide base tires and dual tires on the strains occurring within flexible pavements asphalt concrete surface course. *Canadian Journal of Civil Engineering*. 2012;39(5):526-35.
147. Al-Qadi IL, Wang H. Full-depth pavement responses under various tire configurations: Accelerated pavement testing and finite element modeling. *Journal of the Association of Asphalt Paving Technologists*. 2009;78:721-60.
148. Ann Myers L, Roque R, Ruth BE, Drakos C. Measurement of contact stresses for different truck tire types to evaluate their influence on near-surface cracking and rutting. *Transportation Research Record*. 1999;1655(1):175-84.
149. Yoo P, Al-Qadi IL, Elseifi M, Janajreh I. Flexible pavement responses to different loading amplitudes considering layer interface condition and lateral shear forces. *The International Journal of Pavement Engineering*. 2006;7(1):73-86.
150. Al-Qadi IL, Wang H. Evaluation of pavement damage due to new tire designs. Illinois Center for Transportation (ICT). 2009.
151. Kj B. Finite element procedures in engineering analysis. Prentice-Hall Inc. Englewood Cliffs, NJ. 1982.
152. Yoo PJ, Al-Qadi IL. Effect of transient dynamic loading on flexible pavements. *Transportation Research Record*. 2007;1990(1):129-40.

153. Bayat A. Field and numerical investigation to determine the impact of environmental and wheel loads on flexible pavement. 2009.
154. Group YM. Monthly weather forecast and climate. 2020 [Available from: /web/20200521190122/<https://www.weather-ca.com/en/canada/calgary-climate>].
155. Mohseni A. LTPP seasonal asphalt concrete (AC) pavement temperature models. United States. Federal Highway Administration. Office of Engineering. 1998.
156. Cross SA, Jakatimath Y, KC S. Determination of dynamic modulus master curves for Oklahoma HMA mixtures. Oklahoma State University. 2007.
157. Guide for Mechanistic-Empirical Design, Part 2. Design Inputs, Chapter 2. Material Characterization: National Cooperative Highway Program. 2004.
158. Shafiee MH, Hashemian L, Bayat A. Seasonal Analysis of Flexible Pavement Response to Falling Weight Deflectometer. International Journal of Pavement Research & Technology. 2015;8(5).
159. Alberta Transportation. Pavement design manual. Alberta Transportation and Utilities. 1997.

Appendix A

Investigation of the Impact of Tire Configurations on Different Pavement Structures using Finite Element Analysis

ABSTRACT

In this research, three-dimensional (3D) finite element (FE) models are developed and validated to investigate the impact of new generation wide base tires (NGWBT) and dual tire assemblies (DTA) on different pavement structures. The actual tire-pavement interaction, including the dimensions and shape of the contact area, as well as the contact stress distribution over the contact area, is considered for each load case for both NGWBT and DTA. The impact of each tire type on four pavement structures – arterial, transit collector, non-transit collector, and full-depth asphalt – in the City of Calgary is evaluated, taking into account the viscoelastic behavior of asphalt. Typical climatic conditions (average monthly temperature) for Calgary are also included in the model. Using the 3D FE model, the strain values at critical locations (tensile strain at the bottom of asphalt layer and vertical strain on top of the subgrade) are calculated and used to perform pavement damage analysis. From the calculated strain ratios (NGWBT/DTA), it was found that the weaker the pavement structure, the higher the strains within different pavement layers for NGWBT. Combined damage ratio (CDR) values for both pavement fatigue and rutting are calculated to compare the damage of NGWBT against DTA at different NGWBT market penetration rates. Normalized CDR values ranged from from 1.057 (in the strongest section) to 1.115 (in the weakest section) for a NGWBT market penetration of 20%.

INTRODUCTION

Road systems are an important component of Canada's infrastructure, connecting the country coast to coast as a vital means of transportation. Heavy trucks are used to transport goods on roadways, causing rapid pavement deterioration due to increased truck axle loading and high tire inflation pressure, with pavement damage exacerbated by extreme weather conditions. Modifications have been made to truck tires to improve transportation efficiency, minimize

the impact of high loading on pavement, and reduce costs. One innovation is the introduction of wide base tires to replace dual tires.

First-generation wide base single tires (FGWBT), with tread widths of 385 mm and 425 mm, were introduced in the early 1980s as an alternative to the traditional dual-tire assembly (DTA). FGWBT have advantages over DTA, including lighter weight, better fuel efficiency (127), reduced greenhouse gas emissions, improved handling and braking, less maintenance and reduced cost (128). However, despite the benefits, the impact of wide base tires on road infrastructure has been a major concern since the introduction of FGWBT (129). The behavior of flexible pavements is dependent on the magnitude and frequency of the traffic load imposed on the pavement surface. The traffic loads are transferred to the base structure through the tire/pavement contact area, which depends on multiple factors, including the type, structure, size, and configuration of the tire (130). Although wide base tires were designed to comply with pavement regulations, previous studies conclude that FGWBT significantly increase pavement damage compared to DTA (131, 132).

To overcome this disadvantage, new generation wide base single tires (NGWBT) were introduced. NGWBT are wider than FGWBT (133), with tread widths of 445 mm (445/50R22.5) and 455 mm (455/55R22.5). A report by Ponniah for the Ontario Ministry of Transportation (134) showed that the impact of NGWBT with an axle load of 8,000 kg is same as the impact caused by conventional dual tires (10,000 kg load). NGWBT are increasingly common because of the advantages to the trucking industry, including reduced maintenance cost, increased fuel efficiency, reduced tire noise, etc. (135). Many studies have been done to determine the actual benefits of wide base tires in terms of cost. The results of a study conducted by Genivar for the Ministry of Transportation Quebec suggest that NGWBT consume less fuel due to reduced rolling resistance, have a longer service life, and also have a good safety record (reduced collisions and fatalities) (136).

Due to different stress distributions at the tire-pavement interface (137, 138), a detailed study on NGWBT is needed to analyze their impact on pavements. The modelling of pavement response is complex due to increased truck loading, modification in pavement materials and typical tire designs (139). Currently, to quantify the effects of various tire and wheel load

configurations on pavement performance, there are two major approaches: full-scale field tests and finite element analysis. Full-scale field tests can provide reliable results. However, advancements in computational efficiency have allowed for finite element analysis with satisfying accuracy, with less cost and time expenditure. Due to this, finite element analysis methods have become increasingly attractive to researchers.

Despite the high cost and relatively large amount of time needed for full-scale field tests, significant efforts have been made to measure 3D contact stresses and/or critical strains directly in pavement layers (140-143), which provide convincing, reliable results and analysis aimed at predicting pavement damage. Full-scale field tests can provide efficient guidance for pavement design. Some field studies have previously been carried out on FGWBT to analyze the impact on pavement structure, and these are summarized below. In 1992, research conducted by Akram et al. (144) focused on assessing the damage induced by dual tires and FGWBT using a multi-depth deflectometer on two different sections of asphalt concrete highway to measure the impact of tire on the pavement. The results of the study indicate that FGWBT causes more pavement deflection than dual tires. It also found that wide base single tires are more prone to cause damage to the pavement structure. For instance, on the thin pavement section (11.5 inches), FGWBT were determined to cause 4.8 times more damage than dual tires, whereas on the thick pavement section (27 in), FGWBT caused 2.2 times more damage (144). Based on the study, it was observed that the maximum deflection for wide base tires occurs under the center line of the tire, whereas for dual tires, the maximum deflection occurs under each of the two tires (144, 145). A similar field study conducted by Sebaaly (137) demonstrated that 385/65R22.5 FGWBT produce 20% more strain response at bottom of the asphalt layer than dual tires for a thin flexible pavement section (14 in). From this study, it was concluded that wide base single tires cause more damage to the flexible pavement structure than dual tires (137).

Current studies focus on finite element (FE) analysis to determine the impact of different tire types on pavement structures. In one such study, the pavement damage caused by dual tires, as well as 445/50R22.5 and 455/55R22.5 NGWBT tires was analyzed using three-dimensional FE analysis (132). It was reported that 445/50R22.5 NGWBT increased the damage ratio by 19% at a vehicle speed of 105 km/h compared to conventional dual tires. In contrast, the

damage ratio is 7% for 455/55R22.5 NGWBT (132). Al-Qadi and Wang (138) conducted a study using a three-dimensional FE model to analyze five different failure mechanisms that results in pavement damage on secondary roads. The results of this study indicated that NGWBT caused 1.12 to 1.38 times more damage than conventional dual tires. Compared to conventional dual tires, 455/55R22.5 NGWBT caused 1.94 to 2.50 times more fatigue damage, 1.31 to 2.35 more subgrade rutting, and 1.35 to 1.77 times more HMA rutting (densification). In the case of shear stresses, 455/55R22.5 NGWBT result in a 19% to 78% decrease in HMA rutting (shear) and 4% to 31% less base shear failure (138). Furthermore, 455/55R22.5 NGWBT increases tensile strain by 14% to 30% at the bottom of asphalt concrete layer. However, at shallow depths, tensile strains decreased by 20% near the edge of the tire (146).

The effects of heavy trucks, including tire type and loading levels, on pavement performance, are directly reflected in the distribution of 3D contact stresses. While analyzing pavement damage, it is necessary to consider the different contact stress distributions caused by each tire type. There are three main contact stress components: vertical, transverse, and longitudinal stresses are all generated by vehicular loading on the pavement structure. This three-dimensional computation of tire stresses causes a complex stress state on the pavement surface, which increases the likelihood of pavement damage, including top-down cracking, near-surface cracking and HMA rutting (147, 148). In addition, it is necessary to consider a continuous loading amplitude and non-uniform pressure distribution to simulate a moving wheel. Finally, taking into account the surface shear forces and appropriate layer interface friction improves the ability of FE models to analyze pavement response to vehicular loading (149).

The 3D contact stresses generated at the tire/pavement interface generally have a non-uniform distribution. Accurate characterization of the 3D tire-pavement contact stresses is of paramount importance in pavement response analysis. In the mechanistic-empirical pavement design guide (MEPDG), a circular contact area with constant vertical contact stress was initially used to calculate the mechanical pavement response, without considering shear contact stresses (150). Also, the constant vertical contact stress is usually simplified by using

tire inflation pressure. However, experimental measurements of tire imprints result in shapes that are far from circular, especially for NGWBT.

In addition to the tire configuration, other parameters, including pavement layer thicknesses, climatic conditions, and traffic load, play important roles in pavement damage analysis. Each of these parameters varies according to local conditions. Thus, it is important that studies are conducted based on local conditions to compare the difference in pavement performance for NGWBT and DTA. As a result, a specific analysis is required for each case, including the Calgary pavement structures introduced in this research.

OBJECTIVE AND METHODOLOGY

The objective of this research is to evaluate and compare the impact of NGWBT and DTA on four different pavement structures in the Calgary region, considering local climatic conditions (average monthly temperature). To achieve this, the response of the four pavement structures with varying asphalt layer thickness – arterial, transit collector, non-transit collector, and full-depth asphalt – under loading conditions for NGWBT and DTA was required. The parameters related to each pavement structure in the FE model were set according to the specifications received from the City of Calgary.

For this purpose, 3D FE models were developed and implemented to analyze the problem for each pavement structure and each month of the year. The viscoelastic behaviour of asphalt was taken into account by considering vehicle speed and average asphalt temperature for each month.

The FE simulation approach involves creating a load case (i.e. maximum payload weights) for each of the tire configurations. Each load case takes into account the actual tire-pavement interaction, including the actual dimensions and shape of the contact area, as well as the contact stress distribution over the contact area taken from experimental measurements reported in the literature (149). Load cases for each tire configuration are then used to model the response of each pavement configuration. The strain values at critical locations (that is, the tensile strain at the bottom of the asphalt layer and vertical strain at the top of the subgrade) are calculated and used for the pavement damage analysis. Based on this, strain ratios

(NGWBT/DTA), combined damage ratios (CDR) due to pavement fatigue and rutting, and normalized CDR are determined.

FINITE ELEMENT ANALYSIS

In this study, four different pavement structures for the Calgary region, shown in Figure-1, have been simulated by using the FE software Abaqus (2017 version). These are the structures for the arterial, transit collector, non-transit collector, and full-depth asphalt, with asphalt concrete pavement (ACP) thicknesses of 200 mm, 160 mm, 140 mm, and 200 mm, respectively. The thickness of the granular base course (GBC) in the arterial, transit collector, and non-transit collector is 150 mm. The full-depth asphalt section does not include a GBC layer.

Model Description

Geometry

The general layout for the FE models developed in this work is shown in Figure-2. The x-y dimensions of the model are 2100 mm by 2100 mm. This is large enough that the effect of boundary conditions at the vertical edges of the model can be ignored for analyzing the pavement response under tire loading. In other words, the induced stresses and strains in the pavement layers under the tire-pavement contact area are not considerably influenced by changes in boundary conditions. The dimensions in the depth direction (z-axis) for each specific structure are shown in Figure-1.

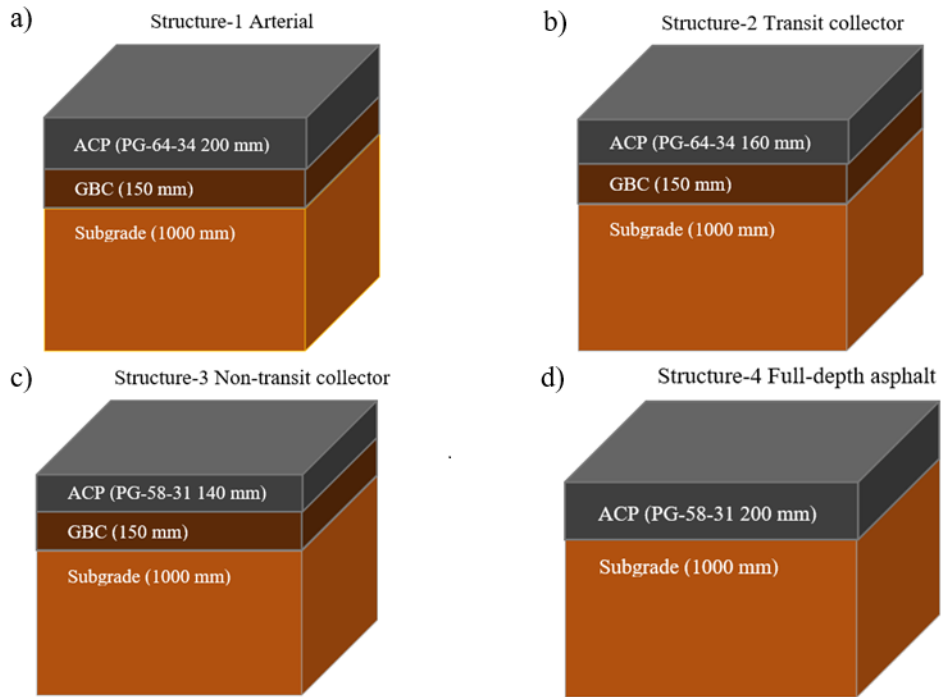


Figure-1 Schematic illustration of pavement structures used in the FE modelling including (a) arterial section, (b) transit collector section, (c) non-transit collector section, and (d) full-depth asphalt

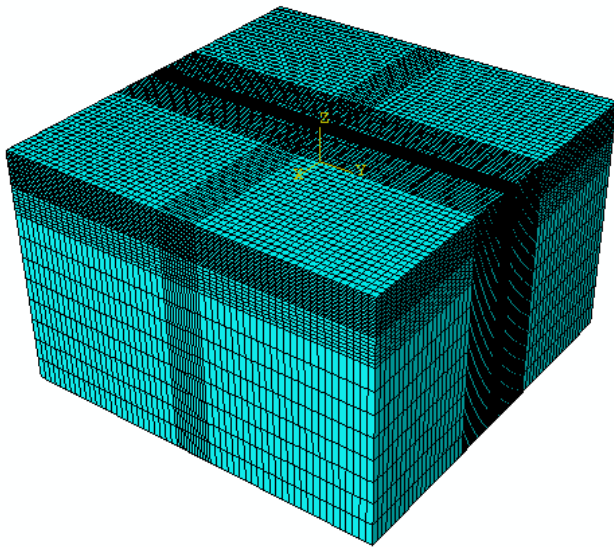


Figure-2 General layout of FE models

Meshing Information

The element type used in the current FE model is the 8-node brick element C3D8R. Generally, a finer mesh is employed near the loading area, while relatively larger element sizes are applied for areas further out. The strains at the bottom of the ACP layer are important outputs of the model. To obtain more accurate results, a finer mesh was applied in the depth direction for the ACP layer, whereas the GBC and subgrade were meshed with relatively larger element sizes. A typical mesh in the x-y plane under DTA and NGWBT loading is shown in Figure-3. The length and width of each element away from the loading area is 36 mm. In the loading area, the length of the elements along the transverse and traffic directions is dictated by the tire rib and groove geometries. For all models in this work, these dimensions are smaller than 20 mm. Furthermore, these element sizes match the sizes reported in the literature (128, 149, 150).

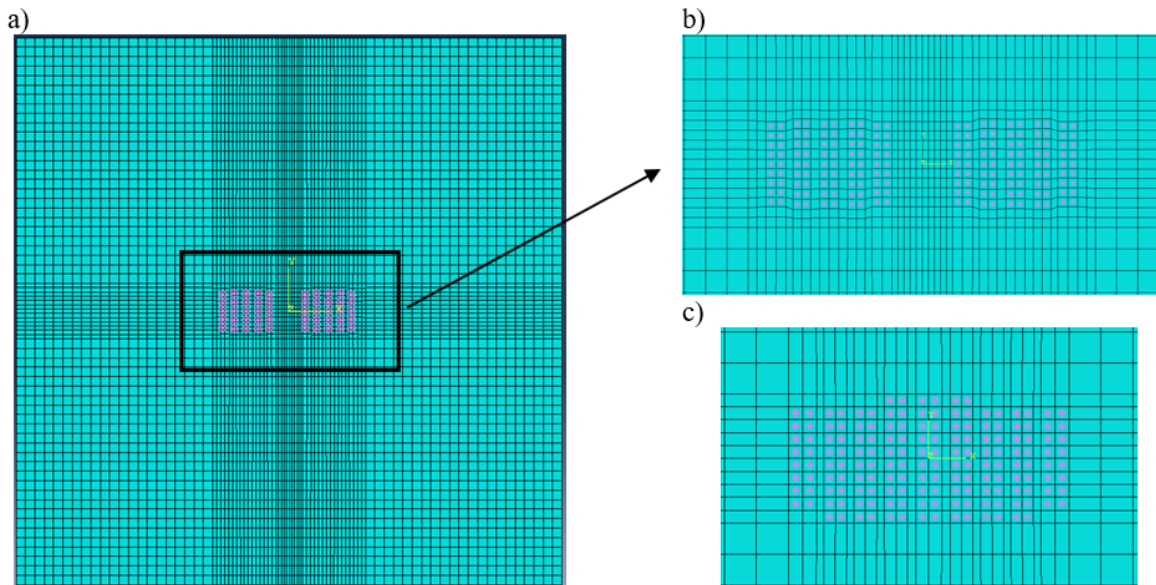


Figure-3 Meshing details in the x-y plane, a) for the entire model under DTA loading, b) for the DTA loading area, and c) for the NGWBT loading area

Convergence Check

In the literature, the continuity of stress across inter-element boundaries has been introduced as a measure for checking the convergence of FE solutions (151). This criterion has been used in previous studies investigating pavement behaviour using FE analysis (128). To check the convergence of the results, different element thicknesses were used in the FE models. The

mesh introduced in the previous section is similar for all layers in the depth direction. Table-1 represents the element thickness in the ACP layer, total number of elements, total number of nodes, vertical stress at the bottom of the ACP layer, and vertical stress jump at the interface between the ACP and GBC layers for each model under a 38 kN load applied by a NGWBT, using the average temperature for January. To ensure accuracy, the non-transit collector structure, which has the lowest ACP layer thickness, was chosen to investigate the convergence of the FE solution. It can be observed that by refining the mesh, the stress jump at the ACP-GBC interface decreases. Considering the maximum load applied to the pavement under the fifth rib of the NGWBT – 956 kPa – the stress jumps vary from 3.09% of the maximum load for an element thickness of 20 mm to 0.47% of the maximum load for an element thickness of 8.7 mm. This range of accuracy is adequate for investigating the pavement response for different tire types. To give a high level of accuracy, an element thickness of 10 mm was chosen for modelling in the ACP layer in this work. Figure-4 illustrates the longitudinal strain at the bottom of the ACP layer for various element thicknesses, demonstrating that the results have converged at an element thickness of 10 mm. After performing the same procedure in the GBC layer, an element thickness of 18.75 mm was selected for meshing the GBC layer of the model.

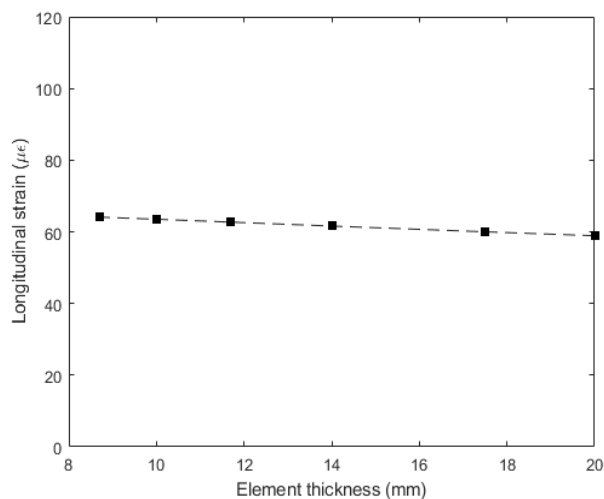


Figure-4 Convergence of longitudinal strain at bottom of ACP layer.

TABLE-1 Convergence check for ACP layer

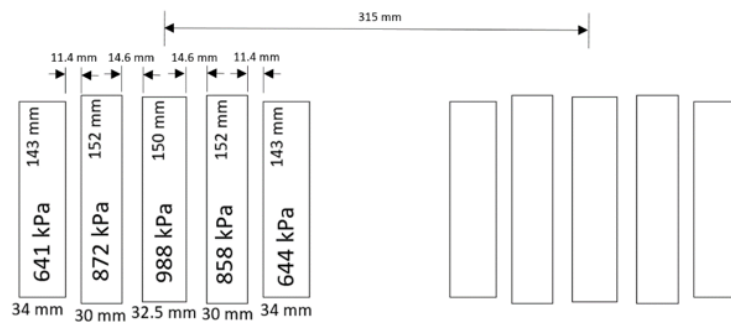
Case	Element Thickness (mm)	Total Number of Elements	Total Number of Nodes	Vertical Stress at Bottom of	Stress Jump at ACP-GBC

				ACP Layer (kPa)	interface (kPa)
1	20	66240	77714	76.7	29.5
2	17.5	69120	80703	63.8	16.5
3	14	74880	86681	57.9	10.6
4	11.7	80640	92659	54.8	7.6
5	10	86400	98637	52.9	5.7
6	8.7	92160	104615	51.7	4.5

Contact Area and Loading Information

For analysis of pavement behaviour under loading from different tire types, it is important to consider the actual tire-pavement interaction, including the dimension and shape of the contact area, and the contact stress distribution over the contact area. In the current research, tire imprints are taken from reported field measurements (149), as shown in Figure-5. The magnitude of the reported loading is equal to a 38 kN wheel load. Contact areas have been measured under a nominal tire pressure of 720 kPa. Due to the lack of field measurements at different temperatures, it is assumed that the loading area remains constant and does not vary with temperature. Furthermore, due to a lack of detailed information about shear contact stresses, it was deemed sufficient to consider vertical contact stresses for the purpose of this work.

a)



b)

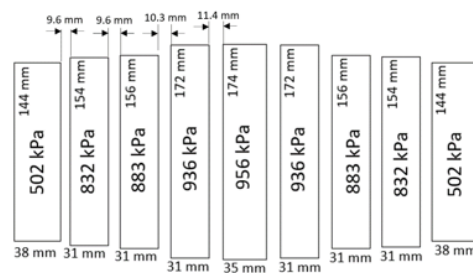


Figure-5 Tire footprints and loading information for a) DTA, and b) NGWBT

Boundary Conditions

At the bottom surface of the model, the displacements are fixed, and a traction-free boundary condition is assumed along the vertical edges. To improve computational efficiency, friction was defined at the ACP-GBC interface, and a tie (fully bounded) boundary condition was applied at the GBC-subgrade interface. In the literature, it is mentioned that a fully bounded boundary condition at the interface between the asphalt layer and GBC may result in underestimation of the strains, leading to compressive strains where tensile strains exist. However, if the bonding is inadequate, this may significantly increase strains throughout the pavement. In this work, a surface to surface contact was defined at the ACP-GBC interface layer, and a simple friction boundary condition with a coefficient of friction of 0.5 was used. This value has previously been suggested for use at a base mixture-granular layer interface (149).

Analysis Type and Material Properties

Although pavement layers have been traditionally considered as linear elastic materials in earlier work, asphalt generally exhibits viscoelastic behavior. Two methods exist in the literature for considering the viscoelastic behavior of asphalt. In the first method, viscoelastic parameters are determined by performing laboratory tests and back-calculations. These parameters include dimensionless relaxation modulus, dimensionless bulk relaxation modulus, and relaxation time (152). Creep tests should be performed to obtain these properties at different temperatures. In cases where the time-dependent parameters are known, they are used in dynamic models as inputs for material properties to represent the viscoelastic nature of the asphalt. In the second method, the elastic modulus of asphalt is determined using laboratory tests at different temperatures and loading frequencies. If the vehicle speed is given, the loading frequency can be determined using the pulse response of asphalt when a vehicle passes over a strain gauge. In this way, an equivalent linear elastic property can be estimated for asphalt at different temperatures and speeds, allowing the problem to be solved using static analysis. This method has been successfully applied to analyze pavement response at the test road in Waterloo, with good agreement between the model and field measurements

(153). Due to lack of details regarding material properties, the second method was employed to account for the viscoelastic nature of asphalt under loading conditions in this work.

The average air temperature for each month was calculated based on Calgary weather information (154). Mid-depth asphalt temperatures were calculated for each pavement structure using the Strategic Highway Research Program (SHRP) model, as in Equation 1 (155).

$$T_d = T_{air} + 0.051d - 0.000063d^2 \dots\dots\dots 1$$

Where, T_d , T_{air} , and d are the pavement temperature at the specified depth (°C), air temperature (°C), and depth (mm), respectively. A frequency of 10 Hz was used, corresponding to a vehicle speed of 60 km/h.

The pavement specifications were PG 58-31 for the full-depth and non-transit collector structures, and PG 64-34 for the arterial and transit collector structures. To increase the model accuracy, the influence of temperature on Poisson’s ratio for the asphalt layer was considered. Table-2 represents the material properties for PG 58-31 and PG 64-34, along with the layer thickness (for calculation of the mid-depth temperature for each month) (156-158). The elastic modulus of the GBC layer is assumed to be a constant value (200 MPa) year round for the pavement structures considered. The elastic modulus of the subgrade was calculated using seasonal factors as provided in the Alberta Transportation Pavement Design Manual (159), as in Table-2. It is assumed that Poisson’s ratio is equal to 0.35 and 0.45 in the GBC and subgrade, respectively, for all months (157).

TABLE-2 Asphalt elastic modulus, Poisson’s ratio, and subgrade modulus in different months

Month	Air Temperature (°C)	Asphalt Temperature (°C)			E (MPa)				Poisson’ s Ratio	Subgrade modulus (MPa)	
					PG 58-31		PG 64-34				
		200 mm ACP thick.	160 mm ACP thick.	140 mm ACP thick.	200 mm ACP thick.	140 mm ACP thick.	200 mm ACP thick.	160 mm ACP thick.		Arterial and Transit Collector	Full-Depth and Non-Transit Collector

Jan	-7	-2.5	-3.3	-3.7	21,962	23,082	22,899	23,617	0.2	100	150
Feb	-5	-0.5	-1.3	-1.7	20,171	21,244	21,139	21,828	0.2	100	150
Mar	-2	2.5	1.7	1.3	17,628	18,632	18,633	19,280	0.2	55	82.5
Apr	4.5	9.0	8.2	7.8	12,709	13,562	13,763	14,316	0.25	12.5	18.75
May	9.5	14.0	13.2	12.8	9,476	10,214	10,535	11,017	0.25	17.5	26.25
Jun	13.5	18.0	17.2	16.8	7,235	7,880	8,278	8,703	0.25	20	30
Jul	16.5	21.0	20.2	19.8	5,755	6,330	6,775	7,157	0.25	20	30
Aug	16	20.5	19.7	19.3	5,989	6,577	7,014	7,403	0.25	20	30
Sep	11	15.5	14.7	14.3	8,599	9,302	9,655	10,115	0.25	20	30
Oct	5.5	10.0	9.2	8.8	12,024	12,854	13,081	13,620	0.25	20	30
Nov	-2.5	2.0	1.2	0.8	18,039	19,055	19,040	19,693	0.2	40	60
Dec	-7	-2.5	-3.3	-3.7	21,962	23,082	22,899	23,617	0.2	80	120

Model Validation

To verify the FE model developed in this work, loads corresponding to DTA and NGWBT were applied to the Virginia Test Road pavement structure (149), and the longitudinal strains at the bottom of the base mix (BM-25) layer were compared against reported field measurements. The results of the current work indicate strain values of 60 $\mu\epsilon$ and 76 $\mu\epsilon$ for DTA and NGWBT, respectively. Field measurements (149) resulted in strain values of approximately 77 $\mu\epsilon$ and 95 $\mu\epsilon$ under DTA and NGWBT, respectively. The results of the current model are in good agreement with these experimental measurements. It is worth noting that the same level of accuracy exists between the numerical model and experimental measurements in Reference (149). Also, the difference in the NGWBT and DTA response is almost the same for experimental results and current FE model.

RESULTS AND DISCUSSIONS

Analysis of Pavement Response in Different Structures

The 3D FE model described in previous sections was implemented to simulate pavement response under DTA and NGWBT loading. The model outputs were determined for four different pavement structures within the City of Calgary. To consider the impact of temperature variation, the outputs are represented for each month. The parameters required for performing pavement damage analysis include the longitudinal strain at the bottom of the ACP layer, and the vertical strain at the top of subgrade (129). These parameters are presented as the outputs of the FE model for each structure. Figure-6 shows the longitudinal strain distribution with depth (z-axis) under DTA loading for the non-transit collector pavement structure in January as a typical result. The results for each pavement configuration will be presented in the following sections.

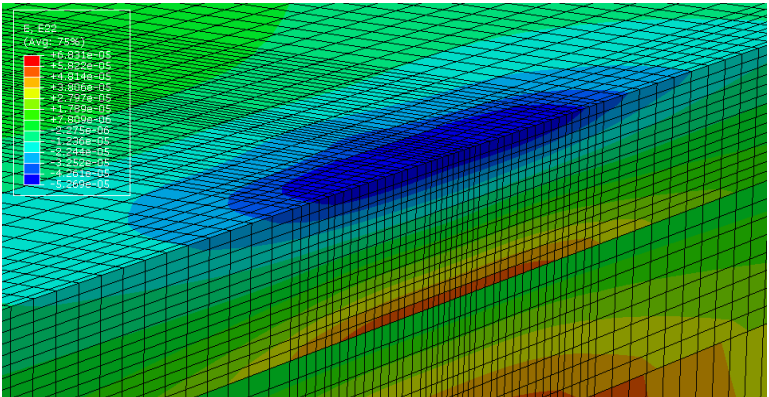


Figure-6 Typical result showing distribution of longitudinal strain under DTA loading for non-transit collector (January)

Figures-7-10 indicate the outputs of the model for each pavement structure. As a general trend, the induced strains are smaller in cold months, with the lowest values in January, and larger in warm months, with the highest values in July.

Higher strains are generated under NGWBT compared to DTA. The magnitude of this difference for longitudinal strains at the bottom of ACP layer, defined as $(\text{NGWBT} - \text{DTA})/\text{DTA}$, does not show significant changes in different months for the arterial (2.2%) and transit collector (2.9%) structures. However, the variation is wider for the non-transit collector (4%) and full-depth asphalt (6.2%) structures. The lowest and highest differences observed correspond to the months of April and February, respectively.

From comparison of longitudinal strains, it can be observed that NGWBT induce higher strains (~13.8%) than traditional DTA in the arterial structure. In the transit collector and non-transit collector structures, NGWBT also result in higher longitudinal strains, about 15.9% and 18.3%, respectively. The increase in the difference in the pavement response under NGWBT and DTA for transit and non-transit collector structures is expected, since the thickness of the ACP layers is lower for these pavement structures compared to the arterial structure. Finally, NGWBT resulted in higher longitudinal strains – from 9.5% (in April) to 15.7% (in February) – in the full-depth asphalt structure compared to DTA.

Arterial Structure

The arterial configuration, which includes 200 mm ACP and 150 mm GBC, has the strongest structure studied in this work. The longitudinal strain at the bottom of ACP and vertical strain at the top of subgrade for the arterial structure are illustrated in Figure 7a and 7b, respectively. The longitudinal strains induced under NGWBT for this structure are on average 13.8% higher than the strains for DTA.

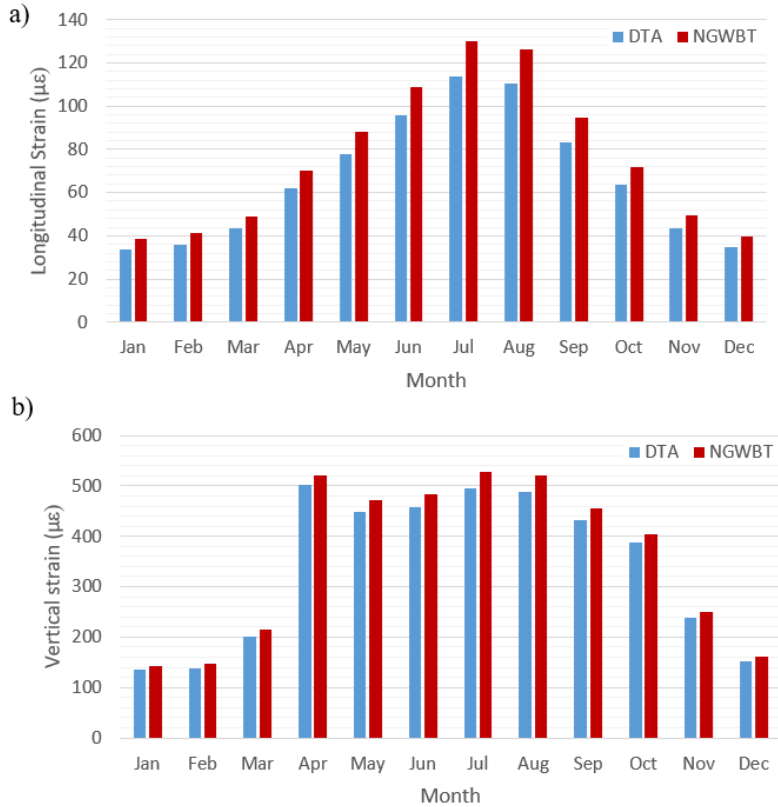


Figure-7 Comparison of a) longitudinal strains at bottom of ACP layer, and b) vertical strains at top of subgrade induced by DTA and NGWBT in the arterial structure

Transit Collector Structure

The transit collector configuration, which includes 160 mm ACP and 150 mm GBC, is weaker than the arterial structure. The strains at the bottom of the ACP layer and top of the subgrade are indicated in Figure-8a and 8b, respectively. The longitudinal strains induced by NGWBT are ~15.9% higher than strains for DTA in the transit collector structure, which is a 2.1% larger difference than for the arterial configuration.

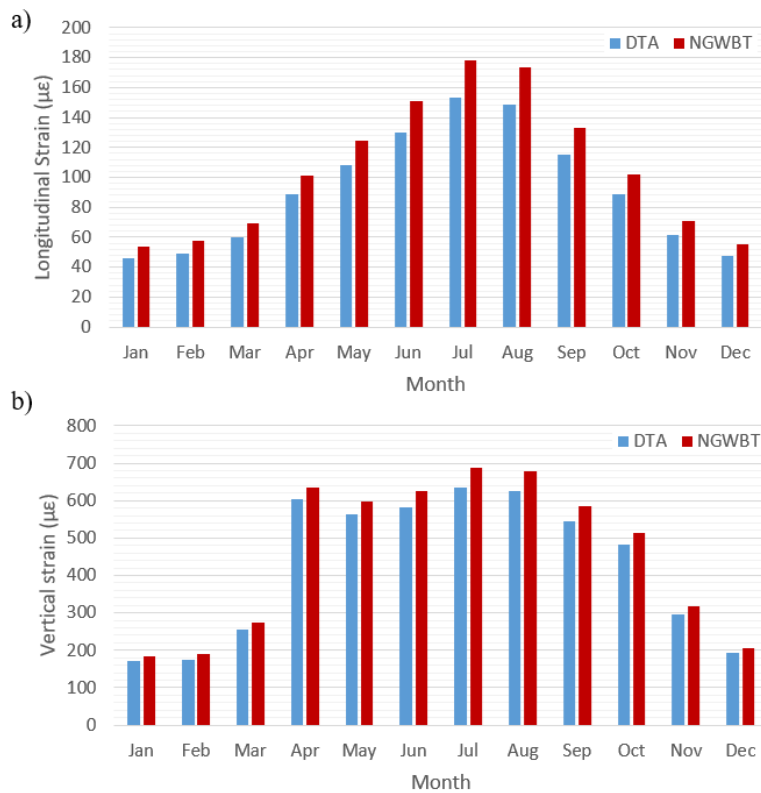


Figure-8 Comparison of a) longitudinal strain at bottom of ACP layer, and b) vertical strain at top of subgrade induced by DTA and NGWBT in the transit collector structure

Non-Transit Collector Structure

The non-transit collector structure, which includes 140 mm ACP and 150 mm GBC, is more prone to damage since the ACP layer thickness is smaller compared to the arterial and transit collector structures. The strains at the bottom of the ACP layer and top of the subgrade are

illustrated for in Figure-9a and 9b for this structure, respectively. The longitudinal strains induced by NGWBT are on average 18.3% higher than the strains induced by DTA for the non-transit collector structure, which are 2.4% and 4.5% larger than the difference observed for the transit collector and arterial configurations, respectively.

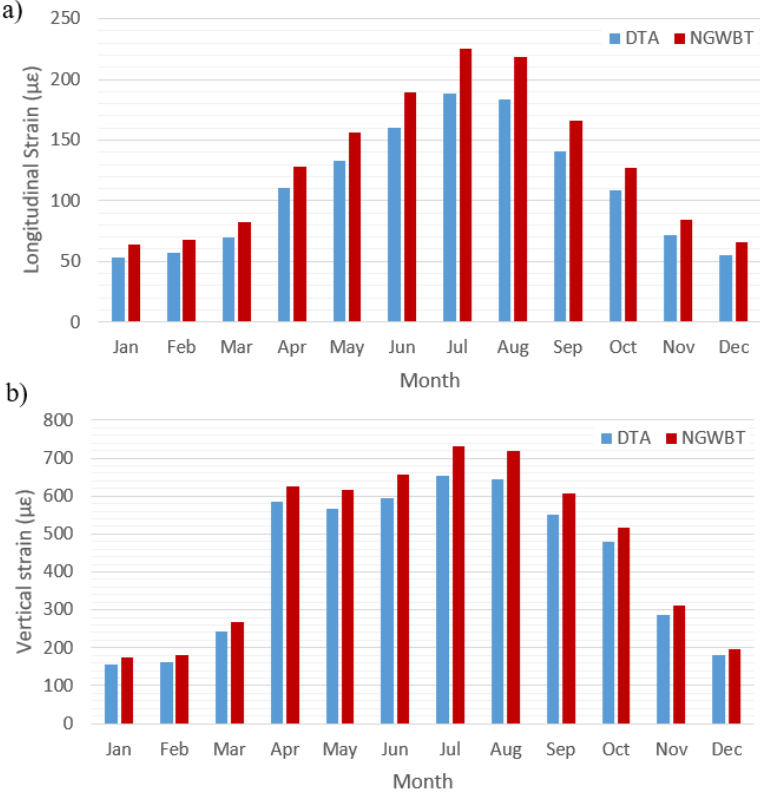


Figure-9 Comparison of a) longitudinal strains at bottom of ACP layer, and b) vertical strains at top of subgrade induced by DTA and NGWBT in the non-transit collector structure

Full-Depth Asphalt Structure

The full-depth asphalt structure has a 200 mm thick layer of ACP on top of the subgrade. There is no GBC layer in this pavement design. The strains at the bottom of ACP and top of the subgrade are shown in Figure-10a and 10b, respectively. The induced longitudinal strains under NGWBT are on average 12.8% higher than strains under DTA in this structure. However, the magnitude of difference in pavement response between NGWBT and DTA loading varies in a wider range compared to the other pavement structures (NGWBT gives 15.7% higher longitudinal strains than DTA in February, and 9.5% higher in April).

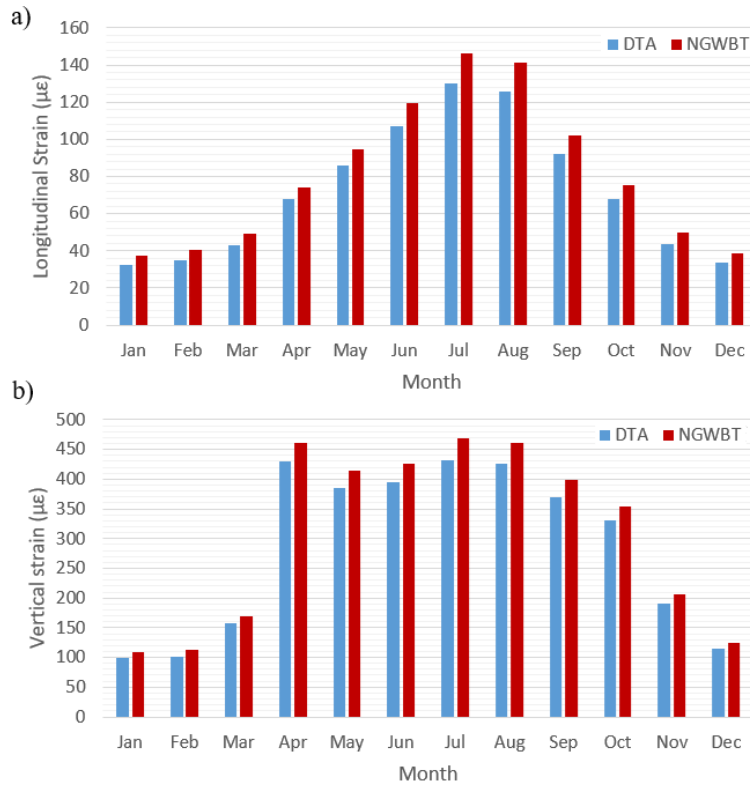


Figure-10 Comparison of a) longitudinal strains at bottom of ACP layer, and b) vertical strains at top of subgrade induced by DTA and NGWBT in the full-depth asphalt structure

Pavement Damage Analysis

The calculation of cumulative pavement damage due to traffic was done similar to the method suggested by Al-Qadi (129). Two pavement distresses were considered: bottom-up (BU) fatigue cracking, caused by strain at the bottom of the asphalt layer; and subgrade rutting (SR), caused by vertical strain at the top of the subgrade. Fatigue and rutting models from the Asphalt Institute were used to calculate the number of repetitions for each criterion (129). The maximum number of repetitions for bottom-up fatigue cracking is given in Equation 2.

$$N_{BU} = 0.0795 \times \varepsilon_t^{-3.291} |E^*|^{-0.854} \dots\dots\dots 2$$

where N_{BU} is the maximum allowed repetition, ε_t is the tensile strain at the bottom of the asphalt layer, and E^* is the stiffness (dynamic modulus) of asphalt (in units of psi). For subgrade rutting (Equation 3),

$$N_{RS} = 1.365 \times 10^{-9} (\varepsilon_c)^{-4.447} \dots\dots\dots 3$$

where NRS is the maximum number of axles loads to the rut depth failure criteria, and ε_c is the vertical compressive strain at the top of the subgrade.

For each distress, the damage ratio, DR, was calculated according to Equation 4

$$DR = \sum_{i=1}^{12} \frac{n_i}{N_i} \dots\dots\dots 4$$

where n_i is the number of load applications for each month (based on information received from the City of Calgary and assuming an equal monthly traffic distribution), n_i is the number of load applications to failure in month i , and i indicates the month.

The combined damage ratio, CDR, for NGWBT compared to DTA was calculated using the method suggested by Al-Qadi et al. (129).

$$CDR = a_1 DR_{BU} + a_2 DR_{RS} \dots\dots\dots 5$$

in which

$$a_i = \frac{\frac{1}{\log(N_i)}}{\frac{1}{\log(N_{BU})} + \frac{1}{\log(N_{RS})}} \dots\dots\dots 6$$

To calculate the number of load applications, N_i , the equivalent single axle load, ESAL, was calculated as:

$$ESAL = 365 \times AADT_{t=0} \times T \times T_f \times GY \times D \times L \dots\dots\dots 7$$

where ESAL is the equivalent single axle load or number of load repetitions, $AADT_{t=0}$ is the average annual daily traffic at time $t=0$, T is the percentage of trucks, T_f is the truck factor, GY is the growth factor for a specific number of years (as in Equation 8), r is the growth rate, Y is the number of years of interest, D is the directional distribution factor, and L is the lane distribution factor.

$$GY = \frac{(1+r)^Y - 1}{r} \dots\dots\dots 8$$

Table 3 shows the traffic data used to perform damage analysis on the various pavement structures. To calculate the pavement damage caused by the presence of NGWBT in the calculated traffic, the normalized cumulative damage ratio (CDR_{WBT}/CDR_{DTA}) was calculated for different market penetration rates for NGWBT (ranging from 0% to 20% at 5% intervals) and normalized with respect to the CDR of DTA (0% of WTB) (3). Table-4 compares the number of load repetitions to failure for each type of distress in the arterial section for DTA and NGWBT. Similarly, the number of load repetitions to failure for each distress is calculated for the other pavement structures. Figure-11 shows the calculated combined damage factors for a design life of 20 years. Note that with an increase the market penetration rate for NGWBT, the normalized CDR increases for all pavement structures. As expected, the non-transit collector structure, which has the lowest strength among the pavement structures studied in this research, is more vulnerable to damage under NGWBT, with a normalized CDR equal to 1.115 at a 20% market penetration for NGWBT. The non-transit collector, full-depth asphalt, and transit collector undergo more damage, with normalized CDR values equal to 1.077 and 1.082 at a 20% market penetration for NGWBT, respectively. Finally, the arterial structure shows the lowest damage with a normalized CDR of 1.057 (20% market penetration).

TABLE-3 Traffic data used for damage analysis

	Arterial	Transit Collector	Non-Transit Collector	Full-Depth Asphalt
AADT	31,000	20,000	20,000	31,000
T	4%	2%	2%	4%
T_f	6%	6%	3%	6%
L	0.8	1	1	0.8
ESAL (first year)	271,560	219,000	109,500	271,560
N_i = ESAL (monthly)	22,630	18,250	9,125	22,630
Y	20	20	20	20
r	3%	3%	3%	3%
G₂₀	26.87	26.87	26.87	26.87

TABLE-4 Load repetitions to failure for bottom-up fatigue cracking and subgrade rutting in arterial section

N_{BU}	N_{SR}
-----------------------	-----------------------

Month	DTA	NGWBT	DTA	NGWBT
Jan	1.15E+08	7.34E+07	2.87E+08	2.22E+08
Feb	9.80E+07	6.24E+07	2.52E+08	1.90E+08
Mar	5.99E+07	3.93E+07	4.73E+07	3.65E+07
Apr	2.34E+07	1.58E+07	8.03E+05	6.85E+05
May	1.40E+07	9.27E+06	1.32E+06	1.07E+06
Jun	8.77E+06	5.71E+06	1.22E+06	9.45E+05
July	5.85E+06	3.78E+06	8.47E+05	6.40E+05
Aug	6.27E+06	4.05E+06	9.03E+05	6.85E+05
Sep	1.21E+07	7.93E+06	1.59E+06	1.25E+06
Oct	2.29E+07	1.53E+07	2.57E+06	2.10E+06
Nov	5.66E+07	3.76E+07	2.27E+07	1.82E+07
Dec	1.05E+08	6.80E+07	1.64E+08	1.27E+08

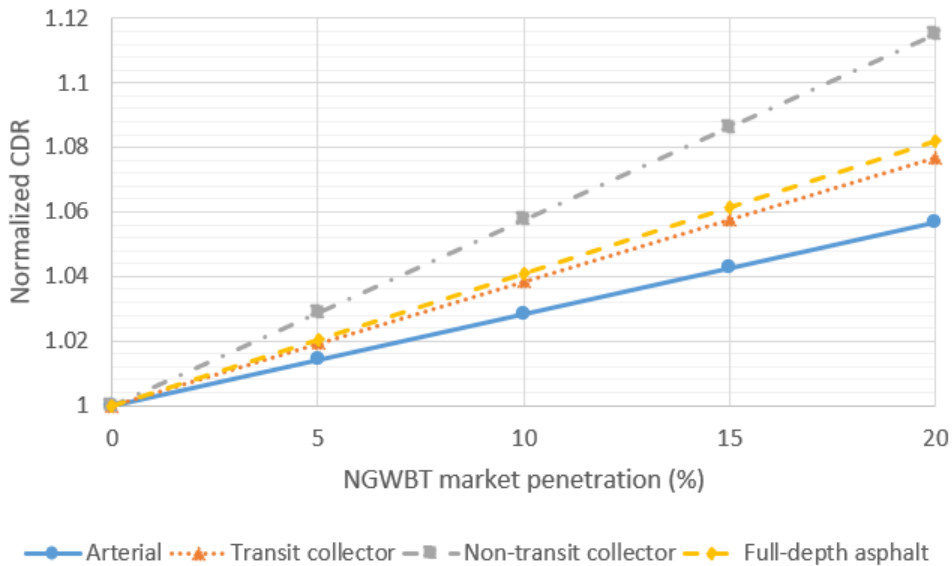


Figure-11 Normalized CDR (CDR_{NGWBT} / CDR_{DTA}) at different market penetration rates in various pavement structures (for a design life of 20 years)

CONCLUSIONS

A 3D FE model was validated to model the behavior of four pavement structures within the City of Calgary for both NGWBT and DTA, considering average monthly temperatures. To account for the viscoelastic behavior of asphalt, material properties were defined by using the average monthly temperature and a loading frequency of 10 Hz. Using this model, strain values were calculated under a loading of 38 kN at critical locations within four pavement

structures (arterial, transit collector, non-transit collector, and full-depth asphalt) with asphalt layers ranging from 140 to 200 mm. There are some limitations in the current work, such as a lack of detailed information about tire-pavement contact stresses and actual asphalt temperatures. However, available data, including tire imprints and contact stresses from the literature, as well as average monthly temperatures were used to analyze the response of four pavement structures to different tire types.

From the comparison between the different pavement structures, the following conclusions were reached.

- The calculated strain ratios (NGWBT/DTA) show that the weaker the pavement structure, the higher the impact of NGWBT on increasing the strains within the pavement layers. The comparison between pavement structures shows the lowest impact for NGWBT on arterials (strongest pavement structure) and highest impact on non-transit collectors (weakest pavement structure).
- Normalized CDR values varied for the four pavement structures considered. CDR ranged from 1.057 (market penetration of 20% in the arterial section) to 1.115 (market penetration of 20% in the non-transit collector section).